PhD

PROGRAM IN MOLECULAR AND TRANSLATIONAL MEDICINE

UNIVERSITY OF MILANO-BICOCCA SCHOOL OF MEDICINE AND SCHOOL OF SCIENCE

Genetic and molecular signatures of glioblastoma stem-like cells

Coordinator: Prof. Andrea Biondi
Tutor: Dr. Gaetano Finocchiaro

Dr. Monica PATANE'
Matr. No. 734626

XXV CYCLE
ACADEMIC YEAR
2011-2012

That's your best friend and your worst enemy - your own brain.
Fred Durst

From a scientist's perspective, to understand everything that you need to know about human beings, you only have to tinker with all the mechanical parts of genes and the brain until there are no more secrets left.
Deepak Chopra

Genetics is crude, but neuroscience goes directly to work on the brain, and the mind follows.
Leon Kass

To my family. To my Dad.
Monica Patanè

TABLE OF CONTENTS

Chapter I: General introduction **pag.7**

1. Pathological features of glioma

2. Molecular and cellular basis of glioblastoma

2.1. Transcriptional and expression profiling:
identification of subtypes and biological programs

2.2 Molecular lesions and critical pathways
in glioblastoma

The RB and p53 pathways

MAPK and PI3K pathways

RTKs

Apoptosis

Angiogenesis

Tumor cell invasion

3. Targeted therapies in GBM

4. Cancer stem-cell hypothesis

5. EGFR and NF-kB pathways in GBM

NF-kB activation

EGFR amplification and EGFRvIII in GBM

EGFR and NF-kB cross-talk in GBM

Scope of the thesis **pag.44**

References

Chapter II: The MET oncogene is a functional marker of a glioblastoma stem-cell subtype **pag. 54**

- **Summary**
- **Introduction**
- **Materials and methods**
- **Results**
- **Discussion**
- **Tables and figures**
- **References**

Chapter III: EGFR and NF-kB cross-talk in glioblastoma stem-like cells **pag. 98**

- **Summary**
- **Introduction**
- **Materials and methods**
- **Results**
- **Discussion**
- **Tables and figures**
- **References**

Summary, conclusions and future perspectives **pag.133**

Publications **pag.134**

CHAPTER I:
GENERAL INTRODUCTION

1. Pathological features of glioma

Primary tumors of the central nervous system (CNS) comprise a heterogenous group of both benign and malignant neoplasm, the most common of which are tumors of glial cells, called gliomas. In western countries the annual incidence is approximately 15 patients per 100000 population, whereas for malignant gliomas is 5 cases per 100000 people (*Riemenschneider et al 2010, 2009; Wen et al 2008*).

Gliomas are histologically classified according to the World Health Organization (WHO) classification, which combines tumor typing with the assignment of a defined malignancy grade: four histological malignancy grades have been defined from benign tumors (grade I) to highly malignant tumors (grade IV) (*Riemenschneider et al 2009).*

Patients with WHO grade I tumors can usually be cured by surgical resection: *pilocytic astrocytoma*, the most common glioma in childhood, is the prototype of this category; this tumor is often well demarcated and only very rarely progresses to anaplasia.

WHO grade II tumors exhibit a rather slow growth, but tend to recur after resection and to progress to anaplastic gliomas or secondary glioblastomas, with a median of survival of 5-8 years after diagnosis; based on morphological similarities with glial cells, we can recognize two type of grade II gliomas, *low grade astrocytomas* and *oligodendrogliomas.*

WHO grade III tumors are termed *anaplastic gliomas*: they are rapidly growing malignant tumors that require, in addition to surgery, aggressive treatment with radio- and chemotherapy, with a median survival time of 2-3 years after diagnosis.

WHO grade IV is assigned to *glioblastoma*, the most common and malignant type of glioma, which preferentially manifests in adult with a peak incidence between 50 and 60 years; patients exhibit a rapid disease progression and a median of survival of just one year after initial diagnosis (*Riemenschneider et al 2009; Pietsch et al 1997).* Glioblastoma (GBM) may arise both *de novo* (*primary glioblastoma*) or through progression from a lower grade glioma (*secondary glioblastoma*): the latter is much less common and is manifested in younger patients (*Wen et al 2008)*. Finally, the presence of necrosis and microvascular proliferation is a histopathological hallmark required for glioblastoma diagnosis (*Dunn et al 2012*).

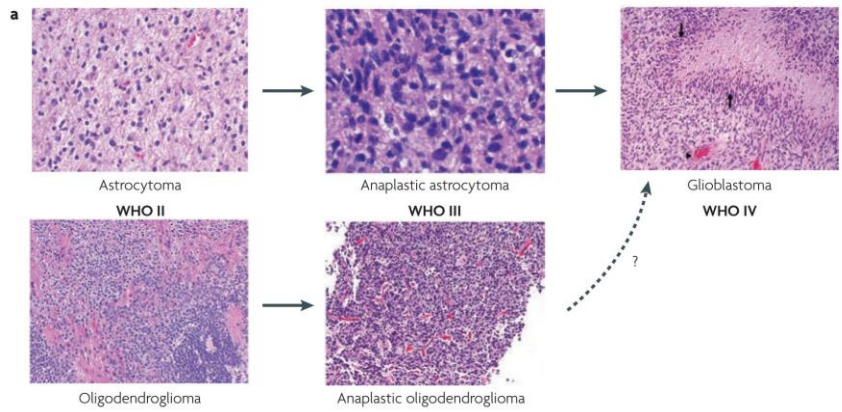

Figure 1. Schematic representation of histopathological hallmarks of diffuse gliomas (astrocytic and oligodendroglial lineages). *Adapted from Huse and Holland 2010*

An accurate distinction between different gliomas is important because of its strong prognostic and therapeutic implications; however, histological classification is often associated with significant interobserver variability; furthermore the clinical behaviour of individual tumors may substantially differ. Thus additional markers are needed for a refined glioma classification and for a better prediction of prognosis.

Like cancer in general, glioma is a result of genetic alterations that accumulate with tumor progression: in the past years the knowledge of these alterations in the various types of gliomas has drastically increased. These molecular markers have both diagnostic and prognostic implications, so they are helpful for the classification of tumors and for the correlation with disease-free and overall survival of the patients; some markers have also a predictive power in order to provide information on the response to a given therapy (*Riemenschneider et al 2010).*

For pilocytic astrocytoma the aberrant activation of *BRAF* proto-oncogene at 7q34 is the most characteristic genetic alteration detected in the 60-80% of these type of tumors: this activation is generated by gene duplication and fusion or less frequently by point mutations and this aberration can be considered both a diagnostis and a prognostic marker for pilocytic gliomas.

A lot of prognostic and diagnostic markers has been identified for WHO grade II and III gliomas: for example mutation of tumor

suppressor gene *TP53* located at 17p13.1 and loss of heterozygosity on chromosome 17p are found in more than half of the WHO grade II diffuse astrocytomas, in contrast oligodendroglial tumors frequently show combined losses of the short arm of chromosome 1 and the long arm of chromosome 19. This typical 1p/19q codeletion is detected in up to 80% of oligodendrogliomas and 60% of anaplastic oligodendrogliomas and is associated with better prognosis and a better response to chemotherapy.

Anaplastic gliomas (WHO grade III), instead, often carry additional genetic changes associated with progression such as losses of tumor suppressor genes *CDKN2A* and *CDKN2B* on 9p21.

Then, the vast majority of low grade diffuse gliomas (WHO grade II) and anaplastic neoplasms (WHO grade III) present somatic mutations in the gene encoding the human cytosolic NAPDH-dependent isocitrate dehydrogenase *(IDH1*): this mutation could be considered a diagnostic marker both for low grade and anaplastic gliomas as well for secondary glioblastoma and is associated with a more favourable outcome (*Yan et al 2009*).

Finally glioblastoma (WHO grade IV) show a very complex set of chromosomal and genetic alterations that involve loss of tumor suppressor genes and activation of proto-oncogenes: primary and secondary glioblastomas show distinct pattern of alterations, because the first arise *de novo*, whereas the latter develop by progression from pre-existing lower grade gliomas; in particular, primary GBM show frequent *EGFR* amplification, *PTEN* mutation and loss of chromosome 10q, whereas secondary GBM is most resembling to low

grade gliomas with mutations in *TP53* and *IDH1* gene (*Riemenschneider et al 2010*).

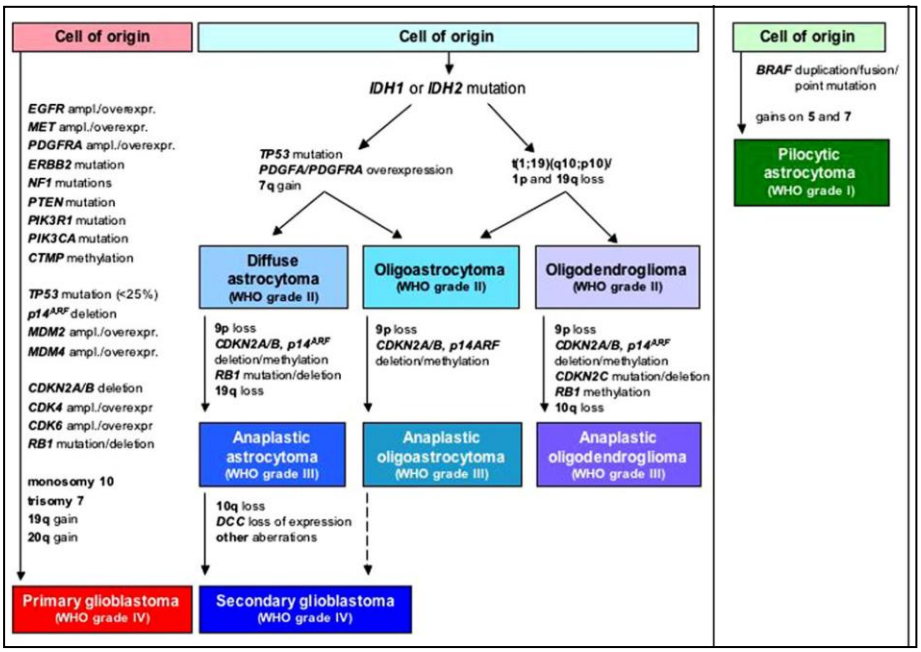

Figure 2. Summary of most frequent molecular alterations in astrocytic, oligodendroglial and oligoastrocytic gliomas. *Adapted from Riemenschneider et al 2010*

2. Molecular and cellular basis of glioblastoma

Glioblastoma multiforme (GBM) is the most common and aggressive of malignant gliomas and is defined by the hallmark features of uncontrolled cellular proliferation, diffuse infiltration, propensity for necrosis, robust angiogenesis, resistance to apoptosis and rampant genomic instability. It presents a significant intratumoral heterogeneity at the cytopathological, transcriptional and genomic level combined with a putative cancer stem cells (CSCs)

subpopulation that make this cancer one of the most difficult to understand and to treat.

On the basis of clinical presentation, GBMs have been further subdivided into the primary and secondary subtypes. Primary GBMs account for the majority of cases in older patients, while secondary GBMs are quite rare and tend to occur in patients below the age of 45 years. Primary GBMs present in acute *de novo* manner with no evidence of prior symptoms or antecedent pathology, whereas secondary GBMs derive from progressive transformation of lower grades astrocytomas with a 70% of grade II transforming into grade III/IV in 5-10 years after diagnosis. Although they share a common phenotype, recent studies have revealed different transcriptional pathways and copy number aberrations (*Furnari et al. 2007*).

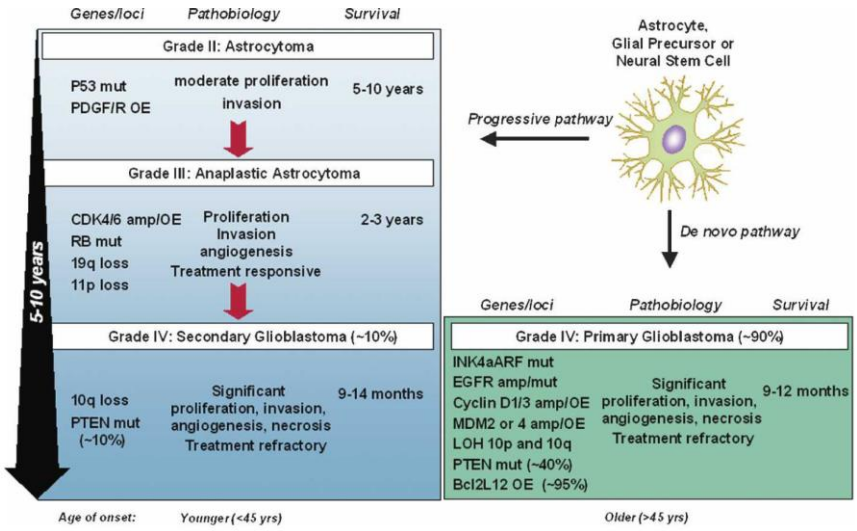

Figure 3.Chromosomal and genetic aberrations involved in the genesis of glioblastoma. Shown are the relationship between survival pathobiology and molecular lesions that lead to primary and secondary glioblastomas. *Adapted from Furnari et al 2007*.

Both primary and secondary glioblastomas arise from precursor cells that may be distinct; besides primary GBMs show a worse prognosis owing to the predominant wild-type *IDH1* genotype; in contrast secondary GBMs are dominated by a mutant *IDH1* genotype that confers a better prognosis and is associated with a more restricted frontal lobe location (*Dunn et al 2012*).

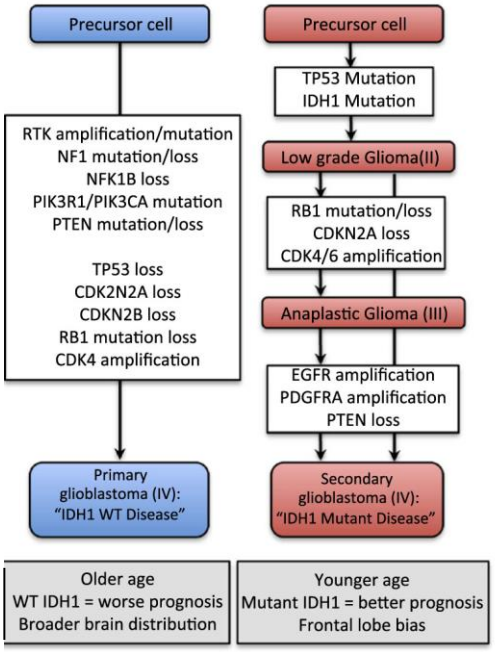

Figure 4. Genomic alterations and clinical outcome of primary and secondary glioblastomas. *Adapted from Dunn et al 2012.*

Glioblastoma, like other human is the cancers, is the product of accumulated genetic and epigenetic alterations: it's characterized by genetic instability and complex alterations in chromosome structure and copy number.

Somatic copy number alterations (SCNAs) are distinguished from germline copy number variations (CNVs) and are extremely common

in cancer. Across the entire genome, the most prevalent SCNAs are either very short (focal) or almost exactly the length of a chromosome arm or whole chromosome (arm-level) (*Beroukhim et al 2010*).

To fully explore these data several group have also developed bioinformatic tools such as Genomic Identification of Significant targets in Cancer (GISTIC), in order to highlight the cancer-derived genomic alterations from the background noise (*Beroukhim et al 2007*). The genomic landscape of glioblastoma has been also clarified by The Cancer Genome Atlas (TCGA) pilot project (*Cancer Genome Atlas Research Network 2008*), which applied multiform profiling as well as array-based platforms to analyze copy number, mRNA expression, and epigenetic state of almost 200 tumors, most of which were untreated primary GBMs.

2.1. Transcriptional and expression profiling: identification of subtypes and biological programs

The glioblastoma transcriptome is highly structured and reflect tumor histology, molecular alterations and clinical outcome; two important studies have provided the foundation for classification of glioblastoma subtypes (*Phillips et al 2006*; *Verhaak et al 2010).*

Phillips et al. (2006) identified three distinct glioblastoma subtypes based on their differences of expression of a panel of genes most strongly correlated with survival: *proneural, mesenchymal* and *proliferative*. *Proneural* subtype (PN) is distinguished by markedly better prognosis and expresses genes associated with normal brain and the process of neurogenesis; it is moreover represented in tumors of

WHO grade III and WHO grade IV and it is characterized by astrocytic or oligondroglial cellular morphology. It may arise in younger patients and determine a longer survival: therefore it may resemble a typical secondary GBM. It is associated with typical markers of adult and fetal brain and with neurogenesis. It doesn't show chromosome gain or loss and *PTEN* and *EGFR* loci are intact.

The *proliferative* subtype (*Prolif*) and the *mesenchymal* subtype (*Mes*) are characterized by a resemblance to highly proliferative cell lines such as lymphoblast or tissue of mesenchymal origin respectively, such as bones, smooth muscles or endothelium. They show activation of gene expression programs of cell proliferation and angiogenesis and typical gain of chromosome 7 and loss of chromosome 10: *PTEN* locus is typically loss and *EGFR* is amplified. They arise in older patients and are associated with a poor survival: therefore they resemble a typical primary GBM. This worse prognosis is probably related to a growth advantage conferred by a rapid rate of cell division or enhanced survival afforded by neovascularization (*Phillips et al 2006*).

	Proneural	Proliferative	Mesenchymal
Histological grade	WHO grade III or WHO grade IV with or without necrosis	WHO grade IV with necrosis	WHO grade IV with necrosis
Cellular morphology	Astrocytic or Oligodendroglial	Astrocytic	Astrocytic
Evolution of signature	Arises in 1° tumor, may persist or convert to *Mes*	Arises in 1° tumor, may persist or convert to *Mes*	Arises in 1° tumor or by conversion from other subtype
Patient age	Younger (~40 yrs.)	Older (~50 yrs.)	Older (~50 yrs.)
Prognosis	Longer survival	Short survival	Short survival
Histological Markers	Olig2, DLL3, BCAN	PCNA, TOP2A	CHI3L1/YKL40, CD44, VEGF
Tissue similarities	Adult and Fetal Brain	HSC, lymphoblast	Bone, cartilage, smooth musc, endothelium, dendritic cells
Biological process	Neurogenesis	Proliferation	Angiogenesis
Analogous forebrain cell	Neuroblast	Neural Stem Cell and/or Transit Amplifying Cell	Neural Stem Cell
Chromosome gain/loss	None	Gain of 7 & Loss of 10 or 10q	Gain of 7 & Loss of 10
PTEN locus	PTEN intact	PTEN loss	PTEN loss
EGFR locus	EGFR normal	EGFR amplified or normal	EGFR amplified or normal
Signaling	Notch activation	Akt activation	Akt activation

Figure 5. Summary of glioblastoma subtypes: proneural, proliferative and mesenchymal. *Adapted from Phillips et al 2006*.

Using unsupervised hierarchical clustering analysis, *Verhaak et al*. (2010) classified 200 TCGA glioblastoma samples into four subtypes, which were subsequently validated using previously published data from 260 independent samples: *Classical*, *Mesenchymal*, *Proneural* and *Neural* subtypes.

The *Classical* subtype is mostly characterized by chromosome 7 amplification and chromosome 10 loss: in the 97% of samples *EGFR* amplification alone account for chromosome 7 aberration; the 50% of them also contained EGFRvIII mutation. Focal homozygous deletion at 9p21.3 (*CDKN2A* locus) is frequently associated in the classical

subclass co-occuring with *EGFR* amplification and mutually exclusive with *RB* pathway aberrations. Neural precursor and stem cell markers such as *Notch* and *Sonic Hedgehog* are highly expressed and there is also a strong association with the astrocytic gene signature, as inherent signature retained from progenitor cells.

In the *Mesenchymal* subtype predominantly occur a focal hemizygous deletion at 17q11.2 containing the gene *NF1* and the majority of samples also have lower *NF1* expression. They display expression of mesenchymal markers, such as MET and YKL40, and astrocytic markers: this combination is reminiscent of the epithelial to mesenchymal transition (EMT) typical of dedifferentiated and transdifferentiated tumors. Genes of the Tumor Necrosis Factor (TNF) pathway and the NF-kB pathway are highly expressed and there is a strong association with the astroglial gene signature.

In the *Proneural* subtype there is a focal amplification at 4q12 harboring the *PDGFRA* locus: this amplification is present in all the subtypes but is much higher in the proneural subtype. This class shows also point mutation of *IDH1* gene, *TP53* and LOH of 17p. The Proneural group was highly enriched with the oligodendrocytic signature and it shows high expression of oligodendrocytic development genes such as *OLIG2*, which is able to downregulate the tumor suppressor gene p21 increasing cell proliferation. Tumors which show a proneural pattern are mostly secondary GBM and WHO grade III gliomas.

Finally the *Neural* subtype is typified by the expression of neuron markers, oligodendrocytic and astrocytic differentiation signature

suggestive of a cell with differentiated phenotype (*Verhaak et al 2010*).

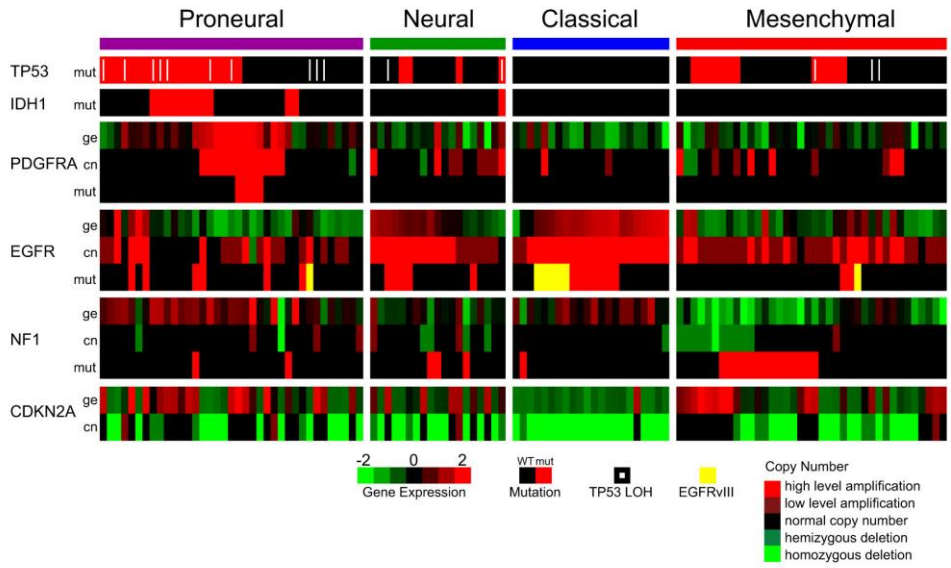

Figure 6. Integrated view of gene expression (ge), copy number variation (cn) and mutations (mut) of glioblastoma subtypes. *Adapted from Verhaak et al. 2010.*

In order to determine whether these genomic subtypes predict biological or clinical differences in glioblastoma, *Brennan et al.* (2009) used a targeted proteomics approach to determine whether glioblastomas also segregated into distinct classes by activation of signal transduction pathways. They identified distinct tumor subgroups defined by EGFR-related signalling, PDGF-related signalling and NF1-related signalling: the *EGFR tumor class* showed EGFR amplification and activating mutations in the extracellular domain, high levels of total and pEGFR proteins such as Notch activity (*EGFR core*); the *PDGF tumor class* show PDGFRA amplification, high levels of PDGFB, pPDGFR and pNFKB1, PTEN

and Ras activity and the typical proneural signature (*PDGF core*); the *NF1 tumor class*, finally, is associated with low levels of NF1 protein, high levels of total and phosphoproteins of the MAPK pathway and higher levels of VEGF, YKL40 according to mesenchymal signature (*NF1 core*) (*Brennan et al. 2009*).

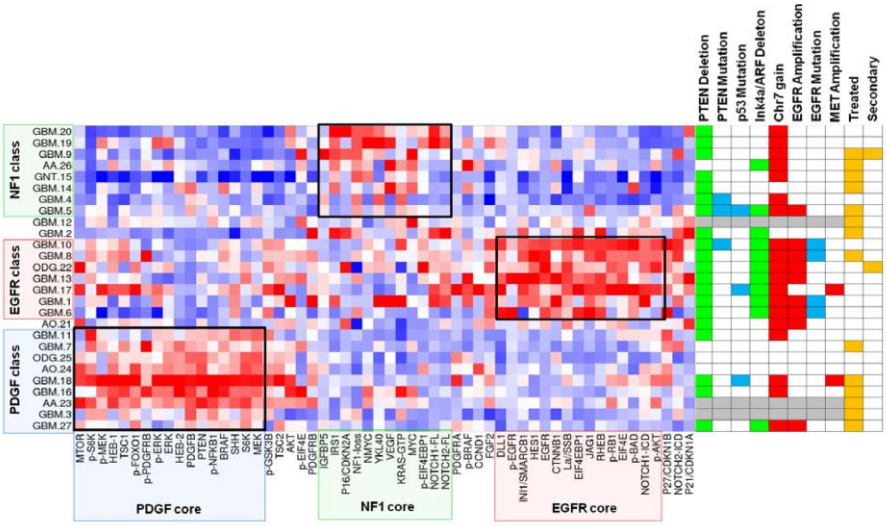

Figure 7. Clustering of gliomas by signature-defining proteins and summary of copy number variations and mutations. *Adapted from Brennan et al 2009.*

2.2. Molecular lesions and critical pathways in glioblastoma

Genetic alterations in glioma target pathways mostly involved in proliferation, cellular survival, apoptosis and necrosis, invasion and angiogenesis (*Dunn et al. 2012*, *Furnari et al. 2007*).

The RB and p53 pathway. These pathways regulates cell cycle primarily by governing the G1-to-S-phase transition and are target of inactivating mutations which render tumors particularly susceptible to inappropriate cell division. In quiescent cells, hypophosphorylated RB protein blocks proliferation binding E2F transcription factors family, which usually transactivates genes for the progression through the cell cycle: the *Rb1* gene on chromosome 13q14 is mutated in 25% of gliomas (*Henson et al. 1994*); besides in the 50%-70% of glioblastomas the *CDKN2A* locus on 9p21 is inactivated by allelic loss and this gene usually transcribes for p16 (*Ink4a*) and p14 (*ARF*), two critical negative regulators for the cell cycle (*Jen et al. 1994*). The *p53* tumor suppressor usually prevents the propagation of cells with unstable genomes by blocking the cell cycle in the G1 phase or activating a program of apoptosis through its function of a transcription factor for more than 2500 potential effector genes: loss of *p53*, in glioma, is determined by point mutations and loss of chromosome 17p (*Louis 1994*), and germ-line mutations are also associated with the Li-Fraumeni syndrome, a familial cancer-predisposition syndrome characterized by an increased incidence of gliomas (*Srivastava et al. 1990*); besides 10% of glioblastomas show amplification of *MDM2* and *MDM4* genes, which usually inhibit p53 activity (*Furnari et al 2007*).

MAPK and PI3K pathways. Proliferation of normal cells requires activation of mitogenic signalling pathways through diffusible growth factor binding or cell-cell adhesion and contact

with extracellular matrix (ECM): this signals are transduced intracellularly by transmembrane receptors which tipically activate MAPK or PI3K pathways. Tumor cells acquire alterations that reduce their dependence on exogenous stimulation by activating constitutively these pathways. MAPK pathways is activated by integrins and tyrosine-kinase receptors (RTK): integrins are membrane-bound ECM receptors which create a focal adhesion complex (FAK) of kinases that allow binding to actin filaments; FAK activates also a cascade of signal transduction which involves effectors, such as Ras and Raf, that phosphorylates MAPK and ERK transcription factor; in glioma high levels of Ras-GTP have been found leading to an appropriate actvation of this pathway (*Guha et al 1997*). The PI3K kinases catalyse the phosphorylation of phosphatidyl-inositol-4,5-biphosphate (PIP_2) to phosphatidyl-inositol-3,4,5-triphosphate (PIP_3), creating a docking site for multiple effector proteins. The *PIK3CA* gene, which encodes for the subunit p110 of PI3K, is mutated in the 15% of malignant gliomas leading to an appropriate activation of this protein (*Samuels et al. 2004*). The PI3K activity is usually antagonized by PIP_3-phosphatase (PTEN): *PTEN* gene is a tumor suppressor which is inactivated in the 50% of glioblastomas by mutation, epigenetic mechanism or loss of chromosome 10q23.3 locus (*Li et al. 1997*). PI3K also activates Akt pathway, which is involved in cell growth and proliferation (*Furnari et al 2007*). Downstream of PI3K pathway we found a very important effector, mTOR: mTOR is a multiprotein complex which functions as serine-threonine kinase. Akt activates mTORC1 which controls

protein synthesis, metabolism and cell growth, whereas mTORC2 phosphorylates at ser473 Akt to promote maximal activity; mTOR complexes response to rapamycin in different ways. (*Tanaka et al 2011*).

RTKs. Gliomas may activate RTKs pathways by different mechanisms: overexpression of both ligands and receptors (autocrine loop), genomic amplification and/or mutation of the receptor.

Epidermal growth factor receptor (*EGFR*) gene amplification occurs in the 40% of glioblastomas and the amplified gene are frequently rearranged (*Lieberman et al.1984, 1985; Ekstrand et al. 1991; Wong et al.1992*). An *EGFR* mutant allele with deletion of exons 2-7 (EGFRvIII) occurs in the 20%-30% of all human GBMs and in 50% of those that have EGFR amplified: EGFRvIII is a constitutively activated receptor which lacks of part of the extracellular domain and is associated with a worse prognosis in GBMs (*Heimberger et al 2005*).

Platelet-derived growth factor receptor alpha (PDGFRA) and its ligands (PDGF-A and PDGF-B) are expressed in high grade gliomas: *PDGFRA* gene is amplified in 15% of all tumors and enriched in the Proneural subtype (*Phillips et al 2006; Verhaak et al. 2010*).

The c-MET tirosyne-kinase receptor is amplified in 5% of glioblastomas and is associated with the Mesenchymal subtype and co-activated in cells with increased levels of EGFR and EGFRvIII (*Beroukhim et al. 2007; Kong et al. 2009; De Bacco et*

al. 2012). Concurrent activation of c-MET with PDGFRA has also been detected in glioblastomas and has been suspected to be a mechanism for resistance to EGFR kinase inhibitors therapy (*Stommel et al. 2007*).

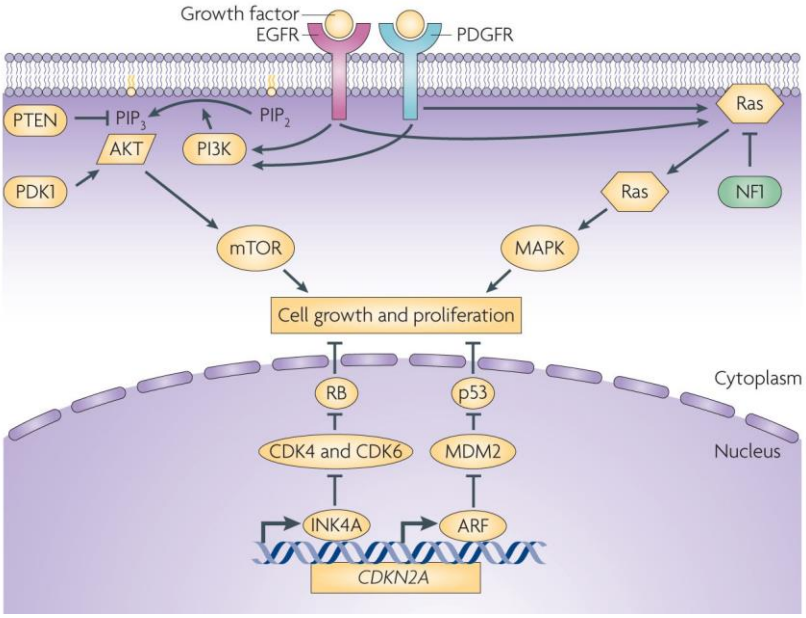

Figure 8. Pathways involved in glioblastoma. *Adapted from Huse and Holland 2010.*

Apoptosis. A hallmark feature of malignant glioma cells is an intense resistance to death-induced stimuli such as radiotherapy and chemotherapy. This property has been linked to genetic alterations of key regulatory proteins as RTKs and PI3K-PTEN-Akt signalling and the effectors of the cell death network, called "death receptors" (TRAIL, TNFR and CD95 receptors), which activate the caspases cascade; or in turn to the anti-apoptotic family Bcl-2, which preserve mitochondrial membrane integrity

and the release of cytochrome c, an activator of the caspases cascade (*Furnari et al. 2007*).

Angiogenesis. GBMs are among the most highly vascular of all solid tumors: microvascular hyperplasia, characteristic of this tumors, consists of proliferating endothelial cells that emerge from normal parent microvessels as tufted microaggretates (glomeruloid bodies) accompanied by stromal elements such as perycites and basal lamina (*Stiver et al. 2004*). Besides, one common feature in the transition from low-grade or anaplastic astrocytomas to secondary GBMs is a dramatic increase in microvascular proliferation such as in the primary GBMs.
The hypothesis that interruption of blood supply to the tumor will lead to regression or dormancy of the tumor had led to the development of several drugs that target multiple steps in angiogenesis. For example, blood vessel formation is regulated by a balance between pro- and anti-angiogenic molecules: VEGFR-2/KDR is considered the central pro-angiogenc factor and is induced by hypoxia via HIF1α. Most approaches target VEGF signalling by interfering with either VEGF ligand or its receptor: actually the anti-VEGF antibody (Bevacizumab) is used heavily in the clinic (*Furnari et al 2007; Dunn et al 2012*).

Tumor cell invasion. Infiltration throughout the brain is prominent feature of low and high-grade glioma and is the principal basis for the lack of surgical cure. In the 90% of cases, the recurrent tumor develops immediately adjacent to the resection

margin or within several centimeters of the resection cavity. Invasion into regions of normal brain is driven by a multifactorial process involving cell interactions with the ECM and with the adjacent cells. Several genes involved in glioma invasiveness has been identified and include, for example, members of the family of metalloproteases (MMPs) and their endogenous tissue inhibitors (TIMPs) that are elevated in high grade glioma or integrins, ephrin receptors and their ligands which are also and overexpressed and linked to poor survival (*Dunn et al 2012*).

3. Targeted therapies in GBM

The standard therapy for newly diagnosed malignant gliomas involves surgical resection when feasible, radiotherapy and chemotherapy. Radiotherapy is the mainstay of treatment for malignant gliomas and its addition to surgery increases survival among patients with glioblastomas from a range of 3 to 4 months to a range of 7 to 12 months. Patients who are older than 70 years of age have a worse prognosis and radiotherapy produces a modest benefit in median survival: so an abbreviated course of radiotherapy or chemotherapy with temozolomide alone may be considered (*Wen et al. 2008*).

Chemotherapy is assuming an increasingly important role in the treatment of malignant gliomas: alkylating agents with a good penetration of the blood-brain barrier such as nitrosoureas or temozolomide have been extensively used. Radiotherapy and concomitant treatment with temozolomide followed by adjuvant temozolomide therapy (*Stupp et al. 2005*) had an acceptable side-

effect profile and, as compared with radiotherapy alone, increased the median survival to 15 months and the survival at 2 years was significantly greater (26%). Further analysis revealed that the survival benefit was largely restricted to those patients whose tumors showed epigenetic silencing of the DNA repair gene *MGMT*: *MGMT* encodes a DNA repair protein that removes alkyl groups from the O^6 position of guanine, which are introduced by alkylating agents such as temozolomide; DNA alkylation triggers cytotoxicity and apoptosis, while high MGMT expression in the tumor cells counteracts the cytotoxic effect and thereby may cause treatment failure. *MGMT* promoter silencing by methylation impedes the transcription of the gene: glioblastoma cells with MGMT promoter hypermethylation thus respond better to temozolomide with a median of survival extended to 2 years and a progression free survival at 6 months (PFS6) of 21% (*Hegi et al.2006*).

The improved understanding of the molecular pathogenesis of malignant gliomas has allowed a more rational use of targeted molecular therapies. Particular interest has focused on inhibitors that target receptor tyrosine kinases such as EGFR (*Erlonitib, Gefinitib* and *Cetuximab*), PDGFR (*Imanitib*), MET; transduction pathway's inhibitors such as mTOR inhibitors and PI3K inhibitors; epigenetic drugs such as HDAC inhibitors (*Vorinostat*); anti-angiogenic drugs such as anti-VEGF (*Bevacizumab*); and immunotherapies such as peptides against EGFRvIII and dendritic cells (*Sathornsumetee et al 2007*). But to date, single agents have only a modest activity with response rates of 0 to 15% and no prolongation of the PFS6; actually most GBMs have coactivation of multiple tyrosine kinases as well as

redundant signalling pathways thus limiting the activity of single agents. This intratumoral heterogeneity and target cooperativity (*Stommel et al 2007*) conspire to create a "multiple dependency" state wherein single-target inhibitors are not sufficient to attenuate tumor growth. The heterogeneity is also at the molecular level, with variable intratumoral distribution of EGFRvIII cells (*Inda et al 2010)* or mutually exclusive SCNAs within distinct populations of the same tumor (*Szerlip et al 2012*).

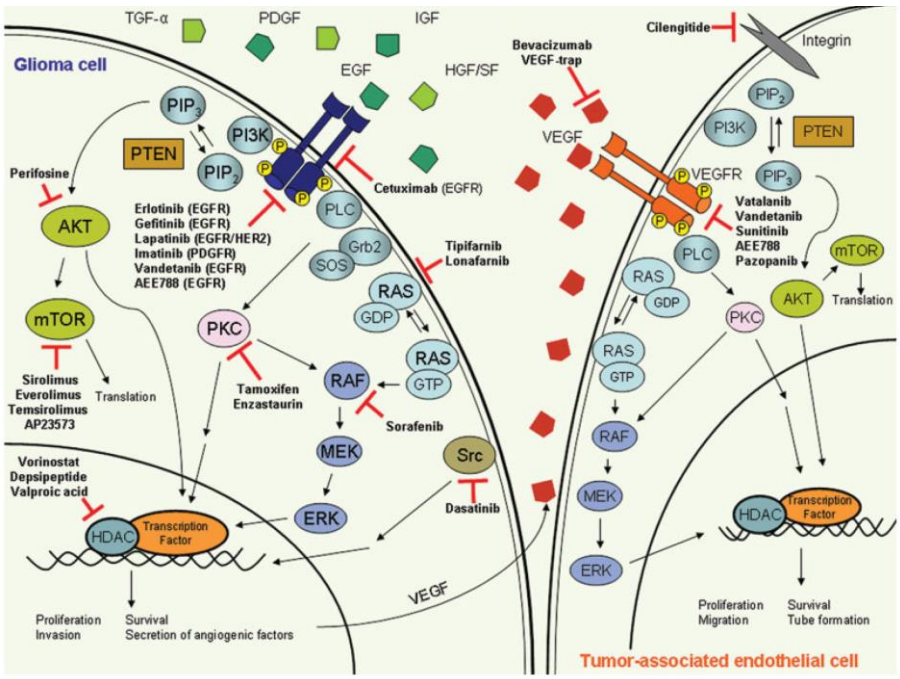

Figure 9. Targeted molecular therapy in glioblastoma. *Adapted from Sathornsumetee et al 2007*

4. Cancer stem-cell hypothesis

The cancer stem-cell hypothesis suggests that not all the cells in the tumor have the same ability to proliferate and maintain the growth of the tumor itself: only a relatively small fraction of cells in the tumor, called cancer stem-cells possess the ability to proliferate and self-renew extensively. To date the traditional hypothesis has been that brain tumors arise from the differentiation of a mature brain cell in response to genetic alterations, but now has found its way the idea that brain tumors may arise from a transformation of a resident immature brain cell, such as neural stem-cell or a progenitor cell. These fraction of cells called "brain tumor stem-cells" (BTSCs) or "glioblastoma stem cells" (GSCs) are considered the real tumor-forming cells: they can be isolated from GBMs and propagate as neurospheres in vitro in serum-free conditions, have self-renewal capacity and recapitulate malignant glioma behaviour in vivo (*Singh et al 2003, 2004*). These self-renewing tumor cells were first identified in GBM by the expression of neural stem cell surface marker CD133 (1%-35% of total population); in contrast the $CD133^-$ cells failed to proliferate and remained in an adherent monolayer in culture expressing mature lineage-specific markers (*Singh et al 2003*). The $CD133^+$ fraction under neural stem cell conditions expressed the stem cell marker Nestin and upon exposure to serum differentiated into a mixed population of neurons, astrocytes and oligodendrocytes which mirrored the heterogeneity found in the original tumor (*Galli et al 2004*).

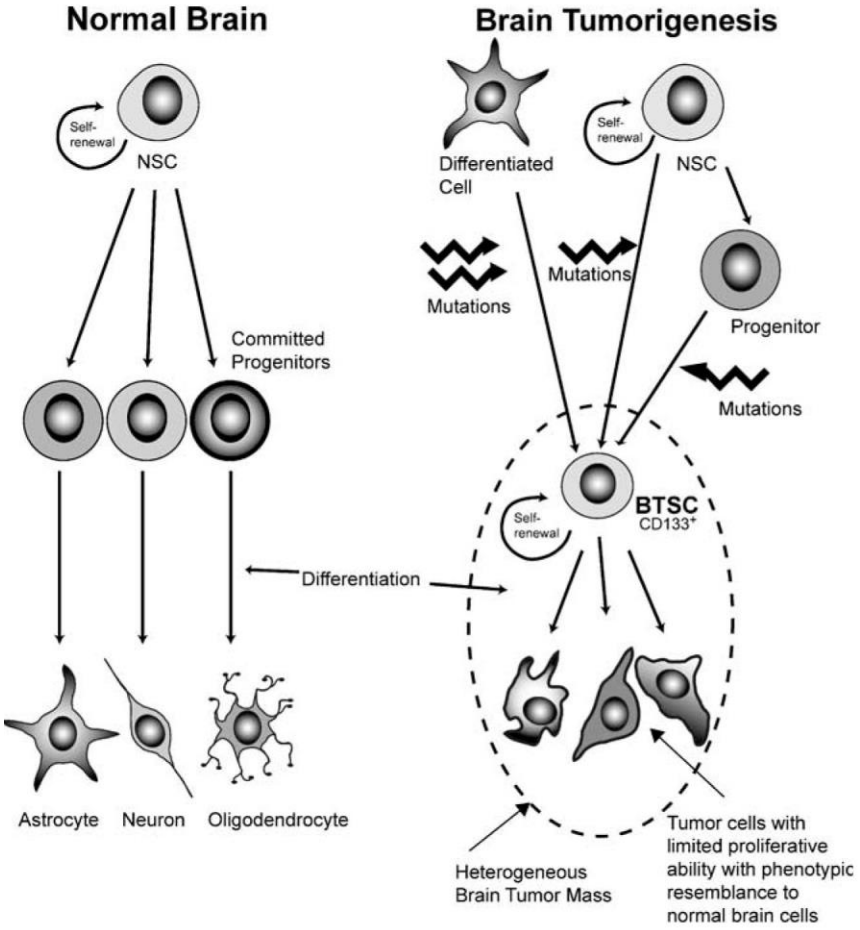

Figure 10. The CSCs hypothesis for brain tumor stem cells (BTSCs).
Adapted from Singh et al 2004

Glioma CSCs (GScs) were among the first solid tumor CSCs described and share significant similarities with normal NSCs including expression of stem cell markers and the capacity to differentiate in multiple lineages but this overlap is incomplete; notably GSCs are also high resistant to chemoradiotherapy. Their behaviour is constantly affected by external signals from their niche that includes stromal cells, immune and non stem tumor cells; these

signals are mediated by cell surface ligand-receptors systems typical of neural stem cells, which are deregulated in GSCs, such as: RTKs, as EGFR, from which depend neurospheres formation and proliferation in vitro; Bone Morphogenetic Proteins (BMPs), which usually regulate proliferation, apoptosis and differentiation; Hedgehog pathway that is a key regulator of embryogenesis and self-renewal of NSCs and GSCs; and Notch which promotes proliferation and supresses differentiation. Transcription factors and epigenetic regulators are also regulators of cancer and normal stem cells such as c-Myc, which is considered an oncoprotein for its role in proliferation, Sox-2, Oct4 and Nanog which regulate self-renewal and differentiation, Olig-2, that is expressed in neural progenitors and finally, Polycomb group genes, such as *EZH2* and *BM1*, which regulate chromatine silencing. These complex signalling of GSCs niche underscoring the importance to elucidate molecular mechanisms in order to develop more efficient therapies against gliomas (*Li et al 2009*).

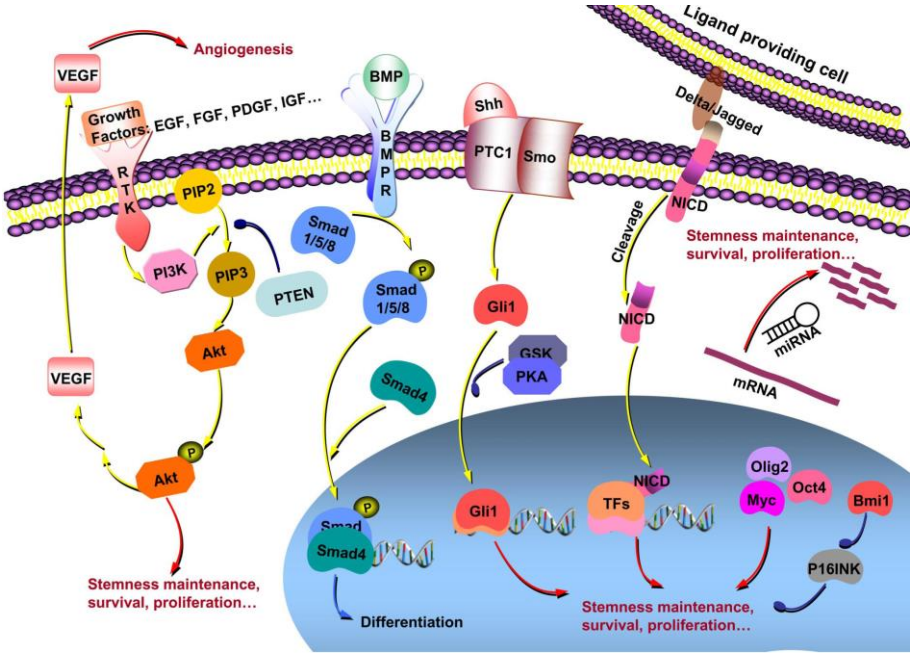

Figure 11. Signalling pathways and cellular factors that regulates GSCs.
Adapted from Li et al 2009.

5. EGFR and NF-kB pathways in GBM

In the past years several studies have showed the importance of EGFR and NF-kB pathways in forming, growth and relapse of many types of cancer including glioblastoma: notably these pathways are strictly intermingled and dependent on each other. Genetic and molecular characterization of alterations involved may be a new challenge in targeted therapy for GBMs.

NF-kB activation. NF-kB is a heterodimeric transcription factor formed by members of a family of proteins that share a conserved N-terminal/DNA binding region called Rel homology domain, which

bind selectively to the kB consensus sequence on the DNA. Based on overall structures and processing, NF-kB family can further subdivided into NF-kB proteins, such as p50/p100 (NFkB1) and p52/p100, and Rel proteins, such as RelA (p65), RelB and RelC: NF-kB proteins are produced by proteolytic removal of C-terminal sequences from a larger precursor, while Rel proteins contain C-terminal transactivation domains. NF-kB complexes are maintained in an inactive form primarily through interactions with the inhibitor of kB proteins (IkB): IkB family has several members including IkBα, IkBβ, IkBε and p100, which are encoded by NFKB inhibitor genes (i.e. *NFKBIA* gene on 14q13.2) and contains ankyrin-like repeats that mediate binding and inhibition of NF-kB complex. Most stimuli activate this pathway by modulating the activity of IkB kinase (IKK) complex which is comprised of three subunits: IKKα, IKKβ and NEMO (IKKγ); IKKα and IKKβ are kinases, whereas NEMO is a scaffold protein for the complex. Upon stimulation IKK complex phosphorylates the IkB proteins which are ubiquitinated and degraded by the 26S proteasome and the NF-kB is finally released. There are, however, two distinct pathways that lead to the activation of NF-kB: the *canonical pathway*, which involves primarily IKKβ for the phosphorylation of IkBα and the release of p65/p50 complex; and the *non-canonical pathway*, which, in turn, involves IKKα to phosphorylate directly p100/RelB complex. These pathways are activated by different stimuli, as it is shown in figure below (*Basserés et al 2006; Brown et al 2008; Nogueira et al 2011*).

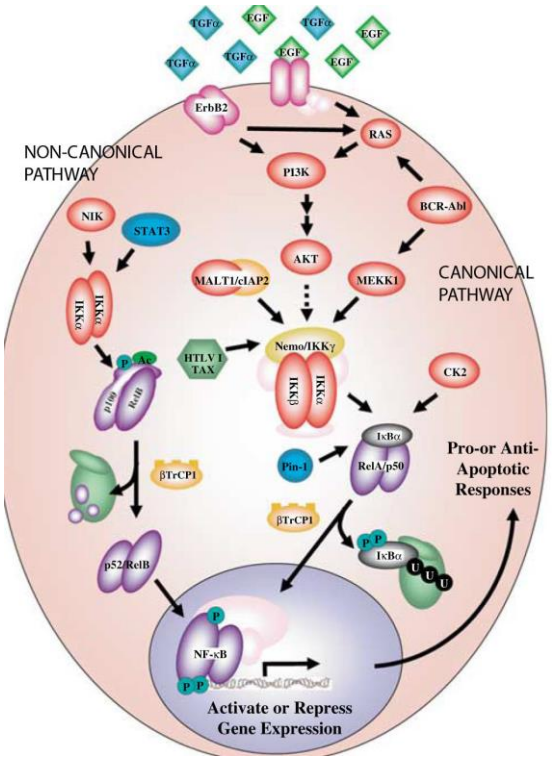

Figure 12. Canonical and non-canonical pathways of NF-kB activation. *Adapted from Basserés et al 2006.*

Complexes bound to IkB continuously shuttle between cytoplasm and the nucleus and a highly efficient nuclear export ensures very low levels of NF-kB in the uninduced state. The transactivation potential of NF-kB activated complex in the nucleus, i.e. the ability to recruit the transcriptional apparatus and stimulate target gene expression, is ensured also by additional modification of the transcriptional factor itself and the surrounding chromatin: C-terminal and Rel-homology domains of p65 are indeed phosphorylated by kinases such as PKA and PKC, and the chromatin surrounding the consensus region may be acetylated and then more accessible (*Vermeulen et al 2002*).

NF-kB is one of the major transcription factors associated with cancer and it has implicated in proliferation, inhibition of apoptosis, tissue

invasion and metastasis: NF-kB is constitutively activated by a number of different mechanisms including genetic and molecular alterations of upstream components of this pathway. NF-kB can promote for example cellular proliferation through regulation of specific target genes such as *RB*, *cyclinD1* and *MYC*, all involved in the regulation of the cell cycle. Interestingly NF-kB directly regulates also a potent anti-apoptotic pathway such as *Bcl-2* e *Bcl-XL* genes. NF-kB then promotes angiogenesis and metastasis in certain tumor models potentially through the regulation of VEGF and metalloproteases (MMPs). Finally NF-kB controls the production of many cytokines and chemokines including IL-8, IL-11, IL-6, IL-1 and IL-15. Complex activation and translocation in the nucleus may be activated by several stimuli, such as growth factors and RTKs (EGFR and PDGFR) which activate, in turn, oncogenic pathways: RAS/MAPK pathway and PI3K/AKT which are primarily involved in the canonical activation of NF-kB, and STAT3, which is activated by IL-6 and phosphorylates p100 in the non-canonical pathway (*Besserès et al 2006; Nogueira et al 2011*). Recently *Nogueira et al (2011)* showed that NF-kB pathway is activated in GSCs under differentiation conditions: treatment with small molecule inhibitors promoted replication arrest and induce senescence by reduced levels of cyclinD1.

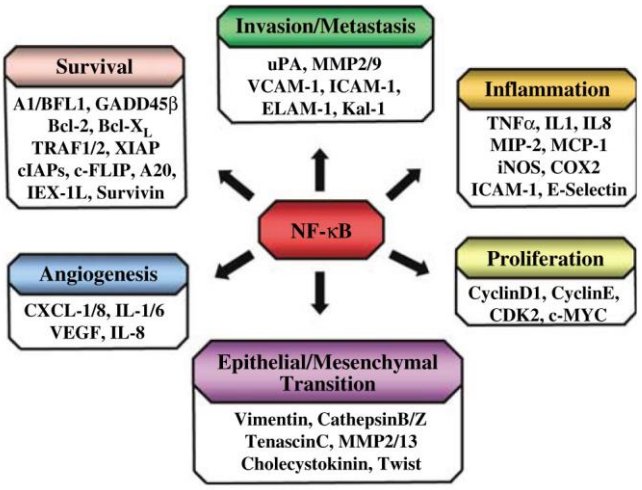

Figure 13. NF-kB-dependent targets involved in oncogenesis. *Adapted from Basserés et al 2006.*

NF-kB activity may be inhibited by different compounds such as: proteasome inhibitors which block IkB degradation; thalidomide which is an anti-infiammatory drug with anti-oncogenic properties; curcumin that has been shown to suppress selectively NF-kB activation; and several IKK inhibitors that specifically bind to IKK family preventing the IkB phosphorylation (*Basserès et al 2006; Zanotto-Filho et al 2011*).

***EGFR* amplification and EGFRvIII in GBMs.** The epidermal growth factor receptor (EGFR) induces proliferation and has a trophic effect on multiple cell types: it's expressed at high levels in various type of cancers including gliomas and actually *EGFR* gene amplification and overexpression are hallmark of GBM and are very

rare in low grade gliomas. The most common EGFR mutant is named EGFRvIII and is generated from a deletion of exons 2 to 7, which results in an in-frame deletion of 267 aminoacids from the extracellular domain of the receptor: EGFRvIII is therefore unable to bind ligand but it signals constitutively (*Hatanpaa et al 2010*).

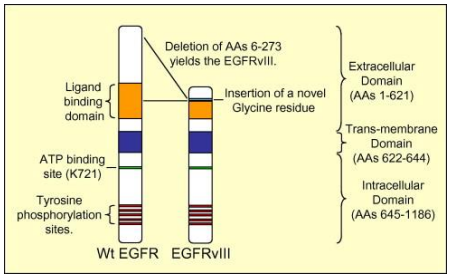

Figure 14. Schematic structure of EGFRvIII
Adapted from Gan et al 2009

EGFR amplification is present in 40% of primary GBMs and EGFRvIII is expressed in the 40% of the *EGFR* amplified tumors. Gene amplification is a hallmark of many cancers and it's visible at the metaphase as chromosomes with homogeneously staining regions or small acentric circular autonomously replicating double minutes (dmins). Dmins comprise in some cases two copies of the amplified sequences linked in inverted orientation; in other cases a single copy of a fragment appears to be circularized by simple ligation of its extremities. These circular molecules, then, are generated by chromosome breakage across replication bubbles or forks, or loops in the G1 or G2 phase. Cytogenetic studies have recurrently disclosed the presence of dmins in GBMs: notably up to 50% of glioblastomas contains *EGFR* dmins and they are generated by fusion of the two ends of a fragment through non-homologous end-joining pathway (NHEJ) (*Vogt et al 2004*); *EGFR* amplification, therefore, may be

easily distinguished from polisomy, which indeed interests the entire chromosome 7 and is also frequent in GBMs.

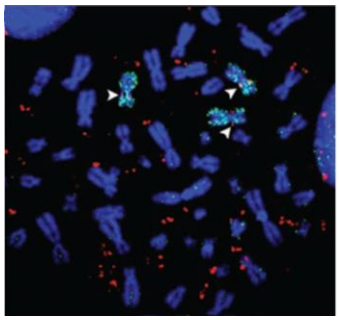

Figure 15. Chromosome 7 polisomy (arrows) and EGFR dmins (red dots). *Adapted from Vogt et al 2004*

Usually binding of the ligand to the wtEGFR results in a rapid internalization of the receptor, followed by dephosphorylation and degradation or recycling of the receptor. Expression of EGFRvIII results in a constitutive tyrosine phosphorylation and, because EGFRvIII doesn't bind EGF, its internalization is slowed, promoting a state of low-level continuous signalling from the activated receptors. In cells expressing EGFRvIII it was reported a constitutive activation of PI3K/Akt pathway and Ras. Besides EGFRvIII induces the expression of Heparin-binding growth factor (HB-EGF) and transforming growth factor α (TGFα): because it doesn't bind these ligands, their binding to wtEGFR generate an autocrine/paracrine loop with EGFRvIII. Finally, EGFRvIII cells contribute to the radioresistance of gliomas by promoting the repair of DNA double strands breaks (DSBs) via hyperactivation of DNA protein kinase of the NHEJ pathway (*Hatanpaa et al 2010*).

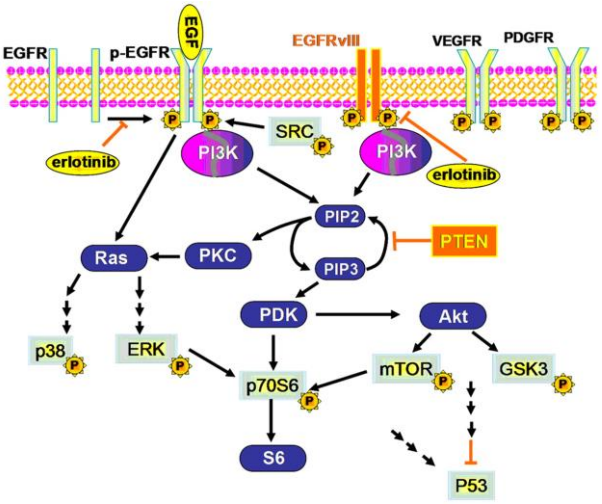

Figure 16. EGFR and EGFRvIII pathways. *Adapted from Shi et al 2012*

EGFR internalization is usually mediated by chlatrin-dependent endocytosis (CME), but *Sigismund et al (2008)* demonstrated that this pathway depends on EGF concentration: in condition of low EGF (1,5ng/ml) the major mechanism for internalization is CME and the receptor is targeted for recycling on the cell surface; in high EGF condition (10-20ng/ml) the internalization is mediated by non-chlatrin endocytosis (NCE), which targets the receptor mostly to degradation; so CME prolongs the duration of signalling, determining longevity of EGFR-mediated pathways and this event depends mostly on ligand concentration.

These results are very interesting, because usually *EGFR* amplification is not maintained in vitro conditions, where the concentration of the ligand in the culture medium is high (10ng/ml): so preclinical studies on EGFR as target are impeded in vitro conditions by the loss of its amplification (*Von Hoff et al 1991*).

Schulte et al (2012) generated paired cell lines from individual tumors supplemented or not with EGF ligand: cell lines in which EGF is omitted, maintained *EGFR* amplification, whereas it's rapidly lost in cultures supplemented with EGF; cell lines with high levels of *EGFR* amplification and co-expression of EGFRvIII formed also highly aggressive tumors in nude mice, whereas non-amplified cells grew significantly more slowly.

EGFR-targeted therapy is limited also by the co-activation of multiple RTKs: several studies showed intratumoral heterogeneity amplification of EGFR and PDGFRA that defines subpopolations with distinct response to growth factors and therefore GBM effective therapy may require combined regimens that target multiple RTKs (*Szerlip et al 2012; Stommel et al 2007*). Tumor heterogeneity is also characterized by different distribution of *EGFR* amplified cells and EGFRvIII mutant cells: *EGFR* amplification and rearrangement are widespread throughout the tumor including regions of no EGFRvIII presence, suggesting that exist mechanisms to modulate EGFRvIII expression, such as epigenetic regulation and this heterogeneity is also maintained in vitro conditions (*Del Vecchio et al 2012*). Enhancement and maintenance of tumor heterogeneity is also maintained by a paracrine model proposed by *Inda et al (2010)*: they showed that cells expressing EGFRvIII secrete elevated levels of IL-6 which promote the in vivo growth of cells with high levels of wtEGFR, maintaining the heterogenic composition of the tumor. IL-6 is a pro-inflammatory cytokine which is released in the micro-environment and bind to a heteromeric receptor on the membrane formed by the specific IL-6 binding receptor, IL6R, and common transducing receptor, gp130.

Upon receptor activation, intracellular signalling is propagated by Janus kinase family (JNK) which activate the signal transducers and activators of transcription family (STAT), in particular STAT3, which is phosphorylated at tyr105. Aberrant production and signalling of IL-6 is common in GBMs and linked to poor outcome and survival (*Wang et al 2009*). EGFRvIII cells release IL-6 in tumor micro-environment, which binds to IL6R/gp130 receptor on *EGFR* amplified cells: this binding activates signalling pathway through JAK and STAT3 and at the same time it is able to transactivate EGF receptor through phosphorylation leading an auto-activating loop (*Inda et al 2010*).

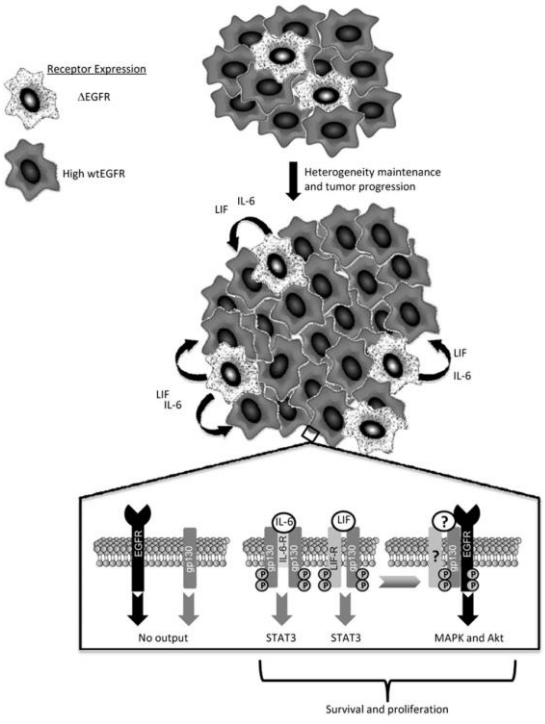

Figure 17. Model of paracrine-mediated tumor enhancement and maintenance of glioma heterogeneity. *Adapted from Inda et al 2010*

***EGFR* and NF-kB cross-talk in GBMs**. The first author that showed a relationship between *EGFR* and NF-kB pathways was Biswas in 2000 in estrogen receptor (ER) negative breast cancer cells: he showed that EGF mitogenic signal is able to activate NF-KB pathway through PI3K signalling, via PKC phosphorylation of IKK complex; NF-kB translocates in the nucleus and transactivates cyclinD1 gene causing tumor proliferation (*Biswas et al 2000*). The first paper that instead shows this cross-talk in GBMs lines was published in 2001: it demonstrated that EGFR was able to activate NF-kB inducing kinase (NIK); NIK is a specific kinase which phosphorylates IKKs that target specifically IkB and so promoting NF-kB activation and translocation into the nucleus (*Habib et al 2001*).

More recently *Bredel et al (2011)* demonstrated a correlation between NF-kB and EGFR status in GBMs: they analysed 790 human glioblastomas and found in almost 20% of them a heterozygous deletion of *NFKBIA* gene, which encodes for IkBα; this deletion is mutually exclusive with *EGFR* amplification and patients who had tumors with *NFKBIA* deletion had outcomes similar to patients with *EGFR* amplification. Restoration of the normal expression of *NFKBIA* in vitro attenuated this malignant phenotype and increased the vulnerability to chemotherapy: these observations suggested that *NFKBIA* may be considered as a tumor suppressor gene. Interestingly they found that *NFKBIA* deletion was more common in non-classical glioblastomas than in classical, mostly in proneural and mesenchymal subtypes. Finally they correlated *NFKBIA* expression with *MGMT* status: hypomethylated *MGMT* is usually linked to a poor response to

temozolomide, but patients with low *MGMT* methylation but high *NFKBIA* expression have a longer survival than low *NFKBIA* patients.

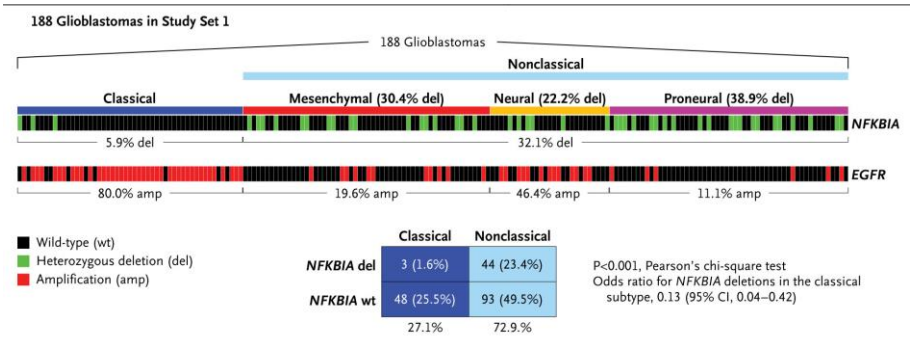

Figure 18. Gene- dosage profile of 188 glioblastomas studied by Bredel et al shows mutual exclusivity with EGFR amplification and the expression in the GBMs subtypes. *Adapted from Bredel et al 2011.*

In the same year also Tanaka showed a relationship between EGFR pathway and NF-kB: he demonstrated that EGFRvIII cells activate NF-kB through PI3K/Akt pathway via mTOR complexes; mTORC2 is able to phosphorylate IKK complex causing translocation in the nucleus of NF-kB and promoting tumor resistance to chemotherapy (*Tanaka et al 2011*).

SCOPE OF THE THESIS

In the past years it was made a very huge effort to understand the genetic and molecular signatures of glioblastoma in order to improve targeted molecular therapy: but to date several things remain still unclear and new markers or new relationships have to been disclosed. Our aim is, therefore, to better clarify genetic signatures and pathways' cross-talks in our glioblastoma-stem like cells model: actually we believe that these cells represent a real reservoir for the tumor of cells, which are able alone to maintain tumor growth, to give raise to a relapse and to determine radio- and chemo-resistance.

In chapter two we present a paper published in collaboration with our laboratory in 2012: in this study we found that the expression of *MET* oncogene was associated with a mesenchymal signature in our glioblastoma stem-like cells model and this expression is mutually exclusive with *EGFR* amplification; these cells also displayed different growth requirements *in vitro* and generated tumors with distinctive features *in vivo*; this suggested that *MET* could be a new target for therapy of a specific subset of GBMs (*De Bacco et al 2012*).

In chapter three we tried to better understand the possible cross-talk between EGFR and NF-kB signalling through a specific genetic signature disclosed in a precedent paper (*Bredel et al 2011*): a heterozygous deletion of *NFKBIA* gene, mutually exclusive with *EGFR* amplification. Surprisingly we found that this signature is a rare event in the primary tumor, but it is very frequent in our glioblastoma stem-like cells model in vitro and has also clear functional consequences. Our results raise the possibility that this

deletion may be amplified in vitro, favored by the presence of EGF, mostly in that lines in which EGFR pathway is predominant; furthermore in these cells seems to be favored the constitutive active mutant of *EGFR* gene, EGFRvIII, probably in order to preserve EGFR-NF-kB axis.

All these data suggest that our model is a much better system than serum-dependent cultures to study GBMs biology, bu at the same time various GSCs subgroups can be defined, that require both different factors to grow and also display different behaviours based on their genetic and molecular signatures.

REFERENCES

Bassères DS, Baldwin AS. *Nuclear factor-kappaB and inhibitor of kappaB kinase pathways in oncogenic initiation and progression.* Oncogene. **2006**;30:6817-30

Beroukhim R, Getz G, Nghiemphu L, Barretina J, Hsueh T, Linhart D, Vivanco I, Lee JC, Huang JH, Alexander S, Du J, Kau T, Thomas RK, Shah K, Soto H, Perner S, Prensner J, Debiasi RM, Demichelis F, Hatton C, Rubin MA, Garraway LA, Nelson SF, Liau L, Mischel PS, Cloughesy TF, Meyerson M, Golub TA, Lander ES, Mellinghoff IK, Sellers WR. *Assessing the significance of chromosomal aberrations in cancer: methodology and application to glioma.* Proc Natl Acad Sci U S A. **2007**;104:20007-12

Beroukhim R, Mermel CH, Porter D, Wei G, Raychaudhuri S, Donovan J, Barretina J, Boehm JS, Dobson J, Urashima M, Mc Henry KT, Pinchback RM, Ligon AH, Cho YJ, Haery L, Greulich H, Reich M, Winckler W, Lawrence MS, Weir BA, Tanaka KE, Chiang DY, Bass AJ, Loo A, Hoffman C, Prensner J, Liefeld T, Gao Q, Yecies D, Signoretti S, Maher E, Kaye FJ, Sasaki H, Tepper JE, Fletcher JA, Tabernero J, Baselga J, Tsao MS, Demichelis F, Rubin MA, Janne PA, Daly MJ, Nucera C, Levine RL, Ebert BL, Gabriel S, Rustgi AK, Antonescu CR, Ladanyi M, Letai A, Garraway LA, Loda M, Beer DG, True LD, Okamoto A, Pomeroy SL, Singer S, Golub TR, Lander ES, Getz G, Sellers WR, Meyerson M. *The landscape of somatic copy-number alteration across human cancers.* Nature. **2010**;463:899-905

Biswas DK, Cruz AP, Gansberger E, Pardee AB. *Epidermal growth factor-induced nuclear factor kappa B activation: A major pathway of cell-cycle progression in estrogen-receptor negative breast cancer cells.* Proc Natl Acad Sci U S A. **2000**;97:8542-7

Bredel M, Scholtens DM, Yadav AK, Alvarez AA, Renfrow JJ, Chandler JP, Yu IL, Carro MS, Dai F, Tagge MJ, Ferrarese R, Bredel C, Phillips HS, Lukac PJ, Robe PA, Weyerbrock A, Vogel H, Dubner S, Mobley B, He X, Scheck AC, Sikic BI, Aldape KD, Chakravarti A, Harsh GR 4th. *NFKBIA deletion in glioblastomas.* N Engl J Med. **2011**;364:627-37

Brennan C, Momota H, Hambardzumyan D, Ozawa T, Tandon A, Pedraza A, Holland E. *Glioblastoma subclasses can be defined by activity among signal transduction pathways and associated genomic alterations.* PLoS One. **2009**;4:7752

Brown KD, Claudio E, Siebenlist U. *The roles of the classical and alternative nuclear factor-kappaB pathways: potential implications for autoimmunity and rheumatoid arthritis.* Arthritis Res Ther. **2008**;10:212

Cancer Genome Atlas Research Network. *Comprehensive genomic characterization defines human glioblastoma genes and core pathways.* Nature. **2008**;455:1061-8

De Bacco F, Casanova E, Medico E, Pellegatta S, Orzan F, Albano R, Luraghi P, Reato G, D'Ambrosio A, Porrati P, Patanè M, Maderna E, Pollo B, Comoglio PM, Finocchiaro G, Boccaccio C. *The MET oncogene is a functional marker of a glioblastoma stem cell subtype.* Cancer Res. **2012**;72:4537-50

Del Vecchio CA, Giacomini CP, Vogel H, Jensen KC, Florio T, Merlo A, Pollack JR, Wong AJ.*EGFRvIII gene rearrangement is an early event in glioblastoma tumorigenesis and expression defines a hierarchy modulated by epigenetic mechanisms*. Oncogene. **2012**

Dunn GP, Rinne ML, Wykosky J, Genovese G, Quayle SN, Dunn IF, Agarwalla PK, Chheda MG, Campos B, Wang A, Brennan C, Ligon KL, Furnari F, Cavenee WK, Depinho RA, Chin L, Hahn WC. *Emerging insights into the molecular and cellular basis of glioblastoma.* Genes Dev. **2012**;26:756-84

Ekstrand AJ, James CD, Cavenee WK, Seliger B, Pettersson RF, Collins VP. *Genes for epidermal growth factor receptor, transforming growth factor alpha, and epidermal growth factor and their expression in human gliomas in vivo.*
Cancer Res. **1991**;51:2164-72

Furnari FB, Fenton T, Bachoo RM, Mukasa A, Stommel JM, Stegh A, Hahn WC, Ligon KL, Louis DN, Brennan C, Chin L, DePinho RA, Cavenee WK. *Malignant astrocytic glioma: genetics, biology, and paths to treatment.* Genes Dev. **2007**;21:2683-710

Galli R, Binda E, Orfanelli U, Cipelletti B, Gritti A, De Vitis S, Fiocco R, Foroni C, Dimeco F, Vescovi A *Isolation and characterization of tumorigenic, stem-like neural precursors from human glioblastoma.* Cancer Res. **2004**;64:7011-21

Gan HK, Kaye AH, Luwor RB. *The EGFRvIII variant in glioblastoma multiforme.* J Clin Neurosci. 2009;16:748-54

Guha A, Feldkamp MM, Lau N, Boss G, Pawson A. *Proliferation of human malignant astrocytomas is dependent on Ras activation.*
Oncogene. **1997**;15:2755-65

Habib AA, Chatterjee S, Park SK, Ratan RR, Lefebvre S, Vartanian T *The epidermal growth factor receptor engages receptor interacting protein and nuclear factor-kappa B (NF-kappa B)-inducing kinase to activate NF-kappa B. Identification of a novel receptor-tyrosine kinase signalosome.*
J Biol Chem. **2001**;276:8865-74

Hatanpaa KJ, Burma S, Zhao D, Habib AA. *Epidermal growth factor receptor in glioma: signal transduction, neuropathology, imaging, and radioresistance.* Neoplasia. **2010**;12:675-84

Hegi ME, Diserens AC, Gorlia T, Hamou MF, de Tribolet N, Weller M, Kros JM, Hainfellner JA, Mason W, Mariani L, Bromberg JE, Hau P, Mirimanoff RO, Cairncross JG, Janzer RC, Stupp R. *MGMT gene silencing and benefit from temozolomide in glioblastoma.* N Engl J Med. **2005**;352:997-1003

Heimberger AB, Hlatky R, Suki D, Yang D, Weinberg J, Gilbert M, Sawaya R, Aldape K. *Prognostic effect of epidermal growth factor receptor and EGFRvIII in glioblastoma multiforme patients.* Clin Cancer Res. **2005**;11:1462-6

Henson JW, Schnitker BL, Correa KM, von Deimling A, Fassbender F, Xu HJ, Benedict WF, Yandell DW, Louis DN. *The retinoblastoma gene is involved in malignant progression of astrocytomas.* Ann Neurol. **1994**;36:714-21

Huse JT, Holland EC. *Targeting brain cancer: advances in the molecular pathology of malignant glioma and medulloblastoma.* Nat Rev Cancer. **2010**;10:319-31

Jen J, Harper JW, Bigner SH, Bigner DD, Papadopoulos N, Markowitz S, Willson JK, Kinzler KW, Vogelstein B. *Deletion of p16 and p15 genes in brain tumors*. Cancer Res. **1994**;54:6353-8

Kong DS, Song SY, Kim DH, Joo KM, Yoo JS, Koh JS, Dong SM, Suh YL, Lee JI, Park K, Kim JH, Nam DH. *Prognostic significance of c-Met expression in glioblastomas.* Cancer. **2009**;115:140-8

Inda MM, Bonavia R, Mukasa A, Narita Y, Sah DW, Vandenberg S, Brennan C, Johns TG, Bachoo R, Hadwiger P, Tan P, Depinho RA, Cavenee W, Furnari F. *Tumor heterogeneity is an active process maintained by a mutant EGFR-induced cytokine circuit in glioblastoma.* Genes Dev. **2010**;24:1731-45

Li J, Yen C, Liaw D, Podsypanina K, Bose S, Wang SI, Puc J, Miliaresis C, Rodgers L, McCombie R, Bigner SH, Giovanella BC, Ittmann M, Tycko B, Hibshoosh H, Wigler MH, Parsons R. *PTEN, a putative protein tyrosine phosphatase gene mutated in human brain, breast, and prostate cancer.* Science. **1997**;275:1943-7

Li Z, Wang H, Eyler CE, Hjelmeland AB, Rich JN. *Turning cancer stem cells inside out: an exploration of glioma stem cell signaling pathways.* J Biol Chem. **2009**;284:16705-9

Libermann TA, Razon N, Bartal AD, Yarden Y, Schlessinger J, Soreq H. *Expression of epidermal growth factor receptors in human brain tumors.* Cancer Res. **1984**;44:753-60

Libermann TA, Nusbaum HR, Razon N, Kris R, Lax I, Soreq H, Whittle N, Waterfield MD, Ullrich A, Schlessinger J. *Amplification, enhanced expression and possible rearrangement of EGF receptor gene in primary human brain tumours of glial origin.* Nature. **1985**;313:144-7

Louis DN. *The p53 gene and protein in human brain tumors.* J Neuropathol Exp Neurol. **1994**;53:11-21

Nogueira L, Ruiz-Ontañon P, Vazquez-Barquero A, Lafarga M, Berciano MT, Aldaz B, Grande L, Casafont I, Segura V, Robles EF, Suarez D, Garcia LF, Martinez-Climent JA, Fernandez-Luna JL. *Blockade of the NFκB pathway drives differentiating glioblastoma-initiating cells into senescence both in vitro and in vivo.* Oncogene. **2011**;30:3537-48

Nogueira L, Ruiz-Ontañon P, Vazquez-Barquero A, Moris F, Fernandez-Luna JL. *The NFκB pathway: a therapeutic target in glioblastoma.* Oncotarget. **2011**;2:646-53

Phillips HS, Kharbanda S, Chen R, Forrest WF, Soriano RH, Wu TD, Misra A, Nigro JM, Colman H, Soroceanu L, Williams PM, Modrusan Z, Feuerstein BG, Aldape K *Molecular subclasses of high-grade glioma predict prognosis, delineate a pattern of disease progression, and resemble stages in neurogenesis.* Cancer Cell. **2006**;9:157-73

Pietsch T, Wiestler OD. *Molecular neuropathology of astrocytic brain tumors.* J Neurooncol. **1997**;35:211-22

Riemenschneider MJ, Reifenberger G. *Molecular neuropathology of gliomas.* Int J Mol Sci. **2009**;10:184-212

Riemenschneider MJ, Jeuken JW, Wesseling P, Reifenberger G. *Molecular diagnostics of gliomas: state of the art.* Acta Neuropathol. **2010**;120:567-84

Samuels Y, Wang Z, Bardelli A, Silliman N, Ptak J, Szabo S, Yan H, Gazdar A, Powell SM, Riggins GJ, Willson JK, Markowitz S, Kinzler KW, Vogelstein B, Velculescu VE. *High frequency of mutations of the PIK3CA gene in human cancers.* Science. **2004**;304:554

Sathornsumetee S, Reardon DA, Desjardins A, Quinn JA, Vredenburgh JJ, Rich JN. *Molecularly targeted therapy for malignant glioma.* Cancer. 2007;110:13-24

Shi Q, Qin L, Wei W, Geng F, Fan R, Shin YS, Guo D, Hood L, Mischel PS, Heath JR. *Single-cell proteomic chip for profiling intracellular signaling pathways in single tumor cells.* Proc Natl Acad Sci U S A. **2012**;109:419-24

Schulte A, Günther HS, Martens T, Zapf S, Riethdorf S, Wülfing C, Stoupiec M, Westphal M, Lamszus K. *Glioblastoma stem-like cell lines with either maintenance or loss of high-level EGFR amplification, generated via modulation of ligand concentration.* Clin Cancer Res. **2012**;18:1901-13

Sigismund S, Argenzio E, Tosoni D, Cavallaro E, Polo S, Di Fiore PP. *Clathrin-mediated internalization is essential for sustained EGFR signaling but dispensable for degradation.* Dev Cell. **2008**;15:209-19

Singh SK, Clarke ID, Hide T, Dirks PB. *Cancer stem cells in nervous system tumors.* Oncogene. **2004**;23:7267-73

Singh SK, Clarke ID, Terasaki M, Bonn VE, Hawkins C, Squire J, Dirks PB. *Identification of a cancer stem cell in human brain tumors.* Cancer Res**. 2003**;63:5821-8

Srivastava S, Zou ZQ, Pirollo K, Blattner W, Chang EH. *Germ-line transmission of a mutated p53 gene in a cancer-prone family with Li-Fraumeni syndrome.* Nature. **1990**;348:747-9

Stiver SI, Tan X, Brown LF, Hedley-Whyte ET, Dvorak HF. *VEGF-A angiogenesis induces a stable neovasculature in adult murine brain.* J Neuropathol Exp Neurol. **2004**;63:841-55

Stommel JM, Kimmelman AC, Ying H, Nabioullin R, Ponugoti AH, Wiedemeyer R, Stegh AH, Bradner JE, Ligon KL, Brennan C, Chin L, DePinho RA. *Coactivation of receptor tyrosine kinases affects the response of tumor cells to targeted therapies.*
Science. **2007**;318:287-90

Stupp R, Mason WP, van den Bent MJ, Weller M, Fisher B, Taphoorn MJ, Belanger K, Brandes AA, Marosi C, Bogdahn U, Curschmann J, Janzer RC, Ludwin SK, Gorlia T, Allgeier A, Lacombe D, Cairncross JG, Eisenhauer E, Mirimanoff RO; European Organisation for Research and Treatment of Cancer Brain Tumor and Radiotherapy Groups; National Cancer Institute of Canada Clinical Trials Group. *Radiotherapy plus concomitant and adjuvant temozolomide for glioblastoma.*
N Engl J Med. **2005**;352:987-96

Szerlip NJ, Pedraza A, Chakravarty D, Azim M, McGuire J, Fang Y, Ozawa T, Holland EC, Huse JT, Jhanwar S, Leversha MA, Mikkelsen T, Brennan CW. *Intratumoral heterogeneity of receptor tyrosine kinases EGFR and PDGFRA amplification in glioblastoma defines subpopulations with distinct growth factor response.*
Proc Natl Acad Sci U S A. **2012**;109:3041-6

Tanaka K, Babic I, Nathanson D, Akhavan D, Guo D, Gini B, Dang J, Zhu S, Yang H, De Jesus J, Amzajerdi AN, Zhang Y, Dibble CC, Dan H, Rinkenbaugh A, Yong WH, Vinters HV, Gera JF, Cavenee WK, Cloughesy TF, Manning BD, Baldwin AS, Mischel PS. *Oncogenic EGFR signaling activates an mTORC2-NF-κB pathway that promotes chemotherapy resistance.*
Cancer Discov. **2011**;1:524-38

Verhaak RG, Hoadley KA, Purdom E, Wang V, Qi Y, Wilkerson MD, Miller CR, Ding L, Golub T, Mesirov JP, Alexe G, Lawrence M, O'Kelly M, Tamayo P, Weir BA, Gabriel S, Winckler W, Gupta S, Jakkula L, Feiler HS, Hodgson JG, James CD, Sarkaria JN, Brennan C, Kahn A, Spellman PT, Wilson RK, Speed TP, Gray JW, Meyerson M, Getz G, Perou CM, Hayes DN; Cancer Genome Atlas Research Network. *Integrated genomic analysis identifies clinically relevant subtypes of glioblastoma characterized by abnormalities in PDGFRA, IDH1, EGFR, and NF1.*
Cancer Cell. **2010**;17:98-110

Vermeulen L, De Wilde G, Notebaert S, Vanden Berghe W, Haegeman G. *Regulation of the transcriptional activity of the nuclear factor-kappaB p65 subunit.* Biochem Pharmacol. **2002**;64:963-70

Vogt N, Lefèvre SH, Apiou F, Dutrillaux AM, Cör A, Leuraud P, Poupon MF, Dutrillaux B, Debatisse M, Malfoy B. *Molecular structure of double-minute chromosomes bearing amplified copies of the epidermal growth factor receptor gene in gliomas.*
Proc Natl Acad Sci U S A. **2004**;101:11368-73

Von Hoff DD, Waddelow T, Forseth B, Davidson K, Scott J, Wahl G. *Hydroxyurea accelerates loss of extrachromosomally amplified genes from tumor cells.* Cancer Res. 1991;51:6273-9

Wang H, Lathia JD, Wu Q, Wang J, Li Z, Heddleston JM, Eyler CE, Elderbroom J, Gallagher J, Schuschu J, MacSwords J, Cao Y, McLendon RE, Wang XF, Hjelmeland AB, Rich JN. *Targeting interleukin 6 signaling suppresses glioma stem cell survival and tumor growth.* Stem Cells. **2009**;27:2393-404

Wen PY, Kesari S. *Malignant gliomas in adults.*
N Engl J Med. **2008**;359:492-507

Wong AJ, Ruppert JM, Bigner SH, Grzeschik CH, Humphrey PA, Bigner DS, Vogelstein B. *Structural alterations of the epidermal growth factor receptor gene in human gliomas.*
Proc Natl Acad Sci U S A. **1992**;89:2965-9

Yan H, Parsons DW, Jin G, McLendon R, Rasheed BA, Yuan W, Kos I, Batinic-Haberle I, Jones S, Riggins GJ, Friedman H, Friedman A, Reardon D, Herndon J, Kinzler KW, Velculescu VE, Vogelstein B, Bigner DD. *IDH1 and IDH2 mutations in gliomas.*
N Engl J Med. **2009**;360:765-73

Zanotto-Filho A, Braganhol E, Schröder R, de Souza LH, Dalmolin RJ, Pasquali MA, Gelain DP, Battastini AM, Moreira JC. *NFκB inhibitors induce cell death in glioblastomas.*
Biochem Pharmacol. **2011**;81:412-24

CHAPTER II

The *MET* oncogene is a functional marker of a glioblastoma stem cell subtype

The MET oncogene is a functional marker of a glioblastoma stem cell subtype

*Francesca De Bacco[1], Elena Casanova[1], Enzo Medico[1], Serena Pellegatta[2,4], Francesca Orzan[1], Raffaella Albano[1], Paolo Luraghi[1], Gigliola Reato[1], Antonio D'Ambrosio[1], Paola Porrati[2], **Monica Patanè[2]**, Emanuela Maderna[3], Bianca Pollo[3], Paolo M. Comoglio[1], Gaetano Finocchiaro[2,4] and Carla Boccaccio[1]*

[1]IRCC - Institute for Cancer Research @ Candiolo, Center for Experimental Clinical Molecular Oncology, University of Turin Medical School, Candiolo, Italy

[2]Unit of Molecular Neuro-Oncology, [3]Unit of Neuropathology, Fondazione I.R.C.C.S. Istituto Neurologico C. Besta, Milan, Italy

[4]Department of Experimental Oncology, IFOM-IEO Campus, Milan, Italy

Cancer Res. 2012;72:4537-50.

Summary

The existence of treatment-resistant cancer stem cells contributes to the aggressive phenotype of glioblastoma. However, the molecular alterations that drive stem cell proliferation in these tumors remain unknown. In this study, we found that expression of the MET oncogene was associated with neurospheres expressing the gene signature of mesenchymal and proneural subtypes of glioblastoma. Met expression was almost absent from neurospheres expressing the signature of the classical subtype, and was mutually exclusive with amplification and expression of the epidermal growth factor receptor (EGFR) gene. Met-positive and Met-negative neurospheres displayed distinct growth factor requirements, differentiated along divergent pathways, and generated tumors with distinctive features. The Met^{high} subpopulation within Met-pos neurospheres displayed clonogenic

potential and long-term self-renewal ability *in vitro*, and enhanced growth kinetics *in vivo*. In Met^{high} cells, the Met ligand HGF further sustained proliferation, clonogenicity, expression of self-renewal markers, migration, and invasion *in vitro*. Together, our findings suggest that Met is a functional marker of glioblastoma stem cells and a candidate target for identification and therapy of a subset of glioblastomas.

Introduction

Glioblastoma, the highest grade glioma variant, is a relatively rare (yearly incidence of 4-5/100,000 people) but very aggressive tumor, associated with high morbidity, mortality and recurrence (median survival of 12-15 months) (1). These meager treatment options prompted a huge effort to achieve comprehensive profiling of gene expression patterns and genetic alterations (2-6), in order to identify molecular targets for innovative - possibly personalized - therapies. By expression profiling, three main glioblastoma subtypes have been recognized: “classical”, “mesenchymal”, and “neural/proneural” (here proneural) (6). The classical subtype mostly displays alterations of the EGFR gene, such as amplification or deletion of the extracellular domain ($EGFR^{vIII}$) (6). The mesenchymal subtype often harbors a normal EGFR gene, and deletion of NF1 or PTEN tumor suppressor genes (6). The proneural subtype preferentially associates with mutations of isocitrate dehydrogenase 1 (IDH1) or 2 (IDH2), or aberrant activation of PDGFRA, resulting from gene amplification/mutation, or occurrence of autocrine loops. This subtype, often evolving from lower grade gliomas, may associate with

a more favorable prognosis, but does not benefit of current therapies (6,7).

To understand glioblastoma pathogenesis it is crucial to identify the driving genetic lesions, and to recognize that glioblastoma onset and progression depend on a (small) subpopulation of "cancer stem cells" (CSCs), which, according to an operational definition, hold replicative immortality *in vitro* and tumor-initiating potential when transplanted *in vivo* (8,9). Despite the controversy arising on the ultimate, elusive nature of these cells, convincing evidence indicates that CSCs possess inherent radio- and chemoresistance, a major cause of treatment failure and disease recurrence (10,11). To envisage new therapeutical strategies, genetic and molecular alterations occurring in glioblastoma stem cells must be identified. Therefore we investigated whether the molecular alterations detectable in the clinically manifest glioblastoma were present in the tumor-initiating subset, allowing classification in subtypes already at the CSC level. From primary glioblastoma tissues, we isolated and propagated extensively self-renewing neurospheres, *i.e*. cultures enriched in stem and progenitor cells (12). These neurospheres displayed mutational profiles largely overlapping with those of the original tumors, and could be classified as classical, mesenchymal or proneural, according to their gene expression profile. We then specifically associated expression of the MET oncogene with mesenchymal and proneural neurospheres, and we showed that Met signaling actively supported the stem-like and invasive phenotype.

Materials and Methods

Neurosphere derivation from patients' specimens and inclusion in the study.

Neurospheres were generated at the Fondazione IRCCS Istituto Neurologico C. Besta starting from tissue samples provided by Surgical Departments. Starting from 269 independent glioblastomas, including primary and recurrent glioblastomas,neurospheres were derived with an overall efficiency of about 45%, with no significant differences between primary and recurrent. No correlation between overallsurvival, age, performance score, EGFR amplification, IDH1 mutation of the tumor, and the ability to form neurospheres was observed. The 18 neurospheres included in this study were randomly chosen among those derived from tumors defined, by clinical and histopathological criteria, as "primary glioblastoma" according to WorldHealth Organization criteria 2007.

Neurospheres derivation, culture, and transfection

Neurospheres were derived by mechanical dissociation and digestion of tumor specimens with collagenase type I (Life Technologies-Invitrogen). Single cell suspensions were plated at clonal density (50 cells/μl) in standard medium containing: DMEM/F-12 (Life Technologies-GIBCO), 2mM glutamine (Sigma), penicillin-streptomycin (1:100, EuroClone), B-27 (1:50, Life Technologies-GIBCO), human recombinant fibroblast growth factor 2 (bFGF, 20ng/ml; Peprotech) and epidermal growth factor (EGF, 20ng/ml; Peprotech). Neurospheres were mechanically dissociated when equal

100-150μm in diameter. When indicated, human recombinant hepatocyte growth factor (HGF, 20ng/ml; Peprotech) was added at the indicated time point to the standard medium. To assess neurospheres multipotency, single cell suspensions were plated in pro-adhesive flasks in DMEM/F-12 containing 2mM glutamine, penicillin-streptomycin, B-27 and 1 to 10% of fetal bovine serum (Lonza). To assess the role of Met in invasion assay, a plasmid containing Met full transcript twas electroporated in Met-neg-NS using the Cell line Nucleofector Kit V and Nucleofector II machine (Amaxa Biosystems) according to manufacturer's instructions, and invasion assay was performed after 48 h.

Evaluation of tumorigenicity

To evaluate tumorigenicity of neurospheres and their sorted Metpos and Met neg subpopulation, dissociated cells were injected ortothopically or subcutaneously into 6-weeks old male NOD.CB17-Prkdcscid/J mice (Charles River Laboratories), according to protocols approved by the Italian Ministry of Health and by the internal Ethical Committee for Animal Experimentation (FPRC-CESA). For ortothopic transplantation, 2μl of a 5×10^7 cells/ml suspension in PBS were delivered into the caudate/putamen nuclei by stereotactic injection (coordinates used were as follows: antero-posterior = 0; medio-lateral = + 2.5mm; dorso-ventral = − 3.5mm). Mice were monitored daily and sacrificed by anesthesia (zoletil 40mg/kg + xylazine 7.5mg/kg) followed by carbon dioxide inhalation when they showed signs of suffering. For subcutaneous transplantation, 10^5 cells were resuspended in v/v PBS/Matrigel (BD Biosciences) and injected

into the right flank. Tumor diameters were measured every 5 days with a caliper, and tumor volume was calculated using the formula: $4/3\pi \times (d/2)^2 \times (D/2)$, where d and D are the minor and major tumor axis respectively.

Immunohistochemical staining

Histological sections from human or xenograft tumors were obtained according to standard methods, and stained with the following antibodies: anti-human mouse monoclonal EGFR (Neomarkers, 1:50), mouse monoclonal p53 (Dako, 1:50), and goat polyclonal YKL-40 (Santa Cruz Biotecnhology, 1:50), rabbit polyclonal Met (C-12, Santa Cruz Biothecnology, 1:100), rabbit polyclonal GalC (Santa CruzBiothecnology, 1:100), goat polyclonal GFAP (Santa Cruz Biothecnology, 1:100), mouse monoclonal Nestin (Santa Cruz Biotecnhology, 1:100), mouse monoclonal Ki- 67 (MIB-1; Dako, 1:200). Immunoreactivity was visualized with DAB (Liquid DAB Substrate Chromogen System, DakoCytomation Carpinteria), and sections were counterstained (H&E). Slides from original tumors were read independently by E.M. and B.P.; from xenograft tumors by F.D.B. and A.D.A.. Tumors were categorized as positive when they exhibited a moderate to strong plasma membrane and/or cytoplasmic staining in the majority of tumor cells, which was easily visible with a low-power objective. Staining intensity was evaluated semi-quantitatively using the following scale: 3+, intensive positive; 2+, positive; 1+, focally positive; 0, no staining.

Nucleic acid extraction

From both primary glioblastoma specimens and established neurospheres, nucleic acids were extracted as follow: genomic DNA (gDNA) using the Wizard® Genomic DNA Purification kit (Promega); total RNA using the mRNeasy Mini kit (Qiagen); and microRNA using the miRNeasy Mini kit (Qiagen), according to the manufacturer's instructions. When indicated, commercial human total brain RNA (Ambion) was used.

Gene copy number evaluation

EGFR, PDGFRA and MET gene amplifications was assessed in gDNA with real-time PCR, using TaqMan® Copy Number Assays (Applied Biosystems) and the ABI PRISM 7900HT sequence detection system (Applied Biosystems). Relative gene copy number data were calculated by normalizing against endogenous controls (TERT GREB1 and RNaseP). A normal diploid human gDNA was used as calibrator to obtain the ΔΔCt. The copy number of each gene was calculated with the formula $2 \times 2^{-\Delta\Delta Ct}$. To discriminate between real EGFR or MET amplification and polysomy of the chromosome harboring the two genes (chr7), the calculated copy number was normalized against the copy number of another gene mapped on chr7, and usually not amplified (HGF). We defined true amplification only when the ratio EGFR/HGF or MET/HGF was > 3. Reported values are the mean ± SEM of two independent experiments in triplicate.

EGFRvIII evaluation

To evaluate EGFR deletion (EGFRvIII), 500ng of purified RNA was reverse transcribed using High Capacity Reverse Transcriptase kit (Applied Biosystem) according to manufacturer's instructions. Amplification of full length EGFR and EGFRvIII was performed on cDNA using Platinum® Taq DNA Polymerase (Invitrogen) and specific primer pairs (Supplementary Table S7). PCR conditions were as follows: 95°C for 3 min; 40 × [95°C for 15 sec, 60°C for 30 sec, and 72°C for 30 sec]; and 72°C for 5 min. PCR products were analyzed onto a 2% agarose gel.

Gene sequencing

IDH1/2 (exon4), TP53, PTEN or MET purified gDNA was amplified using Platinum® Taq DNA Polymerase (Invitrogen) and specific primer pairs (Supplementary Table S7). NF1 was sequenced on mRNA according to (2). PCR conditions were as follows: 95°C for 3 min; 3 × [95°C for 15 sec, 64°C for 30 sec, and 70°C for 1 min]; 3 × [95°C for 15 sec, 61°C for 30 sec, and 70°C for 1 min]; 3 ×[95°C for 15 sec, 58°C for 30 sec, and 70°C for 1 min]; 37 × [95°C for 15 sec, 57°Cfor 30 sec, and 70°C for 1 min]; and 70°C for 5 min. PCR products were purified using ExoSAP-IT® (Affimetrix) according to manufacturer's instruction. Cycle sequencing was carried out using BigDye Terminator v3.1 Cycle Sequencing kit (Applied Biosystems). Sequencing products were purified using Agencourt CleanSeq(Agencourt Bioscience, Beckman Coulter) and analyzed on a 3730 DNA Analyzer ABI capillary electrophoresis system (Applied Biosystems). Sequences were then analyzed using Chromas Lite 2.01

software (http://www.technelysium.com.au/chromas_lite.html) and compared with reference sequences from the Homo sapiens assembly GRCh37 (February 2009). All identified mutations were than compared with those reported in the Catalogue Of Somatic Mutations In Cancer (COSMIC http://www.sanger.ac.uk/genetics/CGP/cosmic/).

Microarray analysis

For gene expression profiling, biotin-labeled cRNA was synthesized from 500ng of total RNA with the Illumina® TotalPrep RNA Amplification Kit according to manufacturer's instructions. The biotin-labeled cRNA was hybridized on Human HT-12 v4 BeadChip (Illumina), according to the manufacturer's instructions. The chip was labeled with streptavidin-Cy3 and the fluorescent signal was scanned with the Illumina BeadArray Reader. Raw data were summarized and cubic-spline normalized with the GenomeStudio software (Illumina). Data filtering, log(2) ratio transformation and mapping of published centroids were carried out with Excel (Microsoft). Clustering was performed with the GEDAS software (3). Data have been deposited in the GEO database, accession number GSE36426.

Quantitative Real-Time PCR

cDNA was obtained as described above. Real-time PCR was performed using primer and probe sets for MET, EGFR, FGFR2, Sox2, OLIG2, Nanog, EZH2, and CD133 (Applied Biosystems), with TaqMan PCR Master Mix (Applied Biosystems) and an ABI PRISM 7900HT sequence detection system (Applied Biosystems). Expression

levels were normalized against endogenous controls (β-actin and β2 microglobulin) and reported as 40-Ct. Where indicated fold increases with respect to control cells were shown. Reported values are the mean ± SEM of at least two independent experiments in triplicate.

MicroRNA quantification

RNA was reverse-transcribed with the Taqman MicroRNA reverse transcription kit and specific stem-loop primers for miR-34a, and miR-23b (Applied Biosystems), according to the manufacturer's instruction, and analyzed with ABI PRISM 7900HT sequence detection system (Applied Biosystems). Expression levels were normalized against endogenous control (RNU48) and reported as 40-Ct. Reported values are the mean ± SEM of two independent experiments in triplicate.

Immunophenotypical analysis and Fluorescence-activated cell sorting

Neurospheres were dissociated and incubated with the following antibodies (forantibodies dilution see Supplementary Table S8): EGFR-PE (clone EGFR.1,Invitrogen); HGF R/c-MET-PE or -APC (clone 95106, R&D System); CD133/2-PE(clone AC141, Miltenyi Biotec GmbH); Sox2-APC (clone 245610, R&D System); Nestin-APC (clone 196908, R&D System); CD15-APC (clone HI98, BioLegend); CD271-APC (clone ME20.4-1.H4, Miltenyi Biotec GmbH); CD44-FITC (clone MEM-85, Invitrogen); and CD29-FITC (clone TDM29, Millipore). For detection of intracellular markers, dissociated cells were previously fixed and permeabilized using

FIX & PERM® (Invitrogen), according to manufacturer's instructions. DAPI (Roche) was used to exclude dead cells. Analysis was performed on a CyAn ADP (Beckman Coulter) equipped with 488nM, 405nM and 642nM solid state lasers. Data were collected and processed using Summit 4.3 software (Beckman Coulter). For fluorescence-activated cell sorting, dissociated cells were stained with anti-HGF R/c-MET-PE antibodies (clone 95106, R&D Systems), and filtered with Filcons filters (50μm, BD Biosciences) to avoid aggregates. Cell sorting was performed on a MoFlo™ XDP nine-color cell sorter (Beckman Coulter). Sorted cells were collected in standard medium or HGF containing medium when indicated. Sorting purity was immediately controlled by CyAn ADP (Beckman Coulter).

Immunofluorescence analysis

For immunofluorescence analysis of differentiated neurospheres, cells underwent differentiation as described above. Differentiated cells were fixed with 3% paraformaldehyde, and stained with rabbit polyclonal MAP2 (Cell Signaling Technology, 1:50), rabbit polyclonal GalC (1:50), goat polyclonal GFAP (1:100), and mouse monoclonal O4 (anti-oligodendrocyte marker O4, Sigma, 1:50) antibodies. Cells were then stained with the appropriate secondary antibodies. Nuclei were counterstained with DAPI (Roche). For immunofluorescence analysis of neurospheres, cells were fixed with 3% paraformaldehyde, included with Shandon Cytoblock® kit (Thermo Scientific) and embedded in Killik (Bio-Optica). Frozen sections of 10μm were cut using a cryostat (Leica), stained with rabbit polyclonal anti-Met antibodies (C-12, Santa Cruz Biothecnology,

1:100), and treated as above. Images shown are representative of results obtained in at least three independent experiments.

Western blotting

Protein expression and phosphorylation were analyzed on whole-cell lysates, solubilized in boiling Laemmli buffer. Equal amounts of proteins were resolved by SDS-PAGE in reducing conditions and analyzed by western blotting with the following antibodies: rabbit polyclonal anti-GalC (Santa Cruz Biotechnology), goat polyclonal anti-GFAP (Santa Cruz Biotechnology), and mouse monoclonal anti-MET (DL21). For control of equal amount of protein loading, blots were stripped with Restore™ Western Blot stripping buffer (Thermo Scientific) according to manufacturer's instruction, and reprobed with mouse monoclonal anti-vinculin or goat polyclonal anti-actin antibodies (Santa Cruz Biothecnology). Antibodies were visualized with appropriate horseradish peroxidase-conjugated secondary antibodies (Amersham), and the enhanced chemi-luminescence system (ECL, Amersham). Blot images were captured using a molecular imager (GelDoc XR; Bio-Rad Laboratories). Western blots shown are representative of results obtained in at least three independent experiments.

Phosphoarray analysis

Neurospheres were grown in standard medium, and, when indicated, further stimulated with HGF for 24 h. Protein extracts (350μg) were analyzed with Phospho-RTK Array Kit or Human Phospho-Kinase Array Kit (R&D Systems) following manufacturer's instructions.

Densitometric analysis was performed with Quantity One 1-D (BioRad Laboratories).

Proliferation assay

An equal number of dissociated cells were plated at clonal density (10 cells/μl) in 96-well plates in a medium devoid of growth factors. 24 h after seeding (day 0), the indicated growth factors were added, and proliferation at day 0, 4 and 8 was measured by Cell Titer Glo™ (Promega) according to manufacturer's instruction, with GloMax 96 Microplate Luminometer (Promega). To assess neurospheres growth rate, proliferation in standard medium was measured every 2 days. The reported values are the mean of two independent experiments in quadruplicate.

Clonogenic assay and long-term propagation of clonal lines

Single Methigh or Metneg cells were sorted and directly seeded by MoFlo™ XDP ninecolor cell sorter (Beckman Coulter) into 96-well plates (1 cells/well) in standard medium or, where indicated, in medium containing HGF (20ng/ml) alone. Neurospheres were counted 14 days after seeding. To assess long-term propagation of clonal lines, sorted Met high or Met neg cells were plated at clonal density in standard medium. Once a week for 20 weeks, the formed neurospheres were dissociated, counted with trypan blue exclusion, and replated at clonal density. Reported values are the mean ± SEM of three independent experiments.

Cell cycle analysis

Cells were fixed in cold 70% ethanol (Sigma) overnight at -20°C. Samples were stained with a 50μg/ml propidium iodide and RNaseA solution (DNAcon3 kit Consul TS) for 3 h at 4°C, with kindly shaking. DNA content and cell cycle were analyzed by flow-cytometry (CyAn ADP, Beckman Coulter).

Migration and invasion assays

Cell migration and invasion assays were performed in Transwell chambers (Corning). For invasion assay, filters were coated with reconstituted Matrigel basement membrane (10μg/cm2). Dissociated cells (10^5 cells/transwell) were seeded on the upper side of the chamber in standard medium. HGF was added to the lower side of the chamber, and cells were incubated for 24 h at 37°C. In some experiments cells were treated with the anti-Met inhibitory antibody DN30-Fab (28μg/ml) or the small molecule kinase inhibitor JNJ-38877605 (500nM). Then, cells on the upper side of the filters were mechanically removed, and cells onto the lower side were fixed, and stained with crystal violet. For quantification, ten fields per experimental condition were randomly selected and micrographed with a 10× objective. Morphometric analysis was performed using MetaMorph 7.1 software (Molecular Devices). Reported values are the mean ± SEM of three independent experiments.

Statistical analysis

Numerical results were expressed as means ± standard error of the mean (SEM). Statistical significance was evaluated using two-tailed Student's t-tests, Fisher's exact tests or χ^2 tests. Multiple comparisons were performed using Bonferroni's correction. $p<0.05$ were considered statistically significant.

Results

Neurospheres harbor genetic lesions specific of glioblastoma subtypes

Eighteen neurospheres were randomly chosen from an ample panel of neurospheres derived from surgical specimens of primary glioblastomas (WHO grade IV) (13) (Table 1). Histological sections of the corresponding tumors were analyzed for mitotic index (invariably high, data not shown), EGFR and p53 expression (14), and traits associated with subtyping, including vascular stroma proliferation and YKL-40 expression (5) (Table 1 and Supplementary Fig. S1A).

Neurospheres and their corresponding tumors were analyzed for the presence of genetic alterations known occurring at high frequency in glioblastoma, such as amplification of EGFR ($EGFR^{amp}$), or deletion of its extracellular domain (exon 2-7, $EGFR^{vIII}$), amplification of PDGFRA, mutations of IDH1/2, TP53, PTEN, and NF1 (6,15) (Table 2; EGFR and PDGFRA gene copy number, and expression of $EGFR^{vIII}$ in Supplementary Fig. S1B,C; TP53, PTEN, and NF1 mutations in Supplementary Table S1).

Eight out of 18 neurospheres displayed EGFR amplification and/or deletion ($EGFR^{amp/vIII}$), a genetic trait preferentially associated with the "classical" glioblastoma subtype, while the remaining harbored a normal EGFR gene ($EGFR^{wt}$), usually found in either "mesenchymal" or "proneural" subtypes (6) (Table 2). No neurospheres displayed the genetic landmarks of the "proneural" subtype, such as PDGFRA amplification or autocrine loop, or IDH1/2 mutations (6) (Table 2 and data not shown). TP53, PTEN or NF1 alterations (mutations or deletions) were found in 9/18, 10/18, and 2/18 neurospheres, respectively (Table 2 and Supplementary Table S1). Mutations of TP53 and NF1 were shown to preferentially associate with $EGFR^{wt}$ glioblastomas (6). In our panel, however, only PTEN deletion/mutation was significantly associated with $EGFR^{wt}$ (for TP53, Fisher exact test, P = 0.637; for PTEN, P = 0.003; for NF1, P = 0.477).

Neurospheres displayed a mutational profile largely overlapping with the corresponding original tumors (Table 2). However, 5/13 neurospheres derived from $EGFR^{amp/vIII}$ tumors, lacked EGFR alterations (Table 2). Moreover, in the remaining $EGFR^{amp/vIII}$ neurospheres, the number of EGFR gene copies was decreased with respect to the corresponding original tumor (Supplementary Table S2). These findings are consistent with previous reports, indicating that *in vitro* culture selects against EGFR genetic lesions (16,17) (see Discussion).

Neurospheres can be classified as classical, mesenchymal or proneural according to gene expression profile

Next we performed genome-wide gene expression profiling of the whole neurosphere panel, and assessed whether they could be subdivided in classical, mesenchymal or proneural subgroups by the transcriptional signature identified in an independent set of glioblastoma tissues by Verhaak (6) (Fig. 1A and Supplementary Fig. S2). The classical, mesenchymal and proneural centroids (i.e. three virtual samples displaying average expression of each signature gene in, respectively, classical, mesenchymal and proneural glioblastomas) were extracted from the published datasets (http://tcga-data.nci.nig.gov/docs/publications/GB_exp), and mapped in the microarray, resulting in 549 probes, corresponding to 532 genes. The three centroids and the neurosphere samples were then hierarchically clustered by unsupervised analysis. The clustering sharply subdivided the neurospheres in three subgroups, including the classical, the mesenchymal and the proneural centroid, respectively (Fig. 1A and Supplementary Fig. S2).

By comparing neurosphere gene expression and mutational profiles, we observed that the majority (7/10) of neurospheres profiled as classical harbored EGFR gene amplification/deletion ($EGFR^{amp/vIII}$) (Fig. 1A). Interestingly, the 3/10 classical neurospheres without EGFR gene amplification displayed high chromosome 7 polisomy and, in two cases, derived from $EGFR^{amp/vIII}$ tumors (Table 2). On the contrary, 7/8 neurospheres profiled as mesenchymal or proneural harbored a normal EGFR gene ($EGFR^{wt}$) (Fig. 1A). Altogether, these data indicate a marked preferential association of $EGFR^{amp/vIII}$ with

classical compared to mesenchymal/proneural neurospheres (χ^2 test, P < 0.04). *Vice versa*, although not statistically significant, PTEN mutation/deletion was preferentially associated with mesenchymal/proneural compared to classical neurospheres (6/8 vs. 4/10 neurospheres, χ^2 test, P = 0.31) (Fig. 1A).

Classical and mesenchymal/proneural neurospheres are discriminated by EGFR or MET expression

Gene expression profiling and qPCR validation (Supplementary Fig. 3A-C), indicated that not only EGFR alteration, but also transcription, was preferentially associated with classical neurospheres (two-sided *t*-test, $p < 0.0001$). *Vice versa*, transcription of the MET gene, known to be expressed in a fraction (≅ 30%) of unclassified human gliomas (18,19), was preferentially associated with mesenchymal/proneural neurospheres (two-sided *t*-test, $p < 0.01$).

To further investigate the role of EGFR and Met as markers of classical and mesenchymal/proneural neurosphere subgroups respectively, we assessed by flow-cytometry the cell-surface expression of the two receptors in the whole neurosphere panel.

As expected, EGFR was detected in the majority (8/10) of classical neurospheres, but only in 2/8 mesenchymal/proneural neurospheres (Fig. 1B and Supplementary Table S3). *Vice versa*, Met was expressed by the majority (7/8) of mesenchymal/proneural neurospheres, with variable percentages of positive cells (5-94%), but only in 2/10 classical neurospheres (Fig. 1B and Supplementary Table S3). Therefore, EGFR protein expression was strongly preferentially associated with the classical neurosphere subgroup (χ^2 test, P <

0.001), while Met protein with the mesenchymal/proneural neurosphere subgroup (χ^2 test, P <0.02). Interestingly, Met expression (in the absence of any gene alteration) was detected in the majority of original tumors that generated neurospheres expressing Met, but was mostly absent from tumors that generated neurospheres not expressing Met, and which harbored EGFR amplification (Supplementary Table S4).

We then analyzed whether other cell-surface markers could be specifically associated with each neurosphere subgroup. CD133, previously used (20), and more recently questioned (21,22), as glioblastoma stem cell marker, was inconstantly expressed (0-90% of positive cells), without association with any subgroup (Fig. 1C-F and Supplementary Table S3). Also expression of Sox2, Nestin and CD15/SSEA1, three markers associated with the neural stem cell phenotype (23), did not display any statistically significant difference among the subgroups (Fig. 1C-F and Supplementary Table S3) (for Sox2, χ^2 test, P = 0.08; for Nestin, P = 0.09; for CD15, P = 0.314). Consistently, transcription of CD133 and Sox2, and other stem cell markers was comparable in all subgroups (Supplementary Fig. S3D). Finally, cell surface expression of CD44 (a gene of the mesenchymal signature, ref. 5,6), or CD271 and CD29 (two markers of "mesenchymal" differentiation of neural progenitors, ref. 24), was not preferentially associated with any subgroup (for CD44, χ^2 test, P = 0.304; for CD271, P = 0.982; for CD29, P = 0.766) (Fig. 1C-F and Supplementary Table S3).

Taken together, these data indicate that, in neurospheres, expression of EGFR and Met are almost mutually exclusive. By combined flow-

cytometric analysis, unlike other markers, the two receptors are sufficient to separate neurospheres in two subgroups: EGFR-pos/Met-neg-NS (hereafter indicated as Met-neg-NS), roughly corresponding to classical neurospheres, and EGFR-neg/Met-pos-NS (hereafter indicated as Met-pos-NS), roughly corresponding to mesenchymal/proneural neurospheres. Consistently, Met-pos-NS, unlike Met-neg-NS, were highly enriched in mesenchymal or proneural, but lacked classical signature genes (Fig. 1G-I). Strikingly, among all these signature genes, EGFR was, concomitantly, the most expressed in the classical subtype, and the least expressed in Met-pos-NS (Fig. 1G).

Met-pos and Met-neg neurosphere subgroups are identified by multiple transcriptional signatures

Neurosphere gene expression profiles were also analyzed by applying additional transcriptional signatures, including two identified in glioblastoma neurospheres (25,26), two in original tumors (5,27), and one in mixed tissues, neurospheres and cell lines (28) (Supplementary Fig. S4 and Supplementary Table S5). The five signatures were almost fully mapped in the microarrays, and hierarchically clusterized neurospheres. In all cases, Met-pos-NS and Met-neg-NS were sharply separated into distinct and homogeneous clusters. By applying the two-cluster signatures, the majority of Met-pos-NS fell into Cluster II (25), or Type II (26), or GSr/lines group (28), while the majority of Met-neg-NS fell into Cluster I (25), or Type I (26), or GSf/tumor group (28). By applying the multi-cluster signatures generated from

tumor tissues (5,27), Met-pos-NS fell into the most aggressive subgroups (Supplementary Fig. S4 and Supplementary Table S5).

Met-pos and Met-neg neurospheres display subtype-specific growth-factor requirements and differentiation patterns

We observed that Met-pos-NS and Met-neg-NS displayed distinctive microscopical features: Met-neg-NS mostly displayed a compact, smooth surface, while Met-pos-NS appeared as aggregates of cells with loose intercellular adhesion (Fig. 2A). Moreover, in standard medium, Met-pos-NS displayed a proliferative rate significantly higher than Met-neg-NS (Fig. 2B). We then systematically analyzed the proliferative response to EGF or bFGF, alone or in combination (Fig. 2C-E and Supplementary Fig. S5A). Met-neg-NS were mostly quiescent in the absence of growth factors (data not shown), and, with one exception, were markedly stimulated by EGF, but weakly by bFGF alone; the two growth factors were not significantly additive (Fig. 2C,E; median fold increase with EGF = 4.54, with bFGF = 1.45, Supplementary Fig. S5A). *Vice versa*, Met-pos-NS grew in the absence of exogenous growth factors (data not shown), and, with some exceptions, were further stimulated by bFGF, but not by EGF; again, the two factors were not additive (Fig. 2D,E; median fold increase with EGF = 0.94, with bFGF = 2.73, Supplementary Fig. S5A).

The ability of Met-pos-NS to proliferate in the absence of exogenous growth factors could be explained by expression of autocrine loops (data not shown). The different sensitivity of Met-neg-NS and Met-pos-NS to EGF was correlated with the different levels of EGFR

expression (Fig. 1B). Consistently, EGFR family members were found significantly phosphorylated, in the presence of EGF, only in Met-neg-NS (Supplementary Fig. S5C). The comparable sensitivity of both Met-neg and Met-pos neurospheres to bFGF correlated with similar expression and ligand-induced tyrosine phosphorylation of FGFR2, the main bFGF receptor (Supplementary Fig. S5B,C).

By culturing dissociated neurospheres in pro-differentiating conditions, Met-neg and Met-pos neurospheres displayed divergent differentiation patterns (Fig. 2F,G, Supplementary Fig. S5D, and data not shown). Met-neg-NS differentiated into neuro-astroglial lineages, as shown by upregulation of the neural marker MAP2 and the astroglial marker GFAP. No oligodendroglial cells were detected after staining with the specific GalC marker. On the contrary, Met-pos-NS differentiated into neuro-oligodendroglial but not into the astroglial lineage.

Finally, a panel of representative Met-neg and Met-pos neurospheres were orthotopically transplanted into immunocompromised mice. Between the two subgroups, no significant differences were reported in mouse survival (Fig. 2H and Supplementary Table S6), tumor proliferative index (Supplementary Table S6) or vascularization (data not shown). In no case, invasion of the contralateral brain hemisphere could be observed (data not shown). However, consistently with the differentiation pattern observed *in vitro*, tumors derived from Met-neg-NS invariably expressed high levels of GFAP, but not GalC. *Vice versa*, those derived from Met-pos-NS invariably expressed high levels of GalC, and traces of GFAP only at the tumor periphery (Fig. 2I, Supplementary Table S6, and data not shown).

The above data showed that, although selected and propagated in the same medium, Met-pos and Met-neg neurospheres have distinct, subtype-specific signaling requirements for proliferation and specific differentiation patterns both *in vitro* and *in vivo*. Altogether, these observations suggest that the corresponding tumors may have different cells of origin (see Discussion).

In Met-pos-NS the Met^{high} subpopulation is enriched with clonogenic and tumorigenic cells

Having established that Met is a marker of a biologically distinct neurosphere subtype, we investigated its functional role. By flow-cytometry (Supplementary Table S3 and Fig. 1B-E) and immunofluorescence (Fig. 3A and data not shown), we observed that Met expression was restricted to cell subpopulations of various extents, which, in some cases, expressed also high levels of stem-cell markers such as Sox2, Nestin, or CD133 (Fig. 3B and data not shown). We thus sorted the Met^{high} from the Met^{neg} subpopulation (for sorting parameters see Supplementary Fig. S6), and performed clonogenic assays by plating and culturing single cells in standard medium. In 9/9 Met-pos-NS, Met^{high} cells invariably displayed higher clonogenic ability as compared with Met^{neg} cells (Fig. 3C and data not shown). Moreover, neurospheres derived from Met^{high} cells maintained their clonogenic ability and differentiative multipotentiality through > 20 serial passages, while those derived from Met^{neg} cells arrested their growth within 3-8 passages (Supplementary Figure S7A, B). Cell cycle analysis of the representative neurospheres BT308 showed that, immediately after

sorting, the Met^{high} subpopulation contained a higher percentage of cells in the S phase (8.2% vs. 3.4%), and a lower percentage of apoptotic cells (3.4% vs. 20.7%), as compared with the Met^{neg} subpopulation (overlapping results were obtained with BT337, data not shown). In another set of experiments, Met^{high} and Met^{neg} cells were sorted, plated at clonal density, and cultured in standard medium. The secondary clones were analyzed by flow-cytometry for Met expression after 7 and 14 days; the clones formed by Met^{high} cells progressively reacquired the same Met immunophenotypic profile (including Met^{high} and Met^{neg}) as the parental neurospheres (Fig. 3D, Supplementary Fig. S7C, and data not shown). In contrast, neurospheres formed by Met^{neg} cells remained entirely composed of Met^{neg} cells.

To investigate the tumorigenicity of the two subpopulations, representative parental Met-pos-NS (BT308 and BT302), and their sorted Met^{high} or Met^{neg} subpopulations, were subcutaneously injected into immunocompromised mice. In the case of BT308, only the parental neurosphere and the Met^{high} subpopulation displayed the ability to form tumors, while, in the case of BT302, even the Met^{neg} subpopulation generated measurable tumors. However, in both cases, tumors formed by Met^{high} cells grew significantly more rapidly than those formed by the parental or its sorted Met^{neg} subpopulation (Fig. 3E). Interestingly, tumors derived by Met^{high} or unsorted cells had a similar histopathological aspect, featuring a mixture of small-rounded and spindle-shaped cells. By immunohistochemistry, the small-rounded cells were positive for Met expression, while spindle-shaped cells were negative. On the contrary, tumors derived by Met^{neg} cells

sorted from BT302 only contained uniform spindle-shaped cells negative for Met expression (Fig. 3F, Supplementary Fig. S8, and data not shown).

Taken together, these findings indicated that, unlike the Met^{neg} subpopulation, the Met^{high} retained long-term clonogenic properties *in vitro*, enhanced growth kinetics *in vivo*, and generated a heterogeneous progeny including Met^{high} and Met^{neg} cells, both *in vitro* and *in vivo*. While Met^{high} might correspond to stem-like cells, Met^{neg} likely correspond to more differentiated cells that exhaust their proliferative potential. Consistently, we observed that Met expression was downregulated when neurospheres (or the sorted Met^{high} subpopulations) were cultured in pro-differentiating conditions (Fig. 3G and Supplementary Fig. S7D). Concomitantly, upregulation of microRNA-34a and microRNA-23b, both targeting the MET transcript (29,30), was observed (Fig. 3H and data not shown). Interestingly, in neurospheres cultured in standard medium, the same microRNAs were more expressed in Met^{neg} than Met^{high} cells (Fig 3I and Supplementary Fig. S7E).

HGF sustains clonogenicity, expression of self-renewal markers, and cell invasion *in vitro*

Next we investigated whether HGF stimulated proliferation of Met-pos-NS, and their sorted Met^{high} and Met^{neg} subpopulations. When supplied to parental neurospheres as the sole growth factor, HGF displayed a negligible proliferative effect, if compared with bFGF (Fig. 4A and Supplementary Fig. S9A). However, in the sorted Met^{high} subpopulation, HGF significantly increased proliferation, although

less intensely than bFGF (two-fold vs. six-fold increase) (Fig. 4A and Supplementary Fig. S9A). As expected, HGF did not stimulate proliferation of Met^{neg} cells (Fig. 4A and Supplementary S9A) and Met-neg-NS (data not shown).

Moreover, HGF supported the clonogenic ability of Met^{high} cells, sorted as single cells from Met-pos-NS, and cultured in the presence or in the absence of HGF as the sole growth factor (Fig. 4B). Conversely, HGF did not stimulate neurosphere formation by Met^{neg} cells (Fig. 4B). Accordingly, in Met-pos-NS, addition of HGF significantly increased the number of $Sox2^{pos}$ or $Nestin^{pos}$ cells (Fig. 4C and Supplementary Fig. S9B), and transcription of self-renewal markers Sox2, Nanog, CD133, and EZH2 (Fig. 4D and Supplementary Fig. S9C), as compared with standard medium. Taken together, these data indicated that HGF sustains the stem-like phenotype of Met-pos-NS.

Met signaling has been associated with induction of epithelial-mesenchymal transition, and the "invasive growth" program (31-33). We thus investigated whether HGF supported the invasive properties of neurospheres. In transwell assays, addition of HGF to standard medium strikingly enhanced migration and invasion of Met-pos-NS (Fig. 5A,B and data not shown). This effect was completely abolished by specific Met inhibitors, including the Fab fragment of the anti-Met antibody DN30 (34) (Fig. 5C), or the specific tyrosine kinase inhibitor JNJ-38877605 (35) (Supplementary Fig. S9D). As expected, HGF did not increase migration or invasion of Met-neg-NS (Fig. 5A,B). In these cells, transfection of Met did not promote invasiveness *per se*, but conferred the ability to respond to HGF (Fig. 5D).

Analysis of intracellular phosphoprotein arrays, showed that, in Met-pos-NS, HGF induced phosphorylation of signal transducers known to control cell invasion, such as JNK, MEK 1/2, several members of Src and STAT families, and p27 (33) (Fig. 5E). Interestingly, the latter was phosphorylated at a residue (T157) that promotes cytoplasmic localization and activation of the cell migratory machinery (36). We also observed decreased phosphorylation of p53 at residues Ser15, Ser46 and Ser392, which results in p53 inhibition (37).

Taken together, these results show that Met activation by HGF concomitantly supports the stem-like and the invasive phenotype of Met-pos-NS *in vitro*, and suggest that this mechanism may promote aggressiveness of a subset of glioblastomas.

Discussion

A unifying model of tumor onset and progression that integrates the "CSC model" and the "Darwinian model" assumes that CSCs accumulate the driving genetic lesions, and transmit them to the genetically and phenotypically heterogeneous progeny forming the tumor bulk (38). The comparative analysis reported in this paper showed that, as a rule, the same mutations of primary glioblastomas are found in their matched neurospheres. This confirms that neurospheres are a faithful *in vitro* model of the original tumor, useful to dissect the relationship between genetics and biology, and to predict the therapeutical response.

Notably, neurospheres derived from $EGFR^{amp/vIII}$ tumors displayed a decreased - or in a few cases an even normal - number of EGFR gene

copies, consistently with previous and recent data (16,17). As EGFR amplification is usually detected only in a fraction of glioblastoma cells (data not shown and ref. 39), these findings can be explained by *in vitro* negative selection of clones harboring EGFR amplification, and positive selection of clones with a normal EGFR gene, coexisting in the same tumor. Growth of clones with normal/low number of EGFR gene copies might be favored by concentrations of exogenous EGF (20 ng/ml), likely exceeding those in brain tissues (17).

Gene expression profiling allowed to classify the neurospheres into classical, mesenchymal and proneural subtypes according to the signatures identified in glioblastoma tissues by Verhaak (6). Interestingly, the classical subgroup encompassed the vast majority of neurospheres harboring EGFR amplification (7/10), confirming an association between the classical expression profile and EGFR genetic alteration already observed in tumors (6). *Vice versa*, the mesenchymal/proneural subgroup included neurospheres mostly harboring a wild-type EGFR gene (7/8) together with deletion/mutation of PTEN tumor suppressor gene (6/8). This association – to our knowledge - was still unreported in tumors or neurospheres.

EGFR is renowned as a prominent player of glioma biology (40), and tumorigenic potential of glioblastoma stem cells (41). However, we found that EGFR was highly expressed in classical neurospheres, consistently with the presence of gene amplification, but barely detectable in most mesenchymal/proneural neurospheres. In search for a functional marker for glioblastoma stem cells lacking EGFR, we considered the MET oncogene. Indeed, we noticed that MET was

listed among genes upregulated in microarrays of glioblastoma tissues, in association with the mesenchymal subtype (6). Moreover, recently, Met was shown to support the stem-like phenotype of unclassified glioblastoma neurospheres (42). The data presented in this paper show, for the first time, that Met expression is preferentially associated with the mesenchymal/proneural subtype of glioblastoma stem cells, and that expression of EGFR and Met are mutually exclusive in neurospheres and, possibly, in original tumors. If further studies will confirm that the cellular distribution of Met and EGFR in patients reflects that observed in neurospheres, there will be far-reaching implications for the molecular diagnostics of glioblastoma. Flow-cytometric or immunohistochemical analysis of the EGFR-Met pair could be proposed as a reliable test to discriminate between classical and mesenchymal/proneural glioblastoma, possibly in addition to previous criteria, such as YKL-40 expression (5).

Interestingly, the neurosphere subgroup expressing Met (Met-pos-NS), irrespectively of their mesenchymal or proneural profile, and the subgroup lacking Met (Met-neg-NS) displayed significant biological differences. They had a different proliferation rate, invariably higher in Met-pos-NS. In this respect, the two subgroups were reminiscent of those previously described (12). Interestingly, Met-pos-NS mostly proliferated even without growth factors, and, as expected, were insensitive to EGF, while Met-neg-NS depended on exogenous growth factor, mostly EGF. Moreover, the two neurosphere subgroups showed a divergent differentiation pattern, either *in vitro*, or in tumors formed by orthotopic transplantation: Met-pos-NS differentiated along the neuro-astroglial, while Met-neg-NS along the neuro-

oligodendroglial pathway. These findings seem consistent with observations in mouse model systems, where brain progenitors inheriting high levels of EGFR give rise to astrocytes, whereas those inheriting low levels generate oligodendrocytes (43).

Strikingly, the Met-pos and Met-neg neurosphere subgroups not only displayed distinct biological features, but were conserved according to five additional transcriptional classifiers, obtained in neurospheres or in original tumors (5,25-28). When two-cluster classifiers found in neurospheres by Gunther *et al*. (25) or Lottaz *et al*. (26) were applied, Met-neg-NS almost fully overlapped with Cluster I/Type I, while Met-pos-NS with Cluster II/Type II.

Taken together, biological and gene expression features of Met-pos and Met-neg neurospheres suggest that Met expression could associate with tumors deriving from different cells of origin. Met-neg-NS (and glioblastoma) could derive from stem or transit amplifying cells of the brain subventricular zone, which depend of EGFR signaling (8,44). Conversely, Met-pos-NS (and glioblastoma) could originate either from the subventricular progenitors inheriting low-levels of EGFR (43), or the diffuse astrocytes of the reactive glia. These cells reactivate their proliferative and regenerative potential in response to injuries (45). The reactive astrocytes are an appealing candidate as a glioblastoma cell of origin also because they are intermingled within the blood-brain barrier, and may be easily exposed to genotoxic agents.

Another novel finding presented in this study is that, in each Met-pos-NS, Met marks and functionally supports a cell subpopulation that retains long-term clonogenic and multi-potential ability *in vitro*, and

enhanced growth kinetics *in vivo*, and thus may retain cancer stem cell properties. Conversely, in Met-pos-NS, loss of Met expression characterizes a cell subpopulation that exhausts its clonogenic activity *in vitro* and *in vivo*. These data strongly suggest that Met is a glioblastoma stem cell marker, which can be proposed for cell isolation as an alternative to CD133.

A further new finding presented in this study indicates that Met supports not only the stem-like, but also the invasive phenotype, at least *in vitro*. Indeed, invasiveness of Met-pos-NS was significantly enhanced by the Met ligand HGF, a key driver of invasive growth (31), and counteracted by specific Met inhibitors. The Met ability to concomitantly support stemness and invasiveness shows that the two phenotypes are functionally associated, and driven by the same signaling circuits and genetic programs, consistently with previous observations (46).

It has been noticed that "the existence of molecularly defined subgroups of glioblastoma raises the question of whether these categories actually represent separate disease entities rather than the expression of minor variability in a single tumor class" (14). Our study suggests that primary glioblastomas contain distinct types of CSCs, each possibly arising from distinct cells of origin, each endowed with specific molecular markers and signaling circuits responsible for stem and tumorigenic properties. These findings contribute to identify separate glioblastoma entities, and to define criteria that might be exploited to guide therapeutic-decision making.

Acknowledgements

We thank Andrea Bertotti, Livio Trusolino, and Claudio Isella for critical discussion; Stefania Giove for histopathology; Daniela Gramaglia, Antonella Cignetto and Michela Bruno for secretarial assistance.

Grant Support

Italian Association for Cancer Research (Investigator Grants and "Special Program Molecular Clinical Oncology 5xMille, N. 9970"), Regione Piemonte (PI-STEM), European Union Framework Programs 7 (N. 201279 and 201640).

Tables and Figures

Table 1. Clinical and neuropathological data of primary glioblastoma (WHO grade IV)

patient code	Gender	Age	OS (weeks)	Location	EGFR	Nuclear p53	Vascular stroma proliferation	YKL-40
BT358	F	63	89	F dx	0	0	1+	2+
BT273	M	58	55	FTP dx	2+	2+	0	0
BT275	F	66	60	P dx	0	0	1+	0
BT373	M	63	60	F dx	0	1+	0	0
BT334	M	63	42	FT dx	1+	0	0	0
BT297	M	54	61	T sx	1+	0	0	3+
BT168	F	78	39	PO sx	1+	0	1+	1+
BT326	M	27	27	F sx	0	0	2+	2+
BT332	M	74	41	PO sx	1+	0	1+	1+
BT347	F	57	12	T sx	1+	1+	2+	0
BT337	M	63	76	FTP sx	0	0	0	0
BT328	M	54	78	F sx	n.a.	n.a.	n.a.	n.a.
BT299	M	49	31	TPO sx	0	0	1+	2+
BT379	M	73	12	FTP dx	0	0	1+	0
BT205	M	73	8	T dx	0	0	1+	2+
BT302	F	18	127*	FP dx	0	1+	2+	2+
BT308	M	76	22	T sx	0	1+	1+	1+
BT314	M	67	76	T sx	0	1+	1+	1+

NOTE: * alive January 2012; OS: overall survival (weeks); n.a.: not assessed. Immunohistochemistry scores: 3+, intensive positive; 2+, positive;1+, focally positive; 0, no staining.

Table 2. Genetic lesions in neurospheres (NS) and the corresponding original glioblastoma tissue specimens (T).

patient code	EGFR^{amp}(§)		EGFR^{vIII} (§)		PDGFRA^{amp}		IDH1/2^{mut}		TP53^{mut}(*)		PTEN^{mut} (*)		NF1^{mut}(*)	
	NS	T	NS	T	NS	T	NS	T	NS	T	NS	T	NS	T
BT358	+	+	+	+	-	-	-	-	-	-	-	-	-	n.a.
BT273	+	+	+	+	-	-	-	-	+	+	-	-	-	n.a.
BT275	+	+	-	+	-	-	-	-	+	+	-	-	-	n.a.
BT373	+	+	-	+	-	-	-	-	-	-	-	-	-	n.a.
BT334	+	+	+	+	-	-	-	-	-	n.a	-	n.a.	-	n.a.
BT297	+	+	-	-	-	-	-	-	-	-	-	-	-	n.a.
BT168	+	+	-	+	-	-	-	-	+	n.a	-	n.a.	-	n.a.
BT326	+	+	-	-	-	-	-	-	-	-	+	+	-	n.a.
*BT332	-^	+	-	+	-	-	-	-	-	-	+	+	-	n.a.
*BT347	-^	+	-	-	-	-	-	-	+	+	+	+	-	n.a.
*BT337	-	+	-	-	-	-	-	-	-	-	-	-	-	n.a.
*BT328	-	+	-	-	-	-	-	-	+	+	+	-	-	n.a.
BT299	-^	-	-	-	-	-	-	-	-	-	+	+	-	n.a.
*BT379	-	-^	-	+	-	-	-	-	+	+	+#	+#	+	n.a.
BT205	-^	-	-	-	-	-	-	-	+	-	+	-	+	n.a.
BT302	-	-	-	-	-	-	-	-	-	-	+	+	-	n.a.
BT308	-^	-^	-	-	-	-	-	-	+	+	+	+	-	n.a.
BT314	-	-	-	-	-	-	-	-	+	+	+	+	-	n.a.

NOTE: (§) analysis of EGFR$^{amp/vIII}$ is shown in Supplementary Figure S1 and reported in Supplementary Table S2; (*) detailed list of mutations is reported in Supplementary Table S1; + presence of genetic alterations; - absence of genetic alterations; ^ chr7 polysomy; # homozygous deletion; n.a. not assessed due to lack of material.

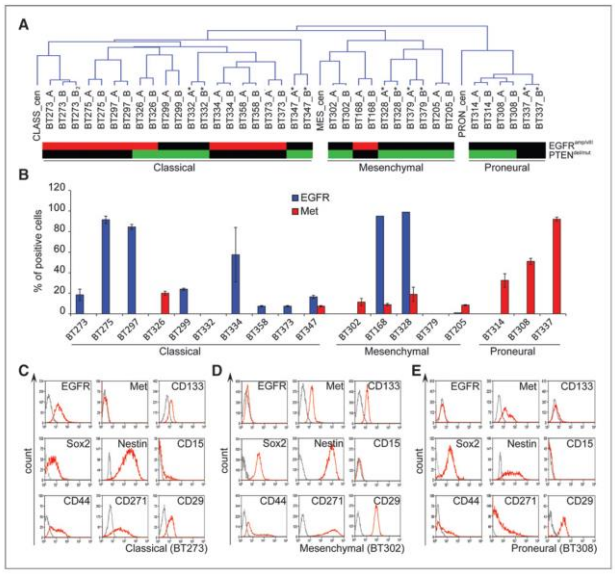

Figure 1. Neurospheres are classified according to gene expression profile, and display subtype-specific EGFR or Met expression. **A**, Unsupervised hierarchical clustering of duplicate neurosphere samples (A and B) and classical (CLASS_cen), mesenchymal (MES_cen) or proneural (PRON_cen) centroids. Red cells: amplification/mutation of EGFR ($EGFR^{amp/vIII}$); green cells: deletion/mutation of PTEN ($PTEN^{del/mut}$); black cells: no lesion. *: derived from tumors with $EGFR^{amp/vIII}$; $BT273\_B_2$: technical replicate. **B**, flow-cytometric detection of EGFR or Met in neurospheres. **C**-**E**, immunophenotype of neurospheres representative of each subtype.

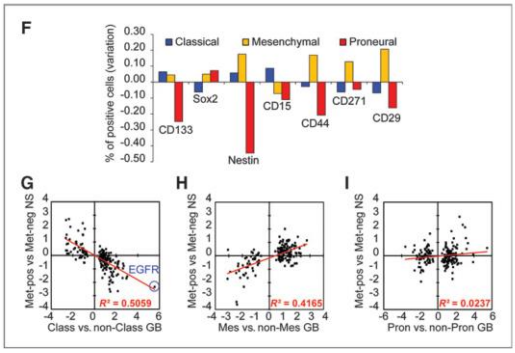

Figure 1. (continued) F, variation of the average number of cells positive for the indicated markers in each subtype with respect to all neurospheres (absolute numbers in Supplementary Table S3). **G-I**, relative expression of 532 signature genes (http://tcga-data.nci.nig.gov/docs/publications/GB_exp) (black dots). x-axis: log2 ratio between glioblastoma (GB) samples of each subtype vs. the other subtypes; y-axis: log2 ratio between Met-pos-NS and Met-neg-NS.

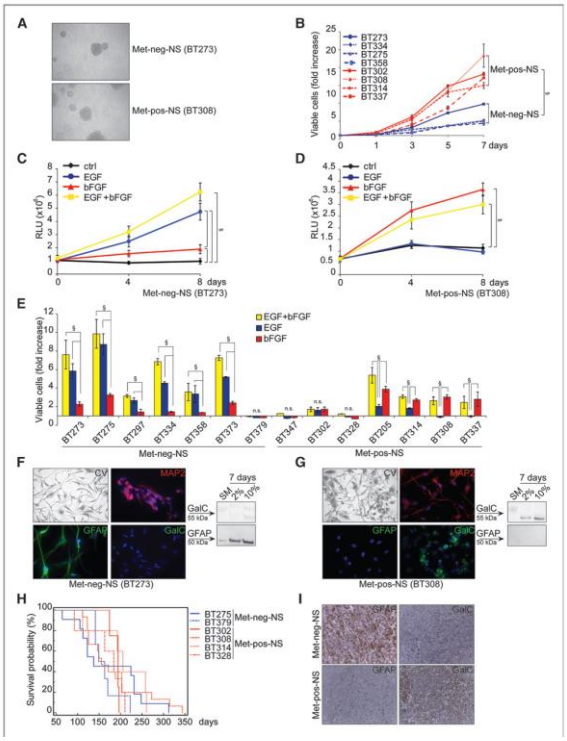

Figure 2. Met-neg-NS and Met-pos-NS display subtype-specific growth-factor requirements and differentiation patterns. **A**, representative micrographs (magnification, x100). **B**, proliferation in standard medium measured by Cell Titer Glo. Fold increase with respect to day 0. §: two-sided *t*-test, $p < 0.05$. **C-D**, proliferation with different growth factors (EGF and/or bFGF) measured as above. RLU: relative light units. §: two-sided *t*-test, $p < 0.05$. **E**, proliferation measured as above after 8 days in standard medium (EGF + bFGF), or EGF, or bFGF alone, with respect to control cells kept in the absence of growth factors. §: two-sided *t*-test, $p < 0.05$. **F-G**, micrographs (magnification, x100) of cells kept in 10% serum for 7 days and stained with crystal violet (CV), or anti-MAP2, anti-GFAP or anti-GalC antibodies. Nuclei counterstained with DAPI. Western blots of cells kept in standard medium (SM) or 2 or 10% serum. **H**, Kaplan-Meier survival curves of mice orthotopically injected with neurospheres. **I**, immunohistochemistry for GFAP or GalC in tumors formed by orthotopically injected neurospheres (Met-neg-NS: BT379; Met-pos-NS: BT308, magnification, x200).

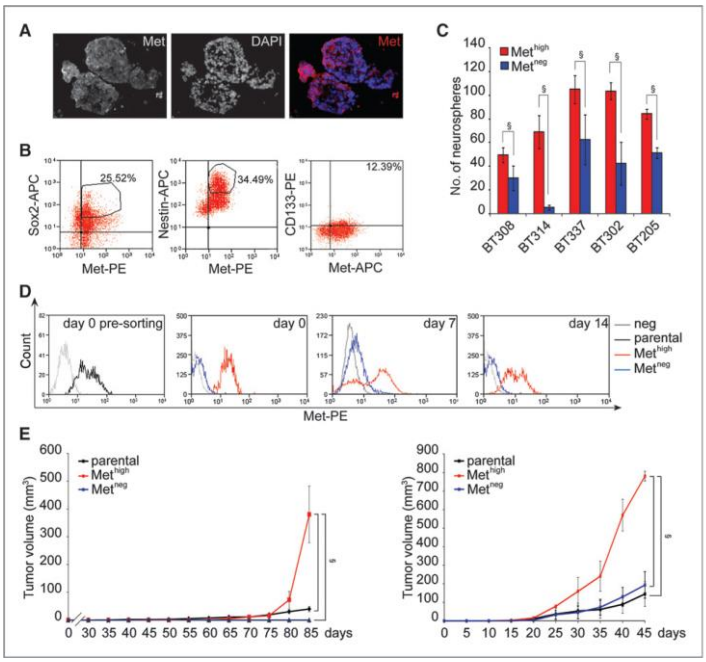

Figure 3. The Met^{high} subpopulation is enriched with clonogenic and tumorigenic cells. **A**, Met staining in a representative Met-pos-NS (BT308; magnification, x400). **B**, flow-cytometry; coexpression of Met with Sox2, Nestin or CD133 in a representative Met-pos-NS (BT308). **C**, clonogenic assay; number of neurospheres formed by Met^{high} or Met^{neg} cells after 14 days in standard medium. §: two-sided *t*-test, $p < 0.05$. **D**, flow-cytometry; Met expression analyzed in the unsorted (parental) BT308 neurosphere (black line) at day 0 pre-sorting, and in its sorted Met^{high} (red line) and Met^{neg} (blue line) subpopulations, at the indicated days after sorting. **E**, volume of subcutaneous tumors formed by BT308 (left) and 302 (right) neurospheres (parental) and their sorted subpopulations (n = 3 in each group). §: two-sided *t*-test, $p < 0.05$.

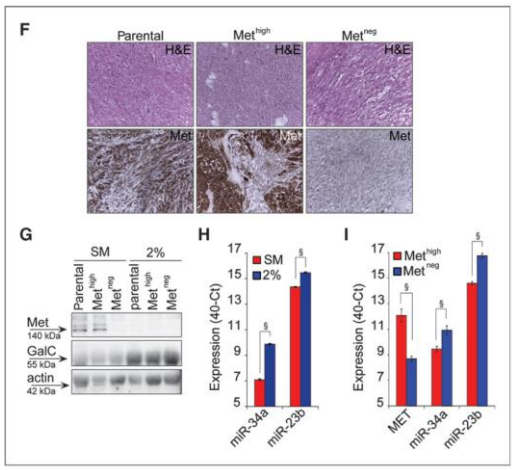

Figure 3 (continued) **F**, H&E and Met immunohistochemical staining (magnification, x200) of the above tumors. Enlarged images in Supplementary Fig. S8. **G**, Met and GalC expression in BT308 neurosphere (parental), and its sorted subpopulations, 7 days after culture in standard medium (SM), or in prodifferentiating medium (2% serum). **H**, qPCR of miR-34a and miR-23b transcripts in BT308 neurosphere grown as in (**G**). §: two-sided *t*-test, $p < 0.05$. **I**, qPCR of MET, miR-34a and miR-23b transcripts in the Met^{high} and Met^{neg} subpopulations immediately after sorting from BT308 neurosphere. §: two-sided *t*-test, $p < 0.05$.

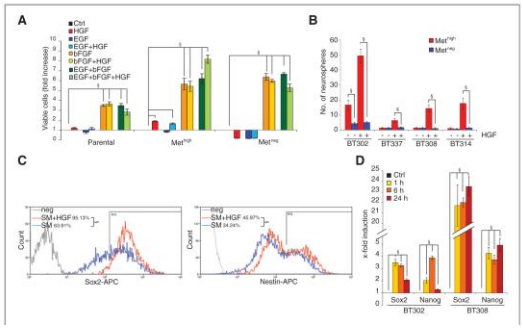

Figure 4. HGF sustains clonogenicity and expression of self-renewal markers. **A**, proliferative effect of growth factors on the Met-pos-NS BT308 (parental), or its sorted subpopulations, with respect to control (no growth factor), after 8 days of culture. §: two-sided *t*-test, $p < 0.05$. **B**, clonogenic assay; number of neurospheres formed by Met^{high} or Met^{neg} cells after 14 days with (+) or without (-) HGF. §: two-sided *t*-test, $p < 0.05$. **C**, flow-cytometry; expression of Sox2 or Nestin in BT308 neurosphere in standard medium (SM) with or without HGF. §: two-sided *t*-test, $p < 0.05$. **D**, qPCR; expression of Nanog and Sox2 in neurospheres treated with HGF with respect to standard medium (ctrl).

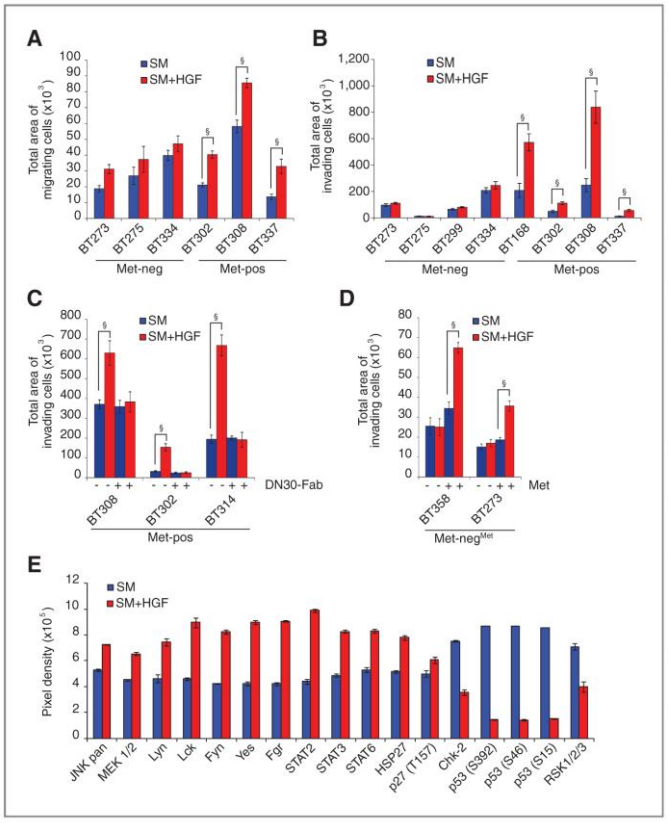

Figure 5. HGF sustains invasive growth. **A**-**B**, transwell assay; neurospheres were dissociated and analyzed for migration (without matrigel coating, **A**), or invasion (with matrigel coating, **B**), in standard medium, with or without HGF. §: two-sided *t*-test, $p < 0.05$. **C**, neurospheres assessed as in (**B**), with (+) or without (–) anti-Met antibodies (DN30-Fab). §: two-sided *t*-test, $p < 0.05$. **D**, representative Met-neg-NS transfected (+) or not (–) with Met and assessed as in (**B**). §: two-sided *t*-test, $p < 0.05$. **E**, phosphorylation of intracellular signal transduces in BT308 neurosphere cultured in standard medium with or without HGF for 24 h. Statistically significantly modulated proteins were represented (two-sided *t*-test, $p < 0.05$).

Supplementary figures and tables

http://cancerres.aacrjournals.org/content/72/17/4537/suppl/DC1

References

1. Wen PY, Kesari S. Malignant gliomas in adults. N Engl J Med 2008;359:492-507.

2. Comprehensive genomic characterization defines human glioblastoma genes and core pathways. Nature 2008;455:1061-8.

3. Brennan C, Momota H, Hambardzumyan D, Ozawa T, Tandon A, Pedraza A et al. Glioblastoma subclasses can be defined by activity among signal transduction pathways and associated genomic alterations. PLoS One 2009;4:e7752.

4. Parsons DW, Jones S, Zhang X, Lin JC, Leary RJ, Angenendt P et al. An integrated genomic analysis of human glioblastoma multiforme. Science 2008;321:1807-12.

5. Phillips HS, Kharbanda S, Chen R, Forrest WF, Soriano RH, Wu TD et al. Molecular subclasses of high-grade glioma predict prognosis, delineate a pattern of disease progression, and resemble stages in neurogenesis. Cancer Cell 2006;9:157-73.

6. Verhaak RG, Hoadley KA, Purdom E, Wang V, Qi Y, Wilkerson MD et al. Integrated genomic analysis identifies clinically relevant subtypes of glioblastoma characterized by abnormalities in PDGFRA, IDH1, EGFR, and NF1. Cancer Cell 2010;17:98-110.

7. Yan H, Parsons DW, Jin G, McLendon R, Rasheed BA, Yuan W et al. IDH1 and IDH2 mutations in gliomas. N Engl J Med 2009;360:765-73.

8. Vescovi AL, Galli R, Reynolds BA. Brain tumour stem cells. Nat Rev Cancer 2006;6:425-36.

9. Dirks PB. Brain tumor stem cells: bringing order to the chaos of brain cancer. J Clin Oncol 2008;26:2916-24.

10. Bao S, Wu Q, McLendon RE, Hao Y, Shi Q, Hjelmeland AB et al. Glioma stem cells promote radioresistance by preferential

activation of the DNA damage response. Nature 2006;444:756-60.

11. Park CY, Tseng D, Weissman IL. Cancer stem cell-directed therapies: recent data from the laboratory and clinic. Mol Ther 2009;17:219-30.

12. Galli R, Binda E, Orfanelli U, Cipelletti B, Gritti A, De VS et al. Isolation and characterization of tumorigenic, stem-like neural precursors from human glioblastoma. Cancer Res 2004;64:7011-21.

13. Louis DN, Ohgaki H, Wiestler OD, Cavenee WK, Burger PC, Jouvet A et al. The 2007 WHO classification of tumours of the central nervous system. Acta Neuropathol 2007;114:97-109.

14. Huse JT, Holland EC. Targeting brain cancer: advances in the molecular pathology of malignant glioma and medulloblastoma. Nat Rev Cancer 2010;10:319-31.

15. Bredel M, Scholtens DM, Yadav AK, Alvarez AA, Renfrow JJ, Chandler JP et al. NFKBIA deletion in glioblastomas. N Engl J Med 2011;364:627-37.

16. Pandita A, Aldape KD, Zadeh G, Guha A, James CD. Contrasting in vivo and in vitro fates of glioblastoma cell subpopulations with amplified EGFR. Genes Chromosomes Cancer 2004;39:29-36.

17. Schulte A, Gunther HS, Martens T, Zapf S, Riethdorf S, Wulfing C et al. Glioblastoma stem-like cell lines with either maintenance or loss of high-level EGFR amplification, generated via modulation of ligand concentration. Clin Cancer Res 2012

18. Koochekpour S, Jeffers M, Rulong S, Taylor G, Klineberg E, Hudson EA et al. Met and hepatocyte growth factor/scatter factor expression in human gliomas. Cancer Res 1997;57:5391-8.

19. Kong DS, Song SY, Kim DH, Joo KM, Yoo JS, Koh JS et al. Prognostic significance of c-Met expression in glioblastomas. Cancer 2009;115:140-8.

20. Singh SK, Hawkins C, Clarke ID, Squire JA, Bayani J, Hide T et al. Identification of human brain tumour initiating cells. Nature 2004;432:396-401.

21. Beier D, Hau P, Proescholdt M, Lohmeier A, Wischhusen J, Oefner PJ et al. CD133(+) and CD133(-) glioblastoma-derived cancer stem cells show differential growth characteristics and molecular profiles. Cancer Res 2007;67:4010-5.

22. Chen R, Nishimura MC, Bumbaca SM, Kharbanda S, Forrest WF, Kasman IM et al. A hierarchy of self-renewing tumor-initiating cell types in glioblastoma. Cancer Cell 2010;17:362-75.

23. Doetsch F. The glial identity of neural stem cells. Nat Neurosci 2003;6:1127-34.

24. Pruszak J, Ludwig W, Blak A, Alavian K, Isacson O. CD15, CD24, and CD29 define a surface biomarker code for neural lineage differentiation of stem cells. Stem Cells 2009;27:2928-40.

25. Gunther HS, Schmidt NO, Phillips HS, Kemming D, Kharbanda S, Soriano R et al. Glioblastoma-derived stem cell-enriched cultures form distinct subgroups according to molecular and phenotypic criteria. Oncogene 2008;27:2897-909.

26. Lottaz C, Beier D, Meyer K, Kumar P, Hermann A, Schwarz J et al. Transcriptional profiles of CD133+ and CD133- Glioblastoma-Derived Cancer Stem Cell Lines Suggest different cells of Origin. Cancer Res 2010;70:2030-40.

27. Freije WA, Castro-Vargas FE, Fang Z, Horvath S, Cloughesy T, Liau LM et al. Gene expression profiling of gliomas strongly predicts survival. Cancer Res 2004;64:6503-10.

28. Schulte A, Gunther HS, Phillips HS, Kemming D, Martens T, Kharbanda S et al. A distinct subset of glioma cell lines with

stem cell-like properties reflects the transcriptional phenotype of glioblastomas and overexpresses CXCR4 as therapeutic target. Glia 2011;59:590-602.

29. Li Y, Guessous F, Zhang Y, Dipierro C, Kefas B, Johnson E et al. MicroRNA-34a inhibits glioblastoma growth by targeting multiple oncogenes. Cancer Res 2009;69:7569-76.

30. Salvi A, Sabelli C, Moncini S, Venturin M, Arici B, Riva P et al. MicroRNA-23b mediates urokinase and c-met downmodulation and a decreased migration of human hepatocellular carcinoma cells. FEBS J 2009;276:2966-82.

31. Boccaccio C, Comoglio PM. Invasive growth: a MET-driven genetic programme for cancer and stem cells. Nat Rev Cancer 2006;6:637-45.

32. Thiery JP, Acloque H, Huang RY, Nieto MA. Epithelial-mesenchymal transitions in development and disease. Cell 2009;139:871-90.

33. Trusolino L, Bertotti A, Comoglio PM. MET signalling: principles and functions in development, organ regeneration and cancer. Nat Rev Mol Cell Biol 2010;11:834-48.

34. Petrelli A, Circosta P, Granziero L, Mazzone M, Pisacane A, Fenoglio S et al. Ab-induced ectodomain shedding mediates hepatocyte growth factor receptor down-regulation and hampers biological activity. Proc Natl Acad Sci U S A 2006;103:5090-5.

35. De Bacco F, Luraghi P, Medico E, Reato G, Girolami F, Perera T et al. Induction of MET by ionizing radiation and its role in radioresistance and invasive growth of cancer. J Natl Cancer Inst 2011;103:645-61.

36. Larrea MD, Wander SA, Slingerland JM. p27 as Jekyll and Hyde: regulation of cell cycle and cell motility. Cell Cycle 2009;8:3455-61.

37. Dai C, Gu W. p53 post-translational modification: deregulated in tumorigenesis. Trends Mol Med 2010;16:528-36.

38. Dick JE. Stem cell concepts renew cancer research. Blood 2008;112:4793-807.

39. Strommer K, Hamou MF, Diggelmann H, de TN. Cellular and tumoural heterogeneity of EGFR gene amplification in human malignant gliomas. Acta Neurochir (Wien) 1990;107:82-7.

40. Nicholas MK, Lukas RV, Jafri NF, Faoro L, Salgia R. Epidermal growth factor receptor - mediated signal transduction in the development and therapy of gliomas. Clin Cancer Res 2006;12:7261-70.

41. Mazzoleni S, Politi LS, Pala M, Cominelli M, Franzin A, Sergi SL et al. Epidermal growth factor receptor expression identifies functionally and molecularly distinct tumor-initiating cells in human glioblastoma multiforme and is required for gliomagenesis. Cancer Res 2010;70:7500-13.

42. Li Y, Li A, Glas M, Lal B, Ying M, Sang Y et al. c-Met signaling induces a reprogramming network and supports the glioblastoma stem-like phenotype. Proc Natl Acad Sci U S A 2011;108:9951-6.

43. Sun Y, Goderie SK, Temple S. Asymmetric distribution of EGFR receptor during mitosis generates diverse CNS progenitor cells. Neuron 2005;45:873-86.

44. Pastrana E, Cheng LC, Doetsch F. Simultaneous prospective purification of adult subventricular zone neural stem cells and their progeny. Proc Natl Acad Sci U S A 2009;106:6387-92.

45. Robel S, Berninger B, Gotz M. The stem cell potential of glia: lessons from reactive gliosis. Nat Rev Neurosci 2011;12:88-104.

46. Mani SA, Guo W, Liao MJ, Eaton EN, Ayyanan A, Zhou AY et al. The epithelial-mesenchymal transition generates cells with properties of stem cells. Cell 2008;133:704-15.

CHAPTER III

EGFR and NF-kB cross-talk in glioblastoma stem-like cells

EGFR and NF-kB cross-talk in glioblastoma stem-like cells

Monica Patanè[1], *Paola Porrati[1]*, *Elisa Bottega[1]*, *Sara Morosini[2]*, *Gabriele Cantini[2]*, *Vita Girgenti[3]*, *Renata Vuono[4]*, *Bianca Pollo[4]*, *Francesca Sciacca[3]*, *Serena Pellegatta[1,2]*, *Gaetano Finocchiaro[1,2]*

[1]Molecular Neuro-Oncology Unit, IRCCS Foundation "C.Besta" Neurological Institute, 20133 Milan, [2]Department of Experimental Oncology, IFOM-IEO Campus, 20139 Milan, [3]Laboratory of Clinical Pathology and Medical Genetics, IRCCS Foundation "C.Besta" Neurological Institute, 20133 Milan, [4]Neuropathology Unit, IRCCS Foundation "C.Besta" Neurological Institute, 20133 Milan

Summary

The NF-kB family of transcription factor is up-regulated in inflammation and different cancers. Recent data described heterozygous deletions of the NF-kB Inhibitor alpha gene (*NFKBIA*) in about 20 % of glioblastomas (GBMs): deletions were mutually exclusive with *EGFR* amplification, a frequent event in GBMs. We have investigated the status of *NFKBIA* and *EGFR* genes in primary GBMs and in GBM neurospheres (NS), containing glioblastoma stem-like cells responsible for tumor perpetuation.

Sixty-nine GBMs and the corresponding NS were included in this study. *NFKBIA* deletion was investigated by copy number variation assay (CNV); whereas *EGFR* amplification by a CNV assay ratio with *HGF*, also located on chromosome 7; expression of *EGFR* and EGFRvIII (a frequent mutant caused by deletion of exons 2-7) were also studied by qPCR and RT-PCR. A fraction of NS was then cultured with EGF and bFGF or with bFGF only, to study the effects of EGF on amplification and expression of *EGFR* and *NFKBIA*.

NFKBIA deletions in heterozygosity were present in 3 of 69 primary GBMs and in 30 of 69 NS. *EGFR* amplification was detected in 36 GBMs and in 23 NS. Furthermore, CNV values decreased significantly in NS versus primary GBMs (47 Vs 10; $p<0.001$). In absence of EGF in the medium, *EGFR* CNV decreased less. In part of NS *NFKBIA* deletion, on the contrary, became detectable in presence of EGF. The CNV assay was validated showing that CN value of the *HPRT1* gene on chromosome X are 2 in females and 1 in males (hemizygosity condition). Furthermore, results of array-CGH performed on 3 primary GBMs and 1 NS line were compatible with the CNV assay when looking at the *EGFR* and *NFKBIA* status. NS cells with *NFKBIA* deletion had increased nuclear activity of p65 (RelA) and increased expression of the NF-kB target IL-6.

Our data point to a low frequency of *NFKBIA* in GBM. Growth factors in the NS culture's medium, and EGF in particular, may significantly affect *EGFR* amplification and related pathways. A thorough assessment of the relevance of NF-kB in GBM biology, also in light of recent data, supporting a pro-differentiation role of NF-kB in neural stem cells, is warranted.

Introduction

Glioblastoma multiforme (GBM) is classified as the highest grade glioma, according to World Health Organization classification (*WHO grade IV, 2007*), with an annual incidence of 5 cases per 100,000 people. It is considered the most aggressive brain tumor, characterized by a rapid disease progression and a median of survival of 12-15 months after diagnosis (*Riemenschneider et al 2009; Wen et al 2008,*

Pietsch et al 1997). This type of tumor is mostly defined by hallmarks of uncontrolled cellular proliferation, invasion, necrosis, robust angiogenesis, genetic and molecular instability. (*Dunn et al 2013; Riemenschneider et al 2009; Wen et al 2008).*

In the last years, it was made a huge effort to achieve a complete characterization of genetic and molecular signatures of glioblastoma in order to identify new molecular targets (*Phillips et al 2006; Berhoukim et al 2007; Verhaak et al 2010*). To date single-target agents have shown only modest activity because most GBMs display a robust intra-tumoral heterogeneity, redundant signalling pathways and target cooperativity, that determine a state in which single-target drugs fail to attenuate tumor growth (*Szerlip et al 2012; Stommel et al 2007; Inda et al 2007*).

By genetic and molecular expression profiling, GBM has been classified into four subtypes with distinct pattern of alterations: *Classical*, *Mesenchymal*, *Proneural* and *Neural* subtypes. The *Classical* subtype is mostly characterized by loss of chromosome 10, *EGFR* gene amplification or activating mutations and high levels of proteins of the EGFR pathway. In the *Mesenchymal* subtype predominantly occur a focal hemizygous deletion at 17q11.2 locus, which contains *NF1* gene and expression of mesenchymal markers such as c-MET receptor. The *Proneural* subtype shows a focal amplification at 4q12, which harbour the *PDGFRA* gene, and point mutations of *IDH1* and *TP53* genes. Finally, the *Neural* subtype shows typical expression of neurons markers and a differentiated phenotype (*Brennan et al 2009; Verhaak et al 2010; De Bacco et al 2012*).

In order to deep understand GBM pathogenesis is also crucial to identify the genetic alterations and the complex signalling of a small fraction of cells called "glioblastoma stem-like cells" (GSCs): these cells are considered the real tumor-forming cells and they are able to self-renew *in vitro* and to recapitulate malignant glioma progression *in vivo*. They can be isolated from GBM specimens and propagate as neurospheres in serum-free culture's conditions, and they could represent a real reservoir for the tumor of cells, which are able alone to maintain tumor growth, to give raise to a relapse and to determine radio- and chemo-resistance. (*Singh et al 2003, 2004; Galli et al 2004; Li et al 2009*).

In the past years several studies have also pointed out the importance of EGFR and NF-kB pathways in forming, growth and relapse of many types of tumors, including glioblastoma: these pathways are now considered strictly intermingled and dependent from each other.

NF-kB is a heterodimeric transcription factor formed by a family of Rel proteins, which share a common N-terminal DNA binding region (RelA/p65, RelB and RelC) and proteins which contain an ankyrin domain (p50, p100). NF-kB complexes are maintained inactive in the cytoplasm through interaction with their inhibitor IkBα, encoded by *NFKBIA* gene on 14q13.2. Most stimuli activate this pathway through phosphorylation of the IKK complex, which in turn is able to phosphorylate IkBα, leading the inhibitor to degradation and the transcription factor NF-kB able to translocate in the nucleus. Here, NF-kB regulates the transcription of several genes involved in proliferation, survival, tissue invasion, inhibition of apoptosis and angiogenesis of tumors and the production of several chemokines and

cytokines. There are almost two distinct pathways of NF-kB activation: canonical and non-canonical, which involve different types of kinases (STAT3, PI3K/Akt, MAPK) and distinct heterodimers (p65/p50; p100/RelB) (*Basserès et al 2006; Brown et al 2008; Nogueira et al 2011a*).

The Epidermal Growth Factor Receptor (EGFR) is involved in proliferation and it is expressed at high levels in many types of cancers, including glioblastoma. It is a typical tyrosine-kinase receptor, which signals through two main pathways: Ras/MAPK kinases and PI3K/Akt/mTOR kinases. Its gene, located on 7p11.2, is amplified in 40% of GBMs, forming typical double-minutes auto-replicative chromosomes: this amplification is distinguished from polisomy of chromosome 7, another hallmark typical of glioblastoma. *EGFR* gene can be also mutated: a deletion of exons 2-7 generates a constitutively activated form, called EGFRvIII, which lacks of the extracellular domain and it is not able to bind EGF ligand and to internalize, leading to a low-level continuous signalling. This mutant is present in almost 50% of *EGFR* amplified GBMs (*Huang et al 1997; Vogt et al 2004; Hatanpaa et al 2010*).

Several studies in the past years have shown the relationship between these two pathways mostly through activation of PI3K/Akt/mTOR signalling (*Biswas et al 2000; Tanaka et al 2011*). However, to date, only one paper (*Bredel et al 2011*) demonstrated a correlation between NF-kB and *EGFR* status at the genetic level, finding a heterozygous deletion of *NFKBIA* gene in 20% of primary GBMs that was mutually exclusive with *EGFR* amplification.

We decided to study this possible correlation in our GSCs model *in vitro* in order to better characterize this relationship at the molecular level and to point out its functional meaning. Surprisingly, we found that this deletion is a rare event in primary tumors, but becomes very frequent in GSCs, an event that seems to depend primarily on culture conditions.

Materials and Methods

Tumor specimens and cell cultures

Human glioblastoma specimens, diagnosed as grade IV gliomas according to WHO criteria, were snap frozen or paraffin-embedded after surgery. Neurospheres (here equivalent to glioblastoma stem-like cells) were derived by mechanical dissociation and digestion of tumor specimens with collagenase type I (Invitrogen, Life technologies, Foster City CA, USA). Single cell suspensions were plated at clonal density (50cells/μl) in standard medium containing: DMEM/F-12 (GIBCO, Life Technologies, Foster City CA, USA), 2mM glutamine (Sigma Aldrich, St.Louis MO, USA), penicillin-streptomycin (1:100, EuroClone, Italy), B-27 supplement (1:50, GIBCO, Life technologies, Foster City CA, USA), human recombinant fibroblast growth factor 2 (bFGF 20ng/ml; Tebu Bio, France) and epidermal growth factor (EGF, 20ng/ml; Tebu Bio, France). Neurospheres were mechanically dissociated when equal 100-150μm in diameter.

Nucleic Acid extraction

Total DNA was extracted using QIAamp DSP DNA Blood Mini Kit (Qiagen, Hilden, Germany) for peripheral blood and PureLink™ Pro

96 Genomic DNA Purification Kit (Invitrogen, Life technologies, Foster City CA, USA) for paraffin-embedded tumors according to protocols of the manufacturers. Total DNA and RNA from neurospheres were instead extracted using All Prep DNA/RNA mini kit (Qiagen, Hilden, Germany). RNA from snap frozen specimens was extracted by TRIZOL® reagent (Invitrogen, Life technologies, Foster City CA, USA) according to manufacturer's protocol. DNA and RNA concentration and purity were measured using Nanodrop® spectrophotometer (Thermo Scientific, Pierce Biotechnology, Rockford IL, USA).

Copy number variation assay

Copy number variation assay was performed on ViiA™ 7 Real-Time PCR System (Applied Biosystems, Life technologies, Foster City CA, USA) using Taqman® copy number assay chemistry (Applied Biosystems, Life technologies, Foster City CA, USA). Briefly, duplex real-time PCR was performed using 5ng/µl of DNA. FAM-labeled assays were used for *EGFR* (Hs4942325_cn), *HGF* (Hs04982672_cn), *NFKBIA* (Hs01379535_cn), *HPRT1* (Hs05654996_cn) (Applied Biosystems, Life technologies, Foster City CA, USA) and VIC-labeled assay was used for reference gene (*TERT* 20X, Applied Biosystems, Life technologies, Foster City CA, USA). DNA extracted from peripheral blood has been used as control. To discriminate between real *EGFR* amplification and polysomy of the chromosome harboring the gene (chr7), the calculated copy number was normalized against the copy number of another gene mapped on chr7, and usually

not amplified (*HGF*): true amplification is considered per *EGFR/HGF* copy number value > 4.

RT-PCR and Real Time PCR

500ng RNA was reverse-transcribed using High Capacity cDNA Reverse Transcription kit on 2720 Thermal Cycler (Applied Biosystems, Life technologies, Foster City CA, USA).

Real Time PCR was performed using Taqman® reagents on ViiA™ 7 Real-Time PCR System (Applied Biosystems, Life technologies, Foster City CA, USA): Taqman Universal Master Mix, *EGFR* assay (Hs_01076078_m1) and *GAPDH* assay as calibrator (Hs_99999905_m1) (Applied Biosystems, Life technologies, Foster City CA, USA). FirstChoice® Human Brain Total RNA has been used as control (Ambion, Life technologies, Foster City CA, USA).

Amplification of full length *EGFR* and EGFRvIII was performed using Taq Gold® DNA Polymerase on 2720 Thermal Cycler (Invitrogen, Life technologies, Foster City CA, USA). PCR conditions were as follows: 95°C for 3 min; 40 × [95°C for 15 sec, 60°C for 30 sec, and 72°C for 30 sec]; and 72°C for 5 min. PCR products were analyzed into a 1,5% agarose gel. Following primers were used: EGFRvIII forward 5'-CTTCGGGGAGCAGCGATGCGA-3' and reverse 5'-ACCAATACCTATTCCGTTACA-3'; wtEGFR forward 5'-CCAGTATTGATCGGGAGAGC-3' and reverse 5'-CCAAGGACCACCTCACAGTT-3' (PRIMM, Italy).

Evaluation of NF-kB activity and IL-6 levels

Cytoplasmatic and nuclear proteins were extracted using the Nuclear extract kit (Active Motif, Carlsbad CA, USA) according to manufacturer's protocol. Protein concentration was measured by MicroBCA Protein Assay kit at OD=540nm (Thermo Scientific, Pierce Biotechnology, Rockford IL, USA) and analyzed using a microplate absorbance reader Multiskan FC (Thermo Scientific, Pierce Biotechnology, Rockford IL, USA).

NF-kB activity was measured in both protein extracts using the TransAM^{TM} NF-kB p65 protein assay (Active Motif, Carlsbad CA, USA), an ELISA-based method on 96-wells plates in which a oligonucleotide containing the NF-kB consensus binding site has been immobilized; p65 subunit was revealed by HRP-conjugated antibodies system and analyzed at OD=450nm.

Interleukin-6 levels were measured from surnatants of our neurospheres using Human IL-6 ELISA kit 96-wells plate, based on standard sandwich enzyme-linked immune-adsorbent technology and revealed by Avidin-Biotin-Peroxidase Complex System (Wuhan Boster Biological Technology, Wuhan China), according to manufacturer's protocol and analyzed at OD=450nm.

Array-CGH

Array-CGH analysis was performed using the CytoChip oligo-array (ISCA) 180K, containing 181,873 oligonucleotide probes (BlueGnome Ldt, Cambridge, UK) with a mean resolution of 16.30 Kb (25 Kb resolution on the backbone, 3.4 Kb resolution on genes). Data analysis was performed using InnoScan 710 Microarray Scanner

(Innopsys Inc. Chicago IL, USA) and Bluefuse software (BlueGnome Ldt, Cambridge, UK). Oligo positions are referred to hg19.

1µg of sample and reference genomic DNAs were digested and then labelled with Cy3 (samples) and Cy5 (references) fluorophores, using random primers. The labelled DNAs were cleaned up using Amicon Ultracel-30 membrane filters (AU-30) (Millipore, Billerica MA, USA) followed by vacuum concentration if required. Labelled DNAs of samples were combined with sex-matched labeled references and then hybridized with oligonucleotide probes of array platform. Hybridization was performed using MaiTaiTM Hybridization System (SciGene, Sunnivale CA, USA). After 24 hours CytoChip oligo-array was washed and scanned. Amplifications or deletions are revealed by green (Cy3) or red (Cy5) signals, due to unbalanced ratio between the two fluorophores.

Probes located at +0.3 and -0.3 in the hg19 are in double copy (normal genotype); probes at +0.40 and +0.60 are in triple copy; more than +0.60 it is referred to gene amplification. Probes at -0.6 and 1 are in single copy, whereas probes at -2 are nullisomic.

Immunohistochemistry

Surgical specimens are fixed in Carnoy, paraffin-embedded and sectioned at 2µm. Sections are mounted on slides, deparaffinized in xylene and blocked in 10% H_2O_2 (Sigma-Aldrich, St. Louise, Missouri, USA). The sections are first incubated with normal goat serum (Dako, Glostrup, Denmark) and then in a humified chamber with mouse monoclonal anti-EGFR (Thermo Scientific, INC, USA). Sections are then incubated with anti-mouse Envision® peroxidase

conjugated (Dako, Glostrup, Denmark). Finally, sections reacted with diaminobenzidine (Liquid DAB Substrate Chromogen System, DakoCytomation Carpinteria, CA, USA), counterstained with hematoxylin and mounted.

For hematoxylin-eosin staining, slides deparaffined in xylene are stained in Carazzi hematoxylin solution, rinsed in running tap water and counterstain in eosin solution.

Data analysis

ΔΔCt method (*Pfaffl, 2001)* was used to determine gene expression and copy number variation; copy number value (CN) was determined as $2(2^{- \Delta\Delta Ct})$, where 2 is the usual copy number of a gene. Numerical results were expressed as means $\pm$ SEM and statistical significance ($P<0.05$) was evaluated using Student *t* test.

Results

Analysis of the *EGFR* status in primary glioblastomas and corresponding neurospheres *in vitro*

We performed a copy number variation assay (CNV) to assess *EGFR* amplification status in 69 primary GBMs and in corresponding neurospheres expanded in vitro in the presence of EGF and bFGF growth factors in the medium. In order to differentiate real *EGFR* amplification from polisomy of chromosome 7, a frequent event in GBM, we studied the ratio between the copy number (CN) of *EGFR* and *HGF* genes, both located on chromosome 7 and normalised with respect to reference gene *TERT*.

Table 1A summarizes results in brain tumors (BT) with or without *EGFR* amplification and in corresponding neurospheres (NS): *EGFR* is amplified in 36 tumors (52%), but only in 23 corresponding NS (33%).

Figure 1A shows the *EGFR/HGF* ratio: in primary tumors the median CN ratio is 47; this value is significantly decreased in vitro, with median CN ratio of 10 ($P<0.001$).

In summary, we have found that the number of samples with *EGFR* amplification and their CN ratios both decrease *in vitro*. Notably 13/36 BT completely lose *EGFR* amplification in corresponding NS.

Analysis of the *NFKBIA* status in primary glioblastomas and corresponding neurospheres *in vitro*

We then performed a CNV assay to assess the *NFKBIA* status on the same tumors and NS tested for *EGFR* amplification. Only 3 BT showed heterozygous deletion of *NFKBIA* and this alteration was mutually exclusive with *EGFR* amplification. Surprisingly, however, the heterozygous deletion of *NFKBIA* was detected in 30/69 NS lines (Table 1B).

The deletion was mutually exclusive with EGFR amplification only in 11/30 NS; notably, 7/30 of these NS had lost *EGFR* amplification *in vitro*; in the remaining 12/30 NS the heterozygous deletion was present concurrently with EGFR amplification (Table 1C).

Figure 1B displays the median copy number of *NFKBIA*: in primary tumors and NS without *NFKBIA* deletion, the CN was almost 2.6, whereas in BT and NS with *NFKBIA* deletion, the copy number was 1.2, suggesting heterozygous deletion.

In order to confirm that the CNV assay is able to distinguish one copy from two copies of a gene, we performed an assay to evaluate *HPRT1* on 6 controls, 3 females and 3 males subjects: this gene maps on chromosome X and therefore only one copy is present in males (hemizygous condition). As shown in supplementary figure 1, females have 2 copies of the gene, and males only one copy, as expected. This result confirms that the gene copy number assay we used to study *NFKBIA* is able to detect hemizygosity and therefore is able to detect also a heterozygous deletion.

Validation of our data also derived from array-CGH experiments: *EGFR* amplification at 7p11.2 (probe position according to hg19 at +0.60) was confirmed in two primary BT (BT418 e BT419) in which we found very high CN ratios with the CNV Assay (74 and 323 respectively) (Figure 2C). BT314 showed trisomy of chromosome 7 (probe position at +0.40) in agreement with lack of amplification with the CNV assay (Figure 2A). BT314 showed *NFKBIA* deletion in primary tumor: this was confirmed by array-CGH, showing complete loss of the long arm of chromosome 14 (Figure 2B). *EGFR* amplification was also found in BT297NS but array-CGH failed to confirm *NFKBIA* deletion at 14q13.2 found in this NS cell line with CNV assay, suggesting the possibility of focal intragenic deletion not detectable by CGH probes that are only flanking *NFKBIA* gene. Taken together the data confirm that the CNV assay is able to detect not only gene amplifications but also heterozygous deletions.

Functional validation of NFKBIA heterozygous deletion

To validate further CNV data, we investigated the functional consequences of *NFKBIA* deletion. We speculated that the deletion could decrease intracellular levels of the NF-kB inhibitor (IkB), causing increased translocation of NF-kB in the nucleus and consequently increased transcription of target genes.

To measure NF-kB activity we used the TransAM NF-kB p65 kit (Active Motif) that specifically detects p65 subunit activation. We compared p65 activity in cytoplasmic and nuclear extracts of 8 NS with *NFKBIA* deletion and in 6 NS without such deletion. As shown in Figure 3, we found that p65 activity was significantly higher in the nuclear extracts of NS with *NFKBIA* deletion compared to others ($P<0.005$), confirming that such deletion may have relevant functional consequences.

Characterization of neurospheres (NS) cultured in different conditions

In order to assess if the presence of EGF in the culture medium affects *EGFR* amplification in NS, we established NS cultures from primary GBMs either in the presence of complete medium (i.e. both EGF and bFGF growth factors) or in presence of bFGF only (modified medium).

We first characterized four NS lines deriving from primary tumors with *EGFR* amplification. Figure 4 shows the comparison of *EGFR/HGF* copy number ratio (fig. 4A) and *NFKBIA* copy number (fig. 4B) in primary tumors (BT), NS in complete medium (EGF+bFGF) and NS in modified medium (bFGF).

All cell lines showed a strong decrease of *EGFR* amplification, with 3 to 20 folds lower levels of *EGFR/HGF* copy number ratio in NS with complete medium versus the corresponding primary tumor. *EGFR* copy number was always higher in the absence of EGF: although this trend was present in all four cell lines, variable levels of *EGFR* amplification were detectable (Fig.4A) from levels comparable to control (BT459) to levels higher than primary BT (BT470).

Two cell lines, BT462 and BT470, showed heterozygous loss of *NFKBIA* in the complete medium, not detected in the original tumor. Interestingly, the deletion was absent in modified medium.

To further investigate the *EGFR* status we performed a quantitative evaluation of *EGFR* expression in BT462 and BT470 by Real Time PCR and investigated by a semi-quantitative method, RT-PCR, wild type *EGFR* and EGFRvIII (the most frequent, constitutively active mutant of *EGFR*) in the same lines (figure 5A). The probe used for Real-Time PCR recognized both wtEGFR and EGFRvIII (see also Methods). BT462 showed increased presence of EGFRvIII and decreased presence of wtEGFR in vitro, particularly in the absence of EGF. BT470, on the contrary, showed a strong decrease of EGFRvIII *in vitro* and an increase of wtEGFR, particularly in the absence of EGF.

In figure 5B we show H&E staining and immunohistochemistry with anti-EGFR antibody of BT462 and BT470 indicating strong EGFR expression, as expected.

Two other cell lines were also considered, BT463 and BT467 that did not show *EGFR* amplification or *NFKBIA* loss in the original tumor.

Under both culture conditions (EGF plus bFGF or bFGF only) the status of these two genes did not change (supplementary figure 2).
Overall the data suggest that loss of *EGFR* amplification in vitro is probably due to EGF presence in the culture medium. Clonal expansion of cells harbouring *NFKBIA* deletion and/or EGFRvIII deletion may take place in this context.

IL-6 expression in cultured cells

Finally, we decided to measure IL-6 levels in the culture medium of BT462 and BT470. This pro-inflammatory cytokine is a known target of NF-kB transactivation. Notably, IL-6 is also produced in EGFRvIII cells and released in the micro-environment to activate adjacent EGFR amplified cells.
Indeed, IL-6 levels showed correlation with the presence of the EGFRvIII variant and *NFKBIA* deletion: they are present in BT462 cells, cultured with EGF or without EGF and in BT470 cells cultured in complete medium, but are very low in the absence of EGF, when EGFRvIII is almost absent (Figure 6: RT-PCR showing EGFR and EGFRvIII are shown below for comparison).

Discussion

***NFKBIA* deletion is low frequency in primary GBM**

In this work we investigated the presence of *NFKBIA* deletion in GBM. After the report by *Bredel et al* (*2011*) no further confirmation was provided if we exclude the report by *Idbaih et al* (*2011*), who found deletions in about 25% GBM but did not confirm mutual

exclusivity of *NFKBIA* deletion with *EGFR* amplification (*Idbaih et al., 2011*). Methods used, however, were not reported. A recent work from TCGA did not mention such a high frequency neither did another report based on TCGA data (*Verhaak et al, 2nd TCGA symposium 2012; Frattini et al, submitted*). In this work we found a 4.3% frequency of the deletion in the primary GBM we studied. It is possible that the presence of normal cells in the surgical specimen underestimates the number of cases with deletion: this, however, seems possibly for a minority of cases. Overall our first conclusion, based on this set of data is that the *NFKBIA* deletion is present but not frequent in primary GBM.

***NFKBIA* deletion in culture is favored by EGF**

This observation is strengthened by the in vitro data we gathered on GBM neurospheres (NS). Unexpectedly, we found that a large fraction of GBM NS showed results of the copy number assay for *NFKBIA* compatible with a heterozygous deletion. In parallel we observed the disappearance of *EGFR* amplification in part of the cases and decreased CN values in others. Two set of observations suggest that the assay we used is appropriate for CNV studies in these cells. First, we validated this technique by showing that *HPRT1*, a gene located in chromosome X, is present with two copies in females and one copy in males (hemizygosity condition). Second we showed that the decreased copy number of *NFKBIA* has functional consequences. We expected that decreased gene dosage of *NFKBIA* may cause increased migration to the nucleus of the NF-kB transcription factor and consequent increased activity of the p65 subunit. This was

actually demonstrated in an ELISA-based testing on GBM NS with or without *NFKBIA* deletion. A third line of evidence is provided by array-CGH tested on primary tumors, where *NFKBI*A deletion, detected by CNV assay, was found associated to the entire loss of chromosome 14. *EGFR* amplification detected by CNV assay was still confirmed by array-CGH in these tumors and in one GBM NS. In this latter case, *NFKBIA* deletion detected by CNV assay was not found by array-CGH: we should consider, however, that specific probes hybridizing to the *NFKBIA* gene are absent in this assay, so the hemizygosity condition is found only in the presence of large deletions or loss of the entire chromosome 14.

The progressive lack of *EGFR* amplification was in good agreement with data from *Schulte et al*, (*2012*), also showing that *EGFR* amplification is progressively lost in culture conditions used for NS growth (*Schulte et al., 2012*). Notably these authors find that *EGFR* amplification is associated to slower growth *in vitro* when compared to cells without such amplification. These observation may explain why *EGFR* amplification is counter-selected *in vitro*. Furthermore, they show that the difference in growth is decreased/canceled if EGF is removed from the culture medium, again in agreement with our findings (*Schulte et al., 2012*). The recent observation that *EGFR* amplification is associated to increased capacity for invasion rather than proliferation is also in agreement with this observation (*Talasila et al., 2013*).

Our results suggests the possibility that also *NFKBIA* deletion may be "amplified" (or created) in vitro in GBM NS that have decreased or lost amplification of *EGFR*. As EGFR signaling may also impinge of

NF-kB, as indicated by data in breast cancer (*Biswas et al., 2000*) and GBMs (*Kapoor et al., 2004*), it seems plausible that in tumor "addicted" to this signaling pathway, *NFKBIA* deletion is a response to loss of this pathway of EGFR signaling.

EGFRvIII may be favored in vitro by lack of EGF

Another response that can be favored in vitro in the absence of EGF-induced signaling by EGFR is the deletion of *EGFR*, as this implies the loss of the extracellular domain of EGFR interacting with its ligand and constitutive activation (*Huang et al., 1997*). EGFRvIII may also activate NF-kB through mTORC2 (*Tanaka et al., 2011*): thus this deletion, that occurs in the majority of GBMs with *EGFR* amplification (*Furnari et al., 2007*), may also preserve the function of EGFR-NF-kB axis in glioma perpetuation.

Genotype of GB-NS may be influenced by EGF and possibly bFGF

Previous data by different group, including ours, have proposed that GBM neurospheres provide a much better system than serum-dependent cultures, *in vitro* and *in vivo*, to study GBM biology (*Tunici et al., 2004*; *Lee et al, 2006; De Bacco et al, 2012*). Present results however indicate that presence of EGF and bFGF may partially skew the molecular signatures present in primary GBMs.

Concluding remarks

The data we have obtained in this study suggest that *NFKBIA* deletions are not frequent in GBMs, in contrast with the initial report

by *Bredel et al* (*Bredel et al., 2011*). Relevant interactions between EGFR, the most important oncogene in GBMs, and NF-kB have been first proposed in breast cancer (*Biswas et al., 2000*). In GBMs association between SHP-2 and Grb2-associated binder 1 (Gab1) was identified as a critical step in the pathway linking EGFR to NF-kB activation *(Kapoor et al., 2004*): these observations were obtained *in vitro* using U87 cells and should be confirmed in an *in vitro* system more representative of GBM biology.

It is plausible that other biological mechanisms independent of EGFR have a major role in NF-kB activation in GBMs. This family of transcription factors is the object of a number of studies pointing at its therapeutic targeting (*Nogueira et al., 2011a*). However its contribution to tumorigenesis in cells of neural origins needs further evaluation.

Data from murine or rat NS showed that loss of both p65 and p50 NF-kB subunits results in a reduced number of progeny and in increased neuronal differentiation (*Young et al., 2006*) and that activation of the canonical NF-kB pathway by TNF-alpha strongly increases NS proliferation (*Widera et al., 2006*).

More recently however it was found that in murine embryonic stem cells Nanog binds to NF-kB proteins, inhibiting their transcriptional activity (*Torres and Watt, 2008*). Overexpression of NF-kB proteins promoted differentiation, whereas inhibition increased expression of pluripotency markers (*Torres and Watt, 2008*). Notably, also in GBM-NS the NF-kB transcriptional pathway was activated after inducing differentiation *(Nogueira et al., 2011b*). Blockade of NF-kB signaling in differentiating NS, by genetic strategies or small-

molecule inhibitors, however, caused replication arrest and senescence, in vitro and in vivo (*Nogueira et al., 2011b*).

Overall our data and available evidence form the literature suggest that more work is required to pinpoint GBM subgroups where NF-kB activation is relevant and mechanisms upstream and downstream such activation. It is likely that genomic data gained within the TCGA project will help unraveling data that are presently looking as contradictory.

Figures and Tables

A

BT	Nr.	
EGFR amplified	36	**52%**
EGFR not amplified	33	
NS	**Nr.**	
EGFR amplified	23	**33%**
EGFR not amplified	**46**	

B

BT	Nr.	
wt NFKBIA	66	
del NFKBIA	**3**	**4%**
NS	**Nr.**	
wt NFKBIA	39	
del NFKBIA	**30**	**43%**

C

del NFKBIA NS	Nr.
wt EGFR	11
amp EGFR	12
loss of EGFR amp	7

Table 1. Analysis of copy number variations (CNVs) in primary GBM (BT) and corresponding neurospheres *in vitro* (NS).
A) Summary of *EGFR* status in primary tumors (BT) and corresponding neurospheres (NS) shows a decrease of *EGFR* amplified samples and an increase of not amplified samples in vitro; B) Summary of *NFKBIA* status in primary BT and corresponding NS shows a very low number of deleted BT and an increase of *NFKBIA* deleted samples in vitro; C) Comparison of *EGFR* status in *NFKBIA* deleted NS shows the presence of the deletion concurrently with *EGFR* amplification.

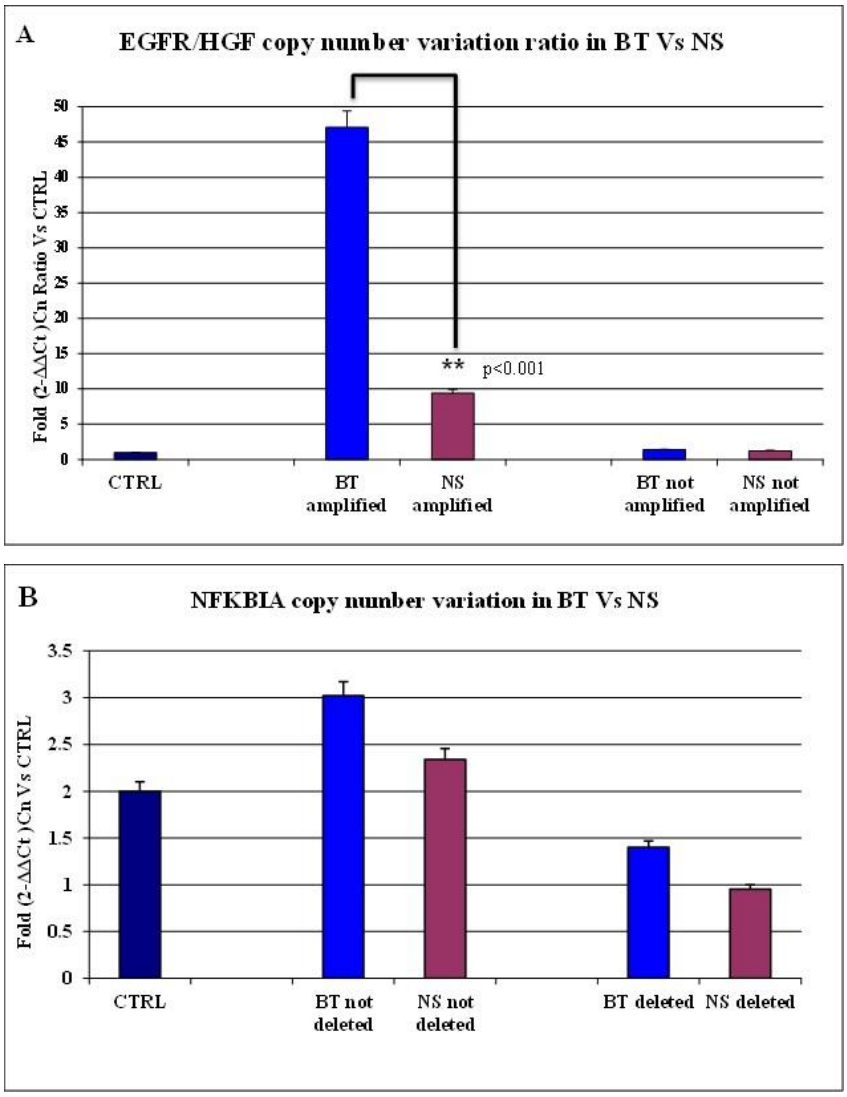

Figure 1. Copy number variation values (CNVs) in primary GBM (BT) and corresponding neurospheres *in vitro* (NS). A) *EGFR* amplification in BT and NS expressed as *EGFR/HGF* ratio in comparison to healthy DNA shows a significant loss of amplification in vitro (**P<0.001; B) heterozygous deletion in BT and NS shows a median CN value of 1.2 compared to healty DNA and not deleted lines.

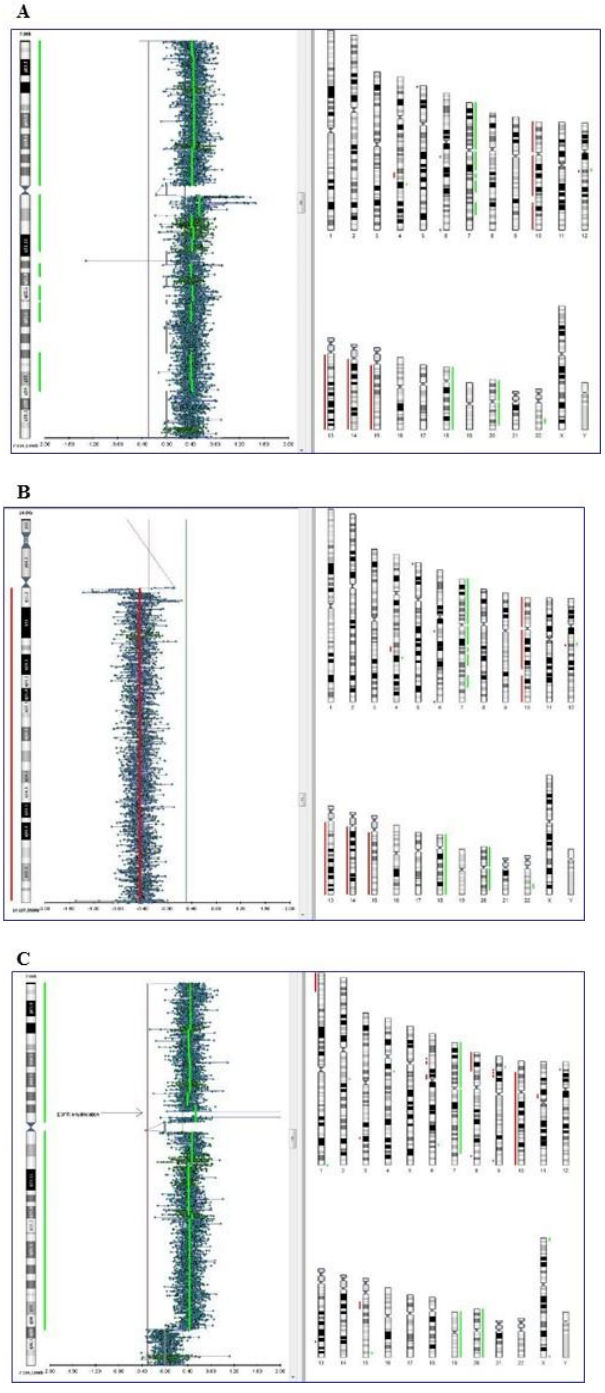

Figure 2. Validation of CNV Assay by array-CGH analysis. A) This figure shows trisomy of chromosome 7 in BT314, but not *EGFR* amplification (probe position at +0.40); B) This figure shows complete loss of chromosome 14q arm in BT314 (probe position at -0.40/0.60); C) This figure shows *EGFR* amplification in BT418 (probe position at +0.60).

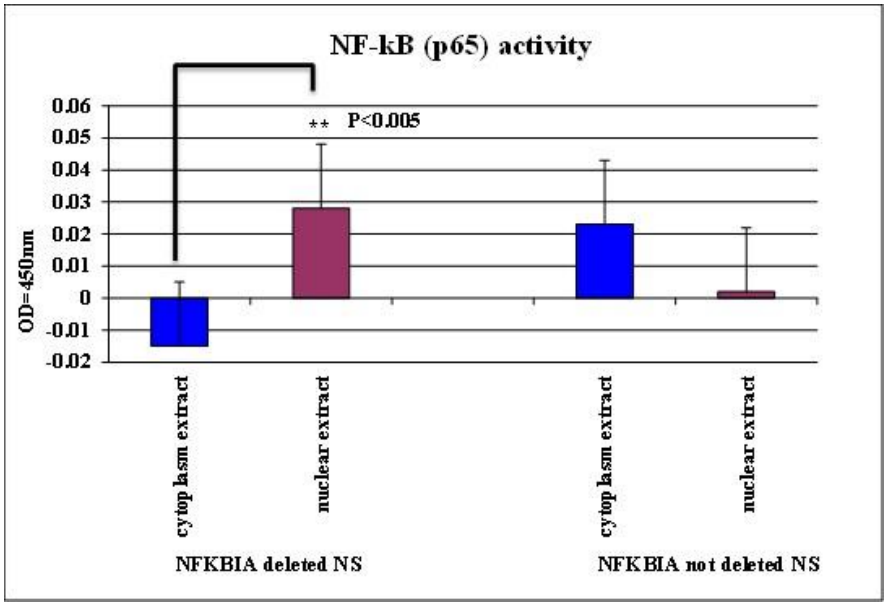

Figure 3. Functional validation of *NFKBIA* heterozygous deletion in NS. A) Comparison of p65 activity in cytoplasmatic proteins versus nuclear proteins in NS shows a significant (** = P<0.005) activity in nuclear extract of *NFKBIA* deleted NS.

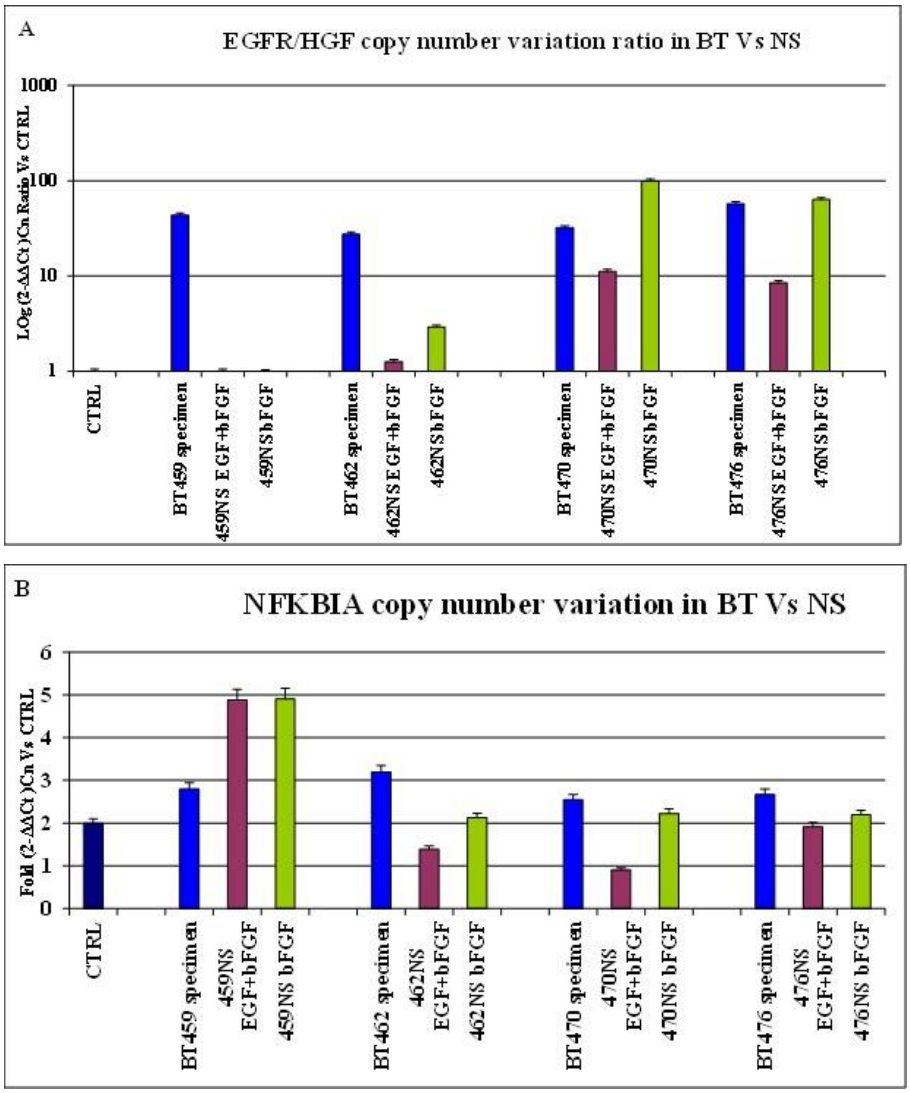

Figure 4. Analysis of copy number variations (CNVs) in primary tumors (BT) and corresponding neurospheres (NS) cultured in different conditions. A) *EGFR* status in NS cultured in presence of both growth factors and in presence of only bFGF shows a strong decrease in complete medium and a retaining of EGFR amplification an absence of EGF with variable levels; B) *NFKBIA* status in NS cultured in presence of both growth factors and in presence of bFGF alone shows an heterozygous NFKBIA deletion only in two NS cultured in complete medium: BT462 and BT470.

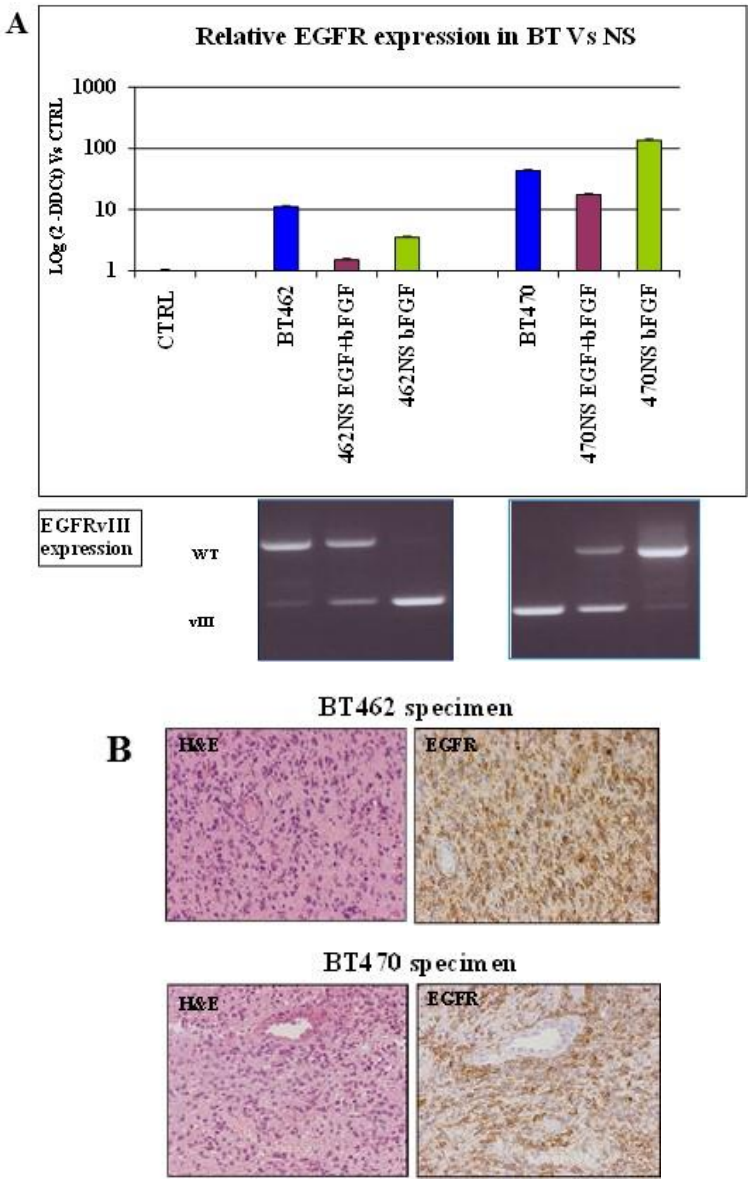

Figure 5. EGFR and EGFRvIII expression in primary tumors (BT) and corresponding neurospheres (NS) cultured in different conditions. A)The upper part shows mRNA levels of *EGFR* in primary tumors and corresponding NS; the lower part shows the presence of wild type *EGFR* and/or the mutant EGFRvIII; B) IHC on tumors specimens shows high levels of EGFR.

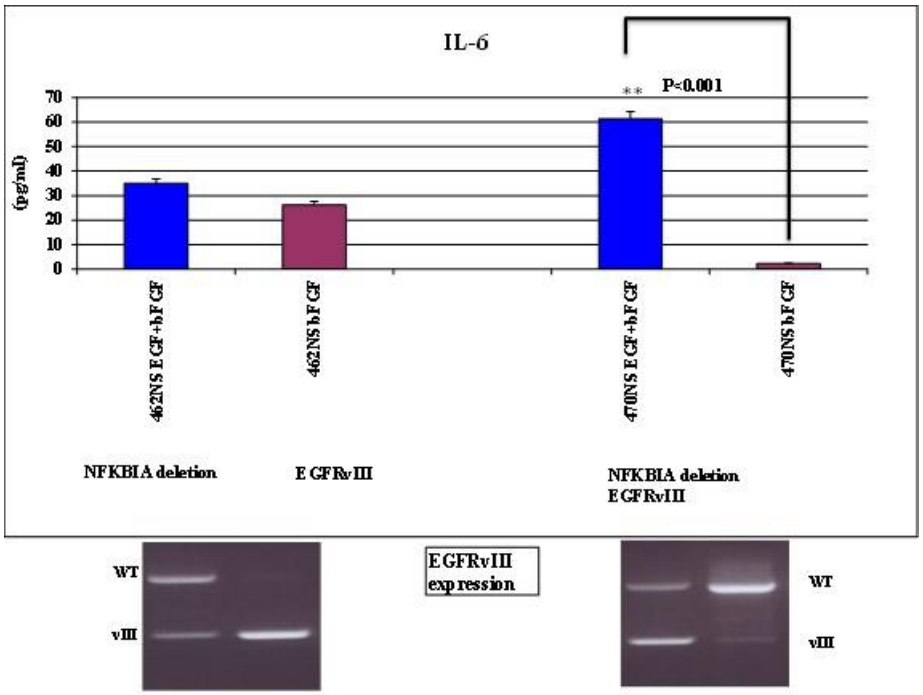

Figure 6. IL-6 expression in cultured cells. Quantification of IL-6 in surnatants of two NS lines cultured in different conditions shows a more IL-6 production in BT470 in complete medium where N*FKBIA* deletion and EGFRvIII are both present (P<0.001).

Supplementary Figures

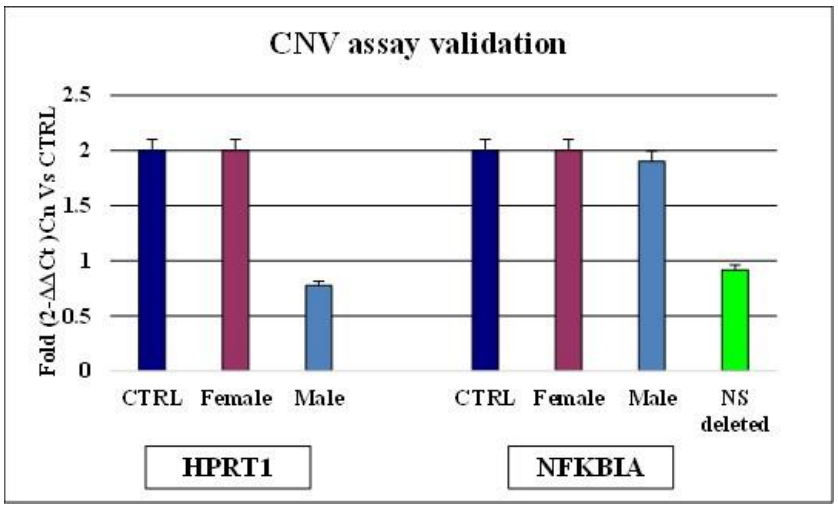

Supplementary figure 1. Copy number validation assay
Validation of Copy Number Variation assay to assess hemizygous or heterozigous condition versus wid type genotype.

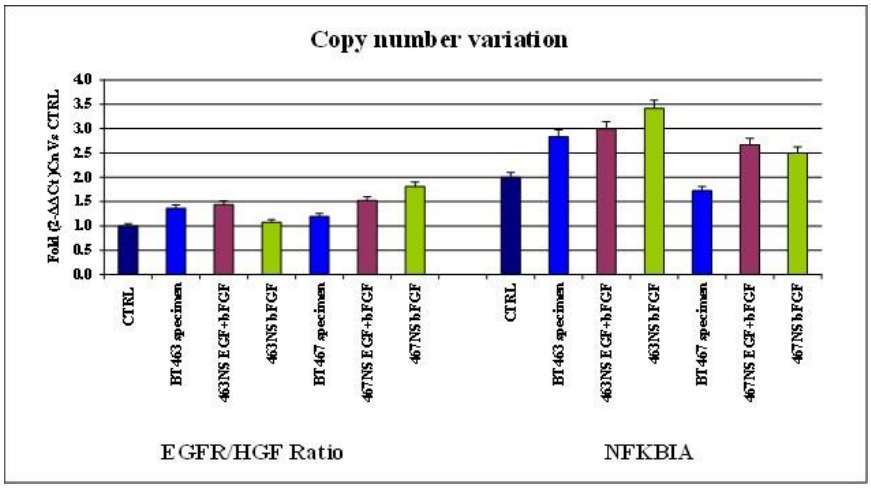

Supplementary figure 2. Analysis of *EGFR* and *NFKBIA* copy number variations (CNVs) in primary tumors (BT) and corresponding neurospheres (NS) cultured in different conditions.
BT463 and BT467 did not show *EGFR* amplification or *NFKBIA* loss in the original tumor.

References

Bassères DS, Baldwin AS. *Nuclear factor-kappaB and inhibitor of kappaB kinase pathways in oncogenic initiation and progression.* Oncogene. **2006**;25:6817-30

Beroukhim R, Getz G, Nghiemphu L, Barretina J, Hsueh T, Linhart D, Vivanco I, Lee JC, Huang JH, Alexander S, Du J, Kau T, Thomas RK, Shah K, Soto H, Perner S, Prensner J, Debiasi RM, Demichelis F, Hatton C, Rubin MA, Garraway LA, Nelson SF, Liau L, Mischel PS, Cloughesy TF, Meyerson M, Golub TA, Lander ES, Mellinghoff IK, Sellers WR. *ssessing the significance of chromosomal aberrations in cancer: methodology and application to glioma.* Proc Natl Acad Sci U S A. **2007**;104:20007-12

Biswas DK, Cruz AP, Gansberger E, Pardee AB.*Epidermal growth factor-induced nuclear factor kappa B activation: A major pathway of cell-cycle progression in estrogen-receptor negative breast cancer cells.* Proc Natl Acad Sci U S A. **2000**;97:8542-7

Bredel M, Scholtens DM, Yadav AK, Alvarez AA, Renfrow JJ, Chandler JP, Yu IL, Carro MS, Dai F, Tagge MJ, Ferrarese R, Bredel C, Phillips HS, Lukac PJ, Robe PA, Weyerbrock A, Vogel H, Dubner S, Mobley B, He X, Scheck AC, Sikic BI, Aldape KD, Chakravarti A, Harsh GR 4th. *NFKBIA deletion in glioblastomas.* N Engl J Med. 2011;364:627-37

Brennan C, Momota H, Hambardzumyan D, Ozawa T, Tandon A, Pedraza A, Holland E. *Glioblastoma subclasses can be defined by activity among signal transduction pathways and associated genomic alterations.* PLoS One. **2009**;4:e7752

Brown KD, Claudio E, Siebenlist U. *The roles of the classical and alternative nuclear factor-kappaB pathways: potential implications for autoimmunity and rheumatoid arthritis.* Arthritis Res Ther.**2008**;10:212

De Bacco F, Casanova E, Medico E, Pellegatta S, Orzan F, Albano R, Luraghi P, Reato G, D'Ambrosio A, Porrati P, Patanè M, Maderna E, Pollo B, Comoglio PM, Finocchiaro G, Boccaccio C. *The MET oncogene is a functional marker of a glioblastoma stem cell subtype.* Cancer Res**. 2012**;72:4537-50

Dunn GP, Rinne ML, Wykosky J, Genovese G, Quayle SN, Dunn IF, Agarwalla PK, Chheda MG, Campos B, Wang A, Brennan C, Ligon KL, Furnari F, Cavenee WK, Depinho RA, Chin L, Hahn WC. *Emerging insights into the molecular and cellular basis of glioblastoma.* Genes Dev. **2012**;26:756-84

Furnari, F.B., Fenton, T., Bachoo, R.M., Mukasa, A., Stommel, J.M., Stegh, A., Hahn, W.C., Ligon, K.L., Louis, D.N., Brennan, C., et al. *Malignant astrocytic glioma: genetics, biology, and paths to treatment. Genes & Development*. **2007**; 21, 2683–2710.

Galli R, Binda E, Orfanelli U, Cipelletti B, Gritti A, De Vitis S, Fiocco R, Foroni C, Dimeco F, Vescovi A *Isolation and characterization of tumorigenic, stem-like neural precursors from human glioblastoma*. Cancer Res. **2004**;64:7011-21

Hatanpaa KJ, Burma S, Zhao D, Habib AA. *Epidermal growth factor receptor in glioma: signal transduction, neuropathology, imaging, and radioresistance.* Neoplasia. **2010**;12:675-84

Huang, H.S., Nagane, M., Klingbeil, C.K., Lin, H., Nishikawa, R., Ji, X.D., Huang, C.M., Gill, G.N., Wiley, H.S., and Cavenee, W.K. *The enhanced tumorigenic activity of a mutant epidermal growth factor receptor common in human cancers is mediated by threshold levels of constitutive tyrosine phosphorylation and unattenuated signaling.* The Journal of Biological Chemistry.**1997**;272, 2927–2935

Idbaih, A., Marie, Y., and Sanson, M. *NFKBIA deletion in glioblastomas. The New England Journal of Medicine*.**2011**; 365, 277; author reply 277–8

Inda MM, Bonavia R, Mukasa A, Narita Y, Sah DW, Vandenberg S, Brennan C, Johns TG, Bachoo R, Hadwiger P, Tan P, Depinho RA, Cavenee W, Furnari F. *Tumor heterogeneity is an active process maintained by a mutant EGFR-induced cytokine circuit in glioblastoma.* Genes Dev. **2010**;24:1731-45

Kapoor, G.S., Zhan, Y., Johnson, G.R., and O'Rourke, D.M. *Distinct domains in the SHP-2 phosphatase differentially regulate epidermal growth factor receptor/NF-kappaB activation through Gab1 in glioblastoma cells.*
Molecular and Cellular Biology.**2004**; 24:823–836

Lee, J., Kotliarova, S., Kotliarov, Y., Li, A., Su, Q., Donin, N.M., Pastorino, S., Purow, B.W., Christopher, N., Zhang, W., et al. *Tumor stem cells derived from glioblastomas cultured in bFGF and EGF more closely mirror the phenotype and genotype of primary tumors than do serum-cultured cell lines*. Cancer Cell.**2006**;9:391–403

Li Z, Wang H, Eyler CE, Hjelmeland AB, Rich JN. *Turning cancer stem cells inside out: an exploration of glioma stem cell signaling pathways.* J Biol Chem. **2009**;284:16705-9

Nogueira L, Ruiz-Ontañon P, Vazquez-Barquero A, Moris F, Fernandez-Luna JL. *The NFκB pathway: a therapeutic target in glioblastoma.* Oncotarget. **2011a**;2:646-53

Nogueira L, Ruiz-Ontañon P, Vazquez-Barquero A, Lafarga M, Berciano MT, Aldaz B, Grande L, Casafont I, Segura V, Robles EF, Suarez D, Garcia LF, Martinez-Climent JA, Fernandez-Luna JL. *Blockade of the NFκB pathway drives differentiating glioblastoma-initiating cells into senescence both in vitro and in vivo.*
Oncogene. **2011b**;30:3537-48

Pfaffl MW. *A new mathematical model for relative quantification in real-time RT-PCR.* Nucleic acids research **2001**

Phillips HS, Kharbanda S, Chen R, Forrest WF, Soriano RH, Wu TD, Misra A, Nigro JM, Colman H, Soroceanu L, Williams PM, Modrusan Z, Feuerstein BG, Aldape K *Molecular subclasses of high-grade glioma predict prognosis, delineate a pattern of disease progression, and resemble stages in neurogenesis.*
Cancer Cell**. 2006**;9:157-73

Pietsch T, Wiestler OD. *Molecular neuropathology of astrocytic brain tumors.* J Neurooncol.**1997**;35:211-22

Riemenschneider MJ, Reifenberger G. *Molecular neuropathology of gliomas.* Int J Mol Sci. **2009**;10:184-212

Riemenschneider MJ, Jeuken JW, Wesseling P, Reifenberger G.*Molecular diagnostics of gliomas: state of the art.*
Acta Neuropathol. **2010**;120:567-84

Schulte A, Günther HS, Martens T, Zapf S, Riethdorf S, Wülfing C, Stoupiec M, Westphal M, Lamszus K. *Glioblastoma stem-like cell lines with either maintenance or loss of high-level EGFR amplification, generated via modulation of ligand concentration.*
Clin Cancer Res. **2012**;18:1901-13

Singh SK, Clarke ID, Hide T, Dirks PB. *Cancer stem cells in nervous system tumors.* Oncogene. **2004**;23:7267-73

Singh SK, Clarke ID, Terasaki M, Bonn VE, Hawkins C, Squire J, Dirks PB. *Identification of a cancer stem cell in human brain tumors.*
Cancer Res. **2003**;63:5821-8

Stommel JM, Kimmelman AC, Ying H, Nabioullin R, Ponugoti AH, Wiedemeyer R, Stegh AH, Bradner JE, Ligon KL, Brennan C, Chin L, DePinho RA. *Coactivation of receptor tyrosine kinases affects the response of tumor cells to targeted therapies.*
Science. **2007**;318:287-90

Szerlip NJ, Pedraza A, Chakravarty D, Azim M, McGuire J, Fang Y, Ozawa T, Holland EC, Huse JT, Jhanwar S, Leversha MA, Mikkelsen T, Brennan CW. *Intratumoral heterogeneity of receptor tyrosine kinases EGFR and PDGFRA amplification in glioblastoma defines subpopulations with distinct growth factor response.* Proc Natl Acad Sci U S A. **2012**;109:3041-6

Talasila, K.M., Soentgerath, A., Euskirchen, P., Rosland, G. V, Wang, J., Huszthy, P.C., Prestegarden, L., Skaftnesmo, K.O., Sakariassen, P.O., Eskilsson, E., et al. *EGFR wild-type amplification and activation promote invasion and development of glioblastoma independent of angiogenesis.* Acta Neuropathologica. **2013**

Tanaka K, Babic I, Nathanson D, Akhavan D, Guo D, Gini B, Dang J, Zhu S, Yang H, De Jesus J, Amzajerdi AN, Zhang Y, Dibble CC, Dan H, Rinkenbaugh A, Yong WH, Vinters HV, Gera JF, Cavenee WK, Cloughesy TF, Manning BD, Baldwin AS, Mischel PS. *Oncogenic EGFR signaling activates an mTORC2-NF-κB pathway that promotes chemotherapy resistance.* Cancer Discov. **2011**;1:524-38

Torres, J., and Watt, F.M. *Nanog maintains pluripotency of mouse embryonic stem cells by inhibiting NFkappaB and cooperating with Stat3.* Nature Cell Biology.**2008**;10:194–201

Tunici, P., Bissola, L., Lualdi, E., Pollo, B., Cajola, L., Broggi, G., Sozzi, G., and Finocchiaro, G. *Genetic alterations and in vivo tumorigenicity of neurospheres derived from an adult glioblastoma.* Molecular Cancer.**2004**;3: 25

Verhaak RG, Hoadley KA, Purdom E, Wang V, Qi Y, Wilkerson MD, Miller CR, Ding L, Golub T, Mesirov JP, Alexe G, Lawrence M, O'Kelly M, Tamayo P, Weir BA, Gabriel S, Winckler W, Gupta S, Jakkula L, Feiler HS, Hodgson JG, James CD, Sarkaria JN, Brennan C, Kahn A, Spellman PT, Wilson RK, Speed TP, Gray JW, Meyerson M, Getz G, Perou CM, Hayes DN; Cancer Genome Atlas Research Network. *Integrated genomic analysis identifies clinically relevant subtypes of glioblastoma characterized by abnormalities in PDGFRA, IDH1, EGFR, and NF1.* Cancer Cell. **2010**;17:98-110

Vogt N, Lefèvre SH, Apiou F, Dutrillaux AM, Cör A, Leuraud P, Poupon MF, Dutrillaux B, Debatisse M, Malfoy B. *Molecular structure of double-minute chromosomes bearing amplified copies of the epidermal growth factor receptor gene in gliomas.*
Proc Natl Acad Sci U S A. **2004**;101:11368-73

Widera, D., Mikenberg, I., Elvers, M., Kaltschmidt, C., and Kaltschmidt, B. *Tumor necrosis factor alpha triggers proliferation of adult neural stem cells via IKK/NF-kappaB signaling.*
BMC Neuroscience.**2006**;7: 64

Wen PY, Kesari S. *Malignant gliomas in adults.*
N Engl J Med. **2008**;359:492-507

Young, K.M., Bartlett, P.F., and Coulson, E.J. *Neural progenitor number is regulated by nuclear factor-kappaB p65 and p50 subunit-dependent proliferation rather than cell survival.*
Journal of Neuroscience Research.**2006**;83:39–49

Authors' contributions and Aknowledgements
P.P., S.M. and E.B. for cells cultures expansion and maintaining; G.C. for EGFRvIII RT-PCR, V.G. and F.S. for array-CGH data; R.V. and B.P. for immunohistochemistry images.

Summary, conclusions and future perspectives

The purpose of this thesis was, therefore, better characterize genetic and molecular signatures of glioblastoma in order to pinpoint new targets for custom therapies: to make this, we used our GSCs model, which is known to ricapitulate *in vitro* genetic and molecular lesions of the primary tumor.

In the first paper this statement seems to be confirmed by *in vitro* and *in vivo* studies: actually we identified distinct subsets of GSCs which displayed different signatures, different *in vitro* requirements and distinct *in vivo* behaviors. So we concluded that primary glioblastomas could contain distinct types of GSCs which arise from different cells of origin and therefore display distinct molecular markers and circuits.

We confirmed these conclusions also in the second paper: here we found that probably the growth factors present in the culture medium could partially skew the molecular signature of the primary tumors driving to a sort of selection of a subtype of GSCs compared to another.

Overall, our data suggest that more work has to be done in order to clarify GSCs behavior *in vitro* and *in vivo* and to characterize all the mechanisms and pathways involved in their genetic and molecular signatures: these findings will contribute to better clarify the characteristic heterogeneity of glioblastoma and to define new criteria for targeted therapies.

Publications

Patanè M, Porrati P, Bottega E, Morosini S, Cantini G, Girgenti V, Vuono R, Pollo B, Sciacca F, Pellegatta S, Finocchiaro G
EGFR and NF-kB cross-talk in glioblastoma stem-like cells
Submitted

De Bacco F, Casanova E, Medico E, Pellegatta S, Orzan F, Albano R, Luraghi P, Reato G, D'Ambrosio A, Porrati P, **Patanè M,** Maderna E, Pollo B, Comoglio PM, Finocchiaro G, Boccaccio C.
The MET oncogene is a functional marker of a glioblastoma stem cell subtype. Cancer Res. 2012;72:4537-50

Calò L, Bruno V, Spinsanti P, Molinari G, Korkhov V, Esposito Z, **Patanè M**, Melchiorri D, Freissmuth M, Nicoletti F. *Interactions between ephrin-B and metabotropic glutamate 1 receptors in brain tissue and cultured neurons.* J Neurosci. 2005;25:2245-54